STUDY OF ARTIFICIAL GROUNDWATER RECHARGE FROM A POND IN A SMALL WATERSHED

A THESIS

Submitted in partial fulfilment of the requirements for the award of the degree

of

DOCTOR OF PHILOSOPHY

in

HYDROLOGY

by

SHAKIR ALI

DEPARTMENT OF HYDROLOGY
INDIAN INSTITUTE OF TECHNOLOGY ROORKEE
ROORKEE - 247 667 (INDIA)

DECEMBER, 2009

INDIAN INSTITUTE OF TECHNOLOGY ROORKEE
ROORKEE

CANDIDATE'S DECLARATION

I hereby certify that the work which is being presented in the thesis entitled **STUDY OF ARTIFICIAL GROUNDWATER RECHARGE FROM A POND IN A SMALL WATERSHED** in partial fulfilment of the requirements for the award of the degree of Doctor of Philosophy and submitted in the Department of Hydrology of Indian Institute of Technology Roorkee, Roorkee, is an authentic record of my own work carried out during a period from July 2004 to December 2009 under the supervision of Dr. Ranvir Singh, Professor, Department of Hydrology, Indian Institute of Technology Roorkee, Roorkee, and Dr. N. C. Ghosh, Scientist F, Groundwater Hydrology Division, National Institute of Hydrology, Roorkee.

The matter presented in this thesis has not been submitted by me for the award of any other degree in this institute or any other Institute.

(SHAKIR ALI)

This is to certify that the above statement made by the candidate is correct to the best of our knowledge.

30/12/09

(N. C. GHOSH)
Supervisor

(RANVIR SINGH)
Supervisor

Date: 30/12/2009

The Ph.D. Viva-Voce examination of **Mr. Shakir Ali**, Research Scholar, has been held on__________.

Signature of Supervisors

Signature of External Examiner

ABSTRACT

Artificial groundwater recharge (AGR) by conservation of surface runoffs on watershed basis, as a measure to restore back the depleted groundwater level and to augment the groundwater resource in phreatic aquifer, is promoted by both the central and state governments in India. It is as one of the key strategies, for sustainable groundwater management, particularly in the arid and semi-arid regions. A number of AGR schemes are practiced in India; in which, practice of groundwater recharge by pond is very common due to its constructional simplicity and low operational and maintenance cost. For sustainable groundwater management and for economic design of well based on the augmented water from such recharge schemes, one has to know the rate of recharge and its responses to the underneath aquifer.

Each recharge pond has a specific catchment area from where it receives water. The runoff that generates from the rainfall over the pond's catchment, stores in the pond and then infiltrates below for recharge to the aquifer at a rate faster than the normal recharge. The rate of recharge depends on the difference of heads in the pond and the underneath groundwater table in addition to the subsurface soil properties and the saturated hydraulic conductivity. The head of water in the pond is governed by the: (i) surface runoff from its catchment, (ii) direct rainfall over its surface, (iii) evaporation from its water surface, and (v) excess outflow runoff from its storage.

In the present investigations, each of the hydrologic components involved in the water balance of a pond has been studied separately to derive suitable process level models in accordance to the data usually monitored in the field, and thereafter, the derived process level models are integrated in the water balance equation of the pond to arrive at the required recharge estimation models.

The recharge component that constitutes two aspects; the potential recharge and the actual recharge, has been studied using the Green-Ampt (GA) infiltration model for deriving the process based potential recharge model, and the Hantush's approximate analytical solution for deriving the process based actual recharge model.

Approximating the logarithmic term, $\ln(1+L_f/H+\psi_f)$ of the GA model [where L_f = length of the advancement of the wetting front; H = depth of ponding; and ψ_f = suction head) by the segmental second order polynomials; the approximate expressions for L_f are derived satisfying all ranges of $[L_f/(H+\psi_f)]\geq 0$. Five segmental equations are found to fit to $\ln\left[1+L_f/\left(H+\psi_f\right)\right]$ for $[L_f/(H+\psi_f)] \geq 0$ within the error bound of $\pm$ 1%. Unlike estimation of L_f by the trial and error method as required in the GA model, the proposed expressions estimate L_f explicitly. The characteristic behaviors of the derived L_f expressions are studied for four textural classes of soils namely; sand, loam, clay loam and sandy clay, considering depth of water to be constant, and are found have similar responses as described by the GA model. The proposed model for L_f is thereafter used to develop the time varying process based potential recharge estimation model. The responses of the potential recharge model are studied for all the four soil texture groups. The results showed similar behaviors as that of the GA model. The equation to estimate the time for the wetting front to the reach water table is also derived. Using the Hantush's approximate analytical equation that has been derived for predicting the rise of groundwater level due to constant recharge through rectangular basin, the process based actual recharge rate estimation model for time varying depth of water and water spread area is developed. The characteristic behavior of the actual recharge estimation model is also studied.

By linking the normalized antecedent precipitation index (NAPI) with the antecedent soil moisture content (AMC) and AMC to the losses of precipitation, a simple rainfall-runoff model for predicting runoff yields is derived using the basic water balance equation. The model is based on the concept of normalized antecedent precipitation index proposed by Heggen (2001). The model has three watershed specific parameters, which can easily be estimated from historical data of rainfall-runoff events. The model requires single input; rainfall and one rainfall dependant variable 'NAPI'. The performance of the proposed model is compared with the Soil Conservation Service-Curve Number (SCS-CN) model. The parametric relationships between parameters of the proposed model and CN of the SCS-CN model are also studied. The proposed model is tested with the field data collected from three small watersheds located in the semi-arid region in Rajasthan, India. The results exhibited a superior match by the proposed model than the SCS-CN model.

By evaluating the performances of four commonly used evaporation estimate models, namely; Bowen ratio energy balance (BREB), Mass transfer (MT), Priestley-Taylor(PT) and Pan evaporation (PE), based on the experimental field data, the most effective and reliable model for estimating the evaporation rate for the semi-arid region in Rajasthan is identified. The performances of the BREB, the PT and the PE models are found nearly complementary to each other while the MT method is found to deviate. In this study, the BREB model is used for the computation of evaporation rate, as the data required by the BREB model were available from the field investigation.

By extending the process based models derived for rainfall-runoff, evaporation and the recharge estimation in the water balance equation of a trapezoidal pond, the integrated models for computing the time varying depth of water, the potential and actual groundwater recharge have been developed. The models are developed for two different sets of condition: first, till the wetting front touches the water table, and the second one, as the water table rises due to subsequent recharges after the pond is hydraulically connected to the aquifer. The performances of the integrated models have also been tested using the data collected from the experimental trapezoidal pond located in the semi-arid region in Rajasthan. The comparison of the observed and the simulated depths of water are found to have a close match. The correlation coefficients of the statistical parameters have also shown a good agreement between the observed and simulated results. The responses of the integrated process based models in estimation of the potential and the actual recharge rates are found most promising. These process based models can be extended to other areas for quantifying the recharge component for similar or other types of recharge schemes.

For evaluating the performances of two data series, the statistical parameters namely; coefficient of determination, index of agreement, percentage relative error, standard error of estimate, and relative bias are chosen as the guiding factors.

ACKNOWLEDGEMENTS

It is my proud privilege to express my sincere thanks, profound gratitude and indebtedness to my supervisors, Dr. Ranvir Singh, Professor, Department of Hydrology, Indian Institute of Technology Roorkee, Roorkee, and Dr. N. C. Ghosh, Scientist F, Groundwater Hydrology Division, National Institute of Hydrology, Roorkee, for their inspiring guidance, invaluable supervision, constant encouragement and immense help which have enabled me to get this research work satisfactorily done.

I wish to pay a special thank to Dr. N.C. Ghosh, for his untiring guidance, giving me an opportunity to grow up both intellectually and personally, and scarifying lots of his valuable time when my effort seemed so hopeless.

I express my sincere gratitude to Dr G.C. Mishra, Emeritus Fellow, Department of Water Resources Development and Management, for his valuable and constructive remarks and suggestions on this research endeavor. I wish to thank to Dr. M. Parumal, Associate Professor, Department of Hydrology, I.I.T., Roorkee, whose suggestions on the subject were very insightful. I am also thankful to Dr. D. K. Srivastva, Chairman, DRC, Department of Hydrology, I.I.T., Roorkee for his cooperation and help during the study periods.

I express my sincere thanks to the authority of Indian Institute of Technology, Roorkee in general and the Department of Hydrology, I.I.T., Roorkee in particular for providing the necessary facilities to carry out the research work. I am also thankful to all the faculty members of Department of Hydrology, I.I.T., Roorkee

I am very much thankful to my Director, Dr. V. N. Sharda, Central Soil and Water Conservation Research and Training Institute, Dehradun, who has actually encourage me to take up this particular research and granted study leave to complete the course work and this research study leading to Ph. D.

I extend my sincere thanks to the Director, National Institute of Hydrology, Roorkee, for providing me necessary infrastructural and laboratory facilities during my Ph.D Programme.

My special thanks to Dr. S.N. Prasad, Head, Central Soil and Water Conservation Research and Training Institute, Research Centre, Kota, for his encouragement, cooperation and providing the facilities to carry out the necessary work at the Centre.

I am thankful to colleagues, Dr. R.K. Singh, Dr. A.K. Parandiyal, Dr. Ashok Kumar, Er. B.K. Sethy, Mr. H.R. Meena, Mr. B.K. Upadhya, Mr. B.B. Singh, Mohammad Irfan, and K.T. Dewani at Kota for their constant encouragements and supports.

I am grateful to Mr. Hari Om, Mr. P.R. Raibole and A.K. Chaturvedi at Kota, for their assistance in collecting field data, and thanks are due to the farmers of the Badakhera watershed for their cooperation and help to look after the instruments installed at the experimental site.

I am in short of words to express my feelings to my family members. I am grateful to my parents and brothers whose moral support, blessing and pray all the time, helped me to complete the work. I extend my humble thanks to my wife Akbari Begum for cooperating all the ways and for letting me to be away from her in most of time during last five years. It is she, who always told me there is light at the end of the tunnel. I really thankful to my son Tarique Hussain, and daughters Farah Naz and Farheen for cooperating with their mother in my absence, and I am proud of their silent acceptance of the situation.

I want to thank my friends and colleagues, Dr. Salman Hameed, Dr. M.N. Quereshi, Mr. Ajay Kumar, Mr. R. Kale, Mr. Omkar Singh, Dr. Surjeet Singh, Mr. Rajan Vatsa, Dr. Anupma Sharma, Dr. R.P. Pandey, Dr. A. K. Lohani, Mr. A.R.Senthil Kumar, Mr. Shobha Ram, Mr. Avdhesh Kumar, Mr. Hari Das, Sanjay Mittal, and others for helping me directly or indirectly in my work and making my stay happy and memorable at Roorkee.

And, finally my greatest gratitude is towards the Almighty for giving me power to fulfill my promises and duties. All the efforts made in this study have been possible by the grace of the God who is the Authority and Finisher of every good work.

(Shakir Ali)

TABLE OF CONTENTS

LIST OF TABLES

LIST OF FIGURES

NOTATIONS

The following notations are used in this thesis. In chapter-2, which deals with review of literature, original notations have been used.

a	=	watershed specific parameter [dimensionless];
a_c	=	cloud cover parameter[dimensionless];
a_s	=	regression constant of extraterrestrial radiation[-];
A	=	water surface area of the pond [km^2];
$A_{i,}$	=	coefficient of the polynomial [dimensionless];
A_s	=	water surface area of the pond at the top [L^2];
A_w	=	area of the pond's catchment [L^2];
ΔA_{ws}	=	change in water surface area [L^2];
$\overline{A}_{ws}$	=	average water surface area [L^2];
b	=	watershed specific parameter [L^{-1}];
b_s	=	regression constant of extraterrestrial radiation[-];
B_i	=	coefficient of the polynomial [-];
c	=	watershed specific parameter [-];
C	=	proportionate coefficient [L^{-1}];
C_c	=	fraction of the sky obscured by cloud [-];
C_i	=	coefficient of the polynomial [-];
C_k	=	integration constant [-];
CN	=	curve number [dimensionless];
CN_I, CN_{II}, CN_{III}	=	curve number for AMC(I), AMC(II), AMC(III) [-];
d	=	depth of water for temperature measurement [m];
D	=	index of agreements [-];
D_w	=	depth to water table below the pond's bed [L];
e_a	=	actual vapour pressure [kpa];
e_s	=	saturated vapour pressure at water temperature [kpa];
$e^0(T_{min})$	=	saturated vapour pressure at minimum air temperature [kpa];
$e^0(T_{max})$	=	saturated vapour pressure at maximum air temperature [kpa];
E	=	evaporation rate [LT^{-1}];
E_P	=	evaporation rate by the pan evaporation method [mm/day];
E_{pan}	=	class A pan evaporation [mm/day];
E_{BR}	=	evaporation rate estimated by the Bowen method [mm/day];
E_{MT}	=	evaporation rate by the mass transfer method [mm/day];
E_{PT}	=	evaporation rate by the Priestley-Taylor's method [mm/day];
F_1, F_2 and F_3	=	numerical factors [dimensionless];
F	=	cumulative depth of infiltration [L];
F_i	=	integral factor [-];

G_1, G_2 and G_3	=	numerical factors [-];
h	=	rise in groundwater level from the impervious strata [L];
h_0	=	depth of impervious stratum below the water table [L];
$\overline{h}$	=	weighted mean of depth of saturation [L];
H	=	depth of ponding [L];
H_a	=	energy advection into water body [MJm^{-2}/day];
H_b	=	heat flux into bottom of water body [MJm^{-2}/day];
H_f	=	depth of flow over the crest[m].
H_L	=	depth of impervious strata measured below the pond bed [L];
H(t)	=	depth of ponding at time 't' [L];
H ($n\Delta t$)	=	depth of ponding for a descrete time '$n\Delta t$'[L];
Δh	=	potential difference between heads of water above pond [L];
i	=	integer number;
I_a	=	initial abstractions [L];
I_c	=	integration constant;
I_L	=	index of losses [-];
J_1, J_2 and J_3	=	numerical factors [-];
J	=	Julian day [day];
k	=	decay constant [-];
K	=	hydraulic conductivity of the aquifer material [LT^{-1}];
K_p	=	pan coefficient [-];
K_s	=	saturated hydraulic conductivity [LT^{-1}];
L	=	loss of rainfall [L];
L_c	=	length of crest [m];
L_f	=	length of advancement of wetting front [L];
$L_f(t)$	=	length of advancement of wetting front at time 't' [L];
$L_f(n\ \Delta t)$	=	length of advancement of wetting front for time '$n\Delta t$' [L];
M	=	integer number;
n	=	number
n_a	=	actual duration of sunshine[hour];
N_{max}	=	maximum duration of sunshine or daylight hours [hour];
P	=	rainfall rate over the pond [LT^{-1}];
P_a	=	atmospheric pressure [kpa];
PRE	=	relative percentage error [percent];
q	=	rate of overflow over the crest of weir [m^3/s];
q_a	=	volumetric recharge rate [LT^{-3}];
$q_a(\gamma)$	=	volumetric recharge rate during time 'γ'[LT^{-3}];
$q_a(n\Delta t)$	=	volumetric recharge rate a descrete time '$n\Delta t$'[LT^{-3}];
Q	=	runoff rate into the recharge pond [LT^{-1}];

Q_o	=	volumetric rate of outflow from the pond [LT^{-3}];
r	=	ratio of rainfall losses to rainfall [-];
R	=	groundwater recharge rate from pond [LT^{-1}];
R_a	=	actual recharge rate [LT^{-1}];
$R_a(t)$	=	potential recharge rate at time't' [LT^{-1}];
$R_a(n\Delta t)$	=	actual recharge rate for a descrete time '$n\Delta t$' [LT^{-1}];
R_{ar}	=	extraterrestrial radiation [MJm^{-2}/day];
R_p	=	potential recharge rate [LT^{-1}];
$R_p(t)$	=	potential recharge rate at time 't' [LT^{-1}];
$R_p(n\Delta t)$	=	potential recharge rate for a descrete time '$n\Delta t$'[LT^{-1}];
R_n	=	net radiation on the water surface [MJ m^{-2}/day];
R_s	=	seepage rate [LT^{-1}];
R_{sw}	=	incoming solar or short wave radiation [MJm^{-2}];
RH_{min}	=	minimum relative humidity [%];
RH_{max}	=	maximum relative humidity [%];
RB	=	relative bias [L];
R^2	=	coefficient of determination [-];
s	=	rise in groundwater level above the initial position [L];
$\bar{s}$	=	average rise in the water table [L];
$s(x, y, t)$	=	rise in water table at coordinate x and y at time 't' [L];
S	=	maximum potential retention [mm];
SE	=	standard error of estimates [L];
t	=	time [T];
Δt	=	time step size [T];
t_d	=	number of second in a day[-];
T_a	=	air temperature [^0C];
T_d	=	time delay for the wetting front [L];
T_{max}	=	maximum air temperature [^0C];
T_{min}	=	maximum air temperature [^0C];
T_w	=	surface water temperature [^0C];
U_2	=	wind speed at 2 m above the water surface [ms^{-1}];
U_z	=	wind speed at 'z' m above the ground surface [ms^{-1}];
$U(t)$	=	unit step response function for rise in water table at time 't'[-]
w	=	constant rate of recharge [LT^{-1}];
W	=	half of the width of recharge pond [L];
z	=	depth below the ground surface [L];
α	=	Priestley-Taylor's coefficient [-];
β	=	Bowen ratio [-];
λ	=	initial abstraction weight [-];

λ_h	=	latent heat of evaporation of water [MJ/kg];
η	=	porosity [dimensionless];
Δ	=	slope of saturated vapour pressure [kpa $^0C^{-1}$];
γ_c	=	psychometric constant [kpa$^0C^{-1}$];
σ	=	Stefan-Boltzmann constant [MJM^{-2} K^{-4}];
ε_w	=	emissivity of the water surface [-];
α_w	=	albedo or reflection coefficient of water surface [-];
δ	=	solar declination [degree];
$\delta_s(m, \Delta t)$	=	Hantush's discrete kernel coefficients[-];
$\delta_s(\Delta t)$	=	unit pulse response function at time 't' [-];
$\delta_s(t)$	=	unit pulse response function at time 't'[-];
θ	=	latitude [degree];
θ_s	=	volumetric moisture content at near saturation [cm^3/cm^3];
θ_i	=	initial volumetric moisture content [cm^3/cm^3];
ψ_f	=	suction head at wetting front [L];
ε_a	=	emissivity of the atmosphere [-];
ϕ	=	storage coefficient of the aquifer [-];
μ	=	mass transfer coefficient, [mm s m^{-1} kpa^{-1}]

ABBREVIATIONS

The following abbreviations are used in this thesis:

Agric.	=	Agriculture;
ASCE	=	American Society of Civil Engineers;
Eg.	=	For example;
exp	=	Exponential;
Fig.	=	Figure;
Hydrogeol.	=	Hydrogeology
Hydrol.	=	Hydrology;
i.e.	=	That is;
J.	=	Journal;
Manage.	=	Management;
Res.	=	Research;
Sci.	=	Sciences;
SCS	=	Soil Conservation Service;
USA	=	United States of America

CHAPTER-1

INTRODUCTION

1.1 GENERAL

Groundwater is used as an important and dependable source of water for drinking and agricultural purposes in many countries including India, particularly, in rural areas. Over the recent years, its excessive withdrawal, in excess to the quantity, that is replenished annually, to meet the increasing demands in various uses triggered by the population pressure has raised concerns to its sustainability and the livelihood it supports. Artificial groundwater recharge (AGR) is promoted as an effective engineered technique for restoring and reverting back the depleted trend of groundwater resource in many countries. AGR helps to maintain and augment the groundwater resource in areas where natural replenishment is slow, and groundwater levels deplete at a faster rate. It is also practiced to (i) enhance the sustainable yield of groundwater, and (ii) conserve and store monsoon surface runoffs for future requirements. In India, AGR is being promoted by the Central and State governments under the public-private partnership as a key strategy to recharge and augment groundwater resource in water stressed areas particularly, in arid and semi-arid regions. Various AGR methods are practiced in India, these include; recharge pond, check dam, furrow, ditch, and sub-surface barrier. Among these, the recharge pond is the oldest and widely practiced AGR scheme due to its constructional simplicity and low operational and maintenance cost. Rajasthan state, large part of which covers the Thar Desert in India, is the driest and water scarce state in the country. AGR by the recharge pond is very common in the state. Pond is a small reservoir constructed by excavation of soils or created by construction of small earthen dam across the natural stream. A pond thus has a specific catchment area to receive surface runoff. The runoff that generates from rainfall over the pond's catchment is conserved and stored in the pond. The accumulated water in the pond infiltrates through the underneath soils and moves downward to the aquifer at a rate faster than the natural recharge because of artificially created additional head of water. The opportunity time for recharge is also increased as the water is stored in the pond. The known quantity of water available from a pond for groundwater recharge helps in the development and management of groundwater resources; it also helps in assessing the effectiveness of that pond in aquifer recharge. Recharge and evaporation take place simultaneously, however, more often, it is seen that the practicing engineers for design purposes estimate the rate of groundwater recharge from such ponds by simple arithmetic calculations; considering, as if surface runoff and evaporation take place in two separate times. Nevertheless, the requirement of databases and technical skills for uses of widely accepted hydrological models is so intensive that it makes the straightforward applications of those models very difficult. Further, for sustainable groundwater management and economic design of well field in water scarce areas, one has to know the quantity of water that would be available as aquifer recharge from such recharge schemes. The above concerns form the relevance of the present investigations.

In a recharge pond, the process level hydrological components are: (i) surface runoff that generates from its catchment, (ii) direct rainfall over its surface, (iii) evaporation from its water surface, (iv) recharge through its wetted area, and (v) outflow of excess runoff from its storage. All these components are time variant and simultaneous process. Even after the recession of runoff and rainfall, groundwater recharge and evaporation take place as a simultaneous process. In order to accurately quantify the rate and volume of recharge water from a pond or to optimize the design of a pond, one has to essentially consider and integrate all the time varying input and output components in the water balance equation of the pond, and then arrive at an integrated model for determining the recharge component.

Both the natural and AGR are govern by the same basic physical processes, however there are some important differences. Because of the increase in the ponding depth in artificial recharge, the infiltration rate is higher than the infiltration rate that takes place under natural condition. Also the arrival time of the infiltrated water at the water table is less for the artificially infiltrated water than that of the infiltrated water under natural condition. There are two aspects of groundwater recharge; one that takes place since onset of infiltration process and continues till wetting front touches the water table, termed as potential recharge, and the other one the subsequent recharge after the wetting front touches the groundwater table, termed as actual recharge. The Green-Ampt (GA) infiltration model is widely used for estimation of the potential recharge rate through an unsaturated homogeneous soil. To compute the potential recharge rate using the GA model, prior knowledge of the time varying length of the advancement of wetting front is required. It is generally estimated by a trial and error method. The computation becomes more cumbersome when depth of the ponded water varies. These pose a major difficulty for straightforward use of the GA model to real life problems.

Once the saturated wetting front reaches the water table, the recharge rate can be estimated using a groundwater flow model. Several analytical solutions to estimate the actual recharge and the evolution of the water table due to recharge are available. The approximate analytical equation given by Hantush (1967) to predict the rise of groundwater level due to constant recharge is widely used for estimation of the actual recharge. The Hantush's equation has a scope for estimation of the actual recharge under varying depth of water and varying recharge area, when the water table rises close to the pond.

For ascertaining the maximum volume of the water a pond can recharge, it is prior requirement to estimate the volume of water it would receive from the contributing catchment. A number of rainfall-runoff (RR) models are available in literature to estimate the surface runoff. Most of these models require a large database for calibration and validation purposes, and are computationally extensive. The widely used Soil Conservation

Service-Curve Number (SCS-CN) model also requires database related to antecedent moisture condition (AMC), land use, land treatment practices, hydrological soil group and hydrologic condition of the watershed. These data types are commonly found unmonitored or sparsely available, particularly for small watersheds. The lumped normalized antecedent precipitation index model proposed by Heggen (2001) for estimation of surface runoff yields from rainfall events has a promising potential in terms of its performance and data requirement; but the model needs a physical explanation and verification in the context of the most widely used model, to authenticate its theoretical credibility.

The stored water in the pond is subjected to evaporation. A number of methods, which include: empirical, water budget, energy budget, mass transfer, combination of energy and mass, and measurements are used for evaporation estimation. These methods vary from one to another in terms of: types of data requirement, range of applicability, structural and parametric differences and cost involved in collection of the data. It is thus imperative to identify the most suitable and promising model among the available models, which can successfully be applied to the arid and semi-arid region in Rajasthan for estimation of evaporation.

1.2 OBJECTIVES OF THE STUDY

The present research study is aimed at to investigate and meet the followings:

1. To derive an analytical solution for estimation of potential and actual recharge from a recharge pond under variable hydrologic conditions,
2. To develop a simple and less data driven rainfall-runoff model for estimating surface runoff yields from a small watershed,
3. To identify a reliable physically based model for estimation of water surface evaporation,

4. To develop an integrated model incorporating the above process level models for estimation of recharge from a pond,
5. To verify the proposed model using generated field data which are required for estimation of runoff, evaporation and groundwater recharge rate,
6. To assess the performance of a pond for recharging groundwater.

1.3 ORGANIZATION OF THE THESIS

The thesis has been organized in eight chapters as follows:

Chapter–1: Introduction

This chapter explains the relevance of the study, the physical processes involved in the artificial groundwater recharge (AGR) from a pond and the difficulties in quantifying the related hydrologic components followed by the objectives of the present study.

Chapter–2: Review of literature

This chapter covers an overview of the AGR and the AGR schemes practiced in India. It also presents a review of the hydrologic components involved in the water balance of a recharge pond and their significance in the context of the groundwater recharge modeling. The chapter also highlights a critical review of the relevant previous investigations related to modeling of the potential and actual recharge, rainfall-runoff, and water surface evaporation.

Chapter–3: Conceptualization of artificial groundwater recharge problem

This chapter gives the conceptualization and the mathematical formulation of research problem to be studied.

Chapter–4: Derivation for potential and actual groundwater recharge

This chapter presents the mathematical derivations, analysis and development of the models to estimate the potential and actual recharge. The Green-Ampt infiltration model and the Hantush's analytical solution for rising water table condition formed the basis in deriving the models for estimation of the potential and actual recharge, respectively. The chapter also includes the results of the performance testing of the derived models.

Chapter–5: Rainfall-runoff modeling of a watershed

This chapter presents the conceptualization and development of a simple rainfall-runoff model for predicting the runoff yields from a small watershed using the basic water balance equation. The model is based on the concept of normalized antecedent precipitation index proposed by Heggen (2001). Analysis of the characteristic behavior of the developed model and its performances in the context of the SCS-CN model and the field data are also discussed in this chapter.

Chapter–6: Estimating water surface evaporation

This chapter includes a detailed analysis of inter-comparison of four commonly used water surface evaporation estimate models based on the field data, and also identifies the best suited model for the semi-arid region in India.

Chapter–7: Integration of runoff, evaporation and recharge components, and Field Application

This chapter deals with the integration of the models derived for rainfall-runoff simulation, estimation of water surface evaporation, and recharge component estimation in the water balance equation of the recharge pond, and brings out the integrated models for simulating the time varying heads of water, the potential and the actual recharge rate. This chapter also discuses about the study area and the data monitored and used for testing and validation of the derived integrated models.

Chapter–8: Conclusions

This chapter summarizes the salient findings of the investigation, and also brings out the conclusions. It also briefs the specific contribution made from the present study.

CHAPTER-2

REVIEW OF LITERATURE

2.1 GENERAL

Groundwater recharge is broadly defined as the water that reaches an aquifer from any direction (down, up, or laterally) (Lerner et al., 1990; Scanlon et al., 2002; Xu and Beekman 2003). In a watershed, it is considered to occur by different ways, either naturally or artificially by human interventions (Lloyd, 1986; Lerner et al., 1990; Scanlon et al., 2002; de Vries and Simmers, 2002; Weeks, 2002; Xu and Beekman, 2003; Small, 2005). Artificial groundwater recharge (AGR), sometimes called planned recharge, is an engineered system generally designed to increase infiltration and store water in an aquifer (O'Hare et al., 1982; Topper et al., 2004; Bower, 2002). Both natural and AGR involve the same basic physical processes, but with some important differences. In artificial recharge, infiltration rate is higher which decreases the period of infiltrated water to reach aquifer than the natural recharge. The AGR involves constraining surface runoff and increasing infiltration to aquifers through construction of recharge structures (Gale et al., 2002). It is an effective tool for augmentation of groundwater resources where; (i) the natural replenishment of groundwater is slow mainly because of low and highly erratic nature of rainfall and geological conditions of aquifer, and (ii) the groundwater levels deplete at a faster rate due to over development (Selvarajan et al., 1995; Greskowiak et al., 2005). These characteristics are normally seen in arid and semi-arid areas. The concept of AGR is not new. It is in use in about 26 countries in different forms for centuries (Helweg, 1985; Asano, 1992; Pyne, 1995; Topper et al., 2004). Its large scale practices are seen in USA, the Netherlands, German and India (Todd, 1980; Oaksford, 1985; Topper, et al., 2004; CGWB, 1994).

India has about 38.8% of its total geographical area (329 million hectares) as semi-arid and 15.1% as arid areas distributed over stretches in the north, northwestern and southern part of the Country. In the arid regions, rainfall is low and highly erratic that ranges from 100 to 420 mm/year, and evaporation varies from 1500 to 2000 mm/year. In the semi-arid regions, the annual rainfall and evaporation vary from 600 to 750 mm and 800 to 1200mm/year, respectively. Groundwater is the main source of water for drinking and irrigation uses in those areas. The Rajasthan state located between 23° 30′ and 30° 11′ north latitude and 69° 29′ and 78° 17′ east longitude in the northwestern part of India constitutes about 40% of total arid and about 9.6% of total semi-arid areas in India. The western part of the State is situated in the Thar Desert. Two major river systems, the Luni and the Chambal, encompass the drainage area of the State. The river and streams of the Luni and the Chambal travel though the Rajasthan state is of ephemeral type. The Luni catchment encompasses the Thar Desert and constitutes the arid region. The Chambal River catchments are comprised of semi-arid region. Monsoon, which occurs from mid June to mid September, is the main source of flow in all these streams. The peculiarity of surface runoffs in all ephemeral streams is that they flow like a flash flood. These types of flow have less time of opportunity to infiltrate water for replenishment of groundwater. Another feature of these river basins is that they follow criss-cross type undulating topography attributing catchment of small watersheds. These characteristics result in very low natural recharge to the aquifer. Yet the groundwater in those areas is being withdrawn continuously to meet demands for different uses. There are reports on significant and consistent drop of water table (1.5 to 9.5m) during past few years (Bose et al., 1998). It has been reported that out of 237 blocks in the State, 212 blocks are facing the problem of depleted groundwater level (Mathur, 2006). Drinking water scarcity during the summer season is a serious problem in most of the rural villages in Rajasthan (Rathore, 2005). To restore the depleting condition of groundwater level, the Central and State governments under the public-private partnership is promoting the AGR as a potential strategy for restoring back the trend of depleted groundwater table and argumentation of groundwater resources. Numerous AGR schemes namely; recharge pond, check dam, furrow, ditch, sub-surface barrier and infiltration galleries are being practiced under the public-private partnership. A number of investigators (Prasad et al., 2008; Rathore 2005) reported the effectiveness of different AGR schemes implemented in many groundwater depleted areas for maintaining and augmenting the groundwater level. Among those recharge schemes, pond is the oldest and is widely practiced in India due to its simplicity and lower operational and maintenance cost. These ponds are commonly known as recharge or percolation pond or tank. In India, pond is known by different names in different States, viz. it is known by *Johad*, *nadi, paal* and *Khadin* in Rajasthan; by *tal* and *bandhara* in Maharastra; by *bundh* in Madhya Pradesh and Utter Pradesh; *by ahar* and *pyne* in Bihar; *by puzhas in Kerala, by oorani* in Andhra Pradesh and by *eris* in Tamil Nadu (Ali et al., 2002). These traditional ponds are serving as an important source of water for people, animal, pisciculture, supplemental irrigation and groundwater recharge.

These ponds are small reservoir, mostly trapezoidal in shape, constructed by excavation of soil or by small earthen dam across the natural stream to catch and hold the surface runoff generated during the monsoon season. The size of these ponds varies between 0.2 and 1.0 ha, and depth ranges from 1.5 to 3m (Ali et al., 2002). Photographs of a small and a medium size pond are shown in Fig. 2.1. These ponds have their own catchment area from which they receive the surface runoffs.

The hydrological components, which characterize the water balance of a pond, are: (i) surface runoff generated from its catchment, (ii) direct runoff over the pond surface, (iii) evaporation from the pond's water surface, (iv) recharge from the pond bed, and (v) outflow from the pond.

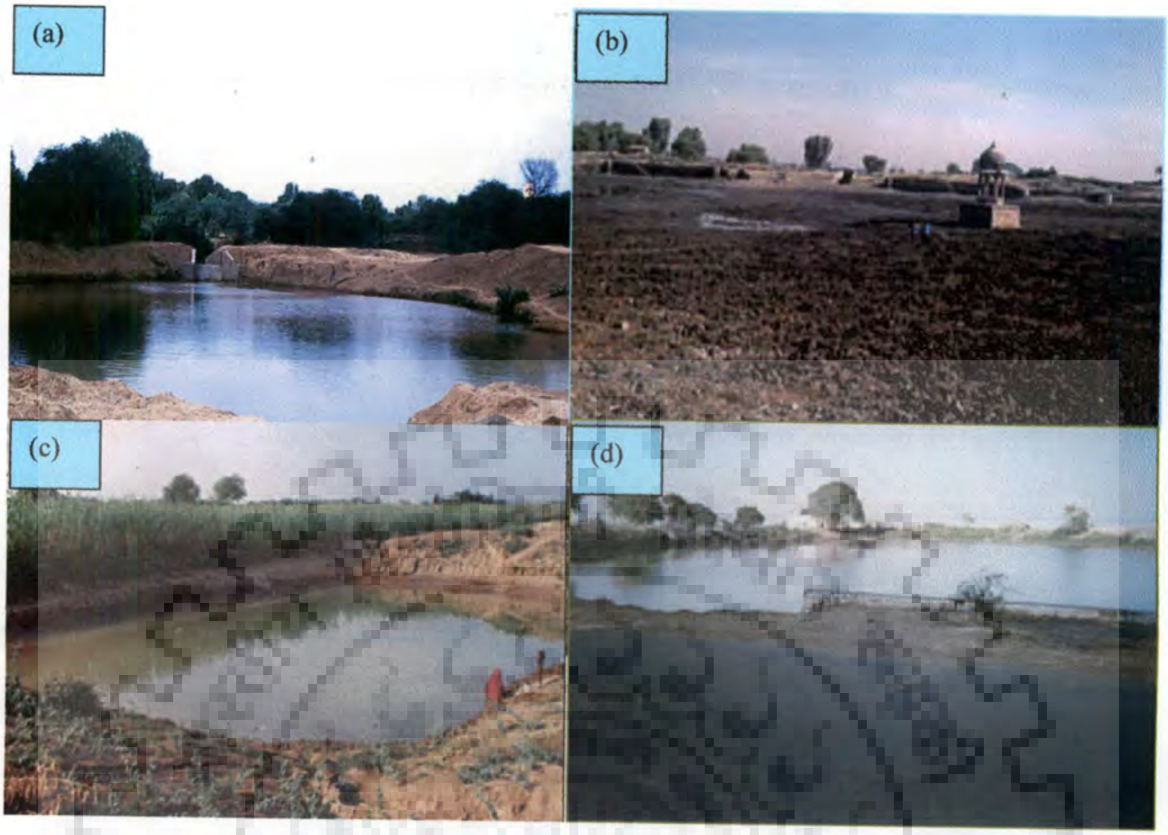

Fig. 2.1. View of recharge ponds in Rajasthan (a) medium size pond with inlet and outlet arrangements in Badakhera watershed, (b) tradition recharge with a temple in Bashyahedi village (c) small size pond in Badakhera watershed, and (d) medium size pond in Chhajawa watershed.

Among the components, surface runoff and evaporation are most important components and its accurate estimation is imperative. Evaporation plays a crucial role particularly for smaller size ponds in the arid and semi-arid regions (Kenabatho and Parida, 2005). Amount of water that received to the pond from its catchment helps in deciding the optimal size and shape of the recharge pond for a given location. Estimation of groundwater recharge from the pond considering all the components is pre-requisite for efficient groundwater resource development and management, and for evaluating the effectiveness of that pond in augmentation of the groundwater resources in a specific location. Keeping the above in view, literature review is focused on groundwater recharge, rainfall-runoff yield and evaporation from a recharge pond. Accordingly, the following sections critically review the significant contributions of various investigators and categorized as:

(i) groundwater recharge ,

(ii) rainfall-runoff modeling,

(iii) evaporation.

2.2 GROUNDWATER RECHARGE

The groundwater recharge process is mainly based on the moisture movement in the unsaturated and saturated zones of the soil. Darcy's law is basis to describe the recharge process. Darcy's law is represented as a relationship between the rate of flow in saturated medium and the hydraulic head gradient. The one-dimensional differential form of Darcy's law (Hillel, 1980) is:

$$q = K_s \frac{\partial h}{\partial z} \tag{2.1}$$

where q is the rate of flow per unit area [LT^{-1}]; K_s is the vertical saturated hydraulic conductivity [LT^{-1}]; h is the hydraulic head [L] and z is the depth below the soil surface [L].

Darcy's law can be extended to unsaturated flow by replacing the saturated hydraulic conductivity K_s term with vertical unsaturated hydraulic conductivity K, which a function of time dependent soil water content, and hydraulic head is changed; $h = z + \psi_f$, and expressed:

$$q = K(\theta) \frac{\partial (z + \psi_f)}{\partial z} \tag{2.2}$$

where $K(\theta)$ is the vertical hydraulic conductivity as a function of water content θ [LT^{-1}]; ψ_f is the pressure head [L].

The pressure head is negative in unsaturated zones of soil ($\psi_f < 0$), whereas it is positive in saturated zone ($\psi_f > 0$). Right at the water table, the pressure head is zero ($\psi_f = 0$). Water pressure heads in unsaturated zone are less than the atmospheric pressure. For this reason, pressure head in the unsaturated zone is also called suction or tension or capillary head (Schwartz and Zhang, 2003)

The recharge has been distinguished as potential and actual recharge by many researchers (Rushton, 1997; Scanlon et al., 2002; de Shilva and Rushton, 2007). The potential recharge is defined as the water that infiltrated through the unsaturated zone of soil which may or may not reach the water table because of unsaturated zone flow processes, while the actual recharge is, that reached the groundwater table. Numerous methods are available to quantify the potential and actual groundwater recharge from the water bodies such as; ponds, reservoirs and lakes (Tracy and Marino, 1987; Lerner et al., 1990; Garg and Ali, 2000; Scanlon et al., 2002; Houston, 2002; Xu and Beekman, 2003; Sharda et al., 2006; Tan et al., 2007; Sarkar et al., 2007). Description of methods of recharge estimation for a variety of climates are presented by Lerner et al.(1990). Scanlon et al.(2002) focused on detailed review of principle and practicalities of assessing groundwater recharge from water bodies, intermittent flow and precipitation. The groundwater recharge estimation methods include: (i) Darcian, (ii) analytical, (iii) numerical, (iv) water balance, (v) empirical (vi) tracer techniques, and (vii) measurements. Each method has its own merits and demerits. Empirical models are usually in the form of an equation. The parameters of the fitted equation are derived by means of curve-fitting to the actual measurement or estimated recharge. They have no apparent physical basis. Empirical models usually relate the recharge to the depth of water, hydro-geological, and meteorological parameters for a specific location (Sharda et al., 2006; Srivastava et al., 2007). There are numerous empirical formulae used to calculate seepage loss from reservoirs and ponds (Kraatz, 1971; Sharda et al., 2006; Srivastava et al., 2007). Empirical methods have limited range of applicability

(Lerner et al., 1990), in the context of (a) difficulty in measurement of variables at other places; (b) their limited range of accuracy in the model structure, (c) difficulty in comparing one method with another due to method-specific model variables, and (d) the limited funds available for data collection. Scanlon et al. (2002) reported that isotopic tracers provide information on recharge sources, however, it is generally difficult to quantify recharge rate. Nair et al. (1980) used the enrichment of deuterium (^{2}H) and Oxygen (^{18}O) in a recharge pond to delineate the area of influenced by the recharge pond in a semi-arid region of India. Some investigators (Sukhija and Reddy, 1987; Sukhija et al., 1997) have demonstrated the usefulness of the chloride (Cl) mass balance method to detect the presence of percolated water in a well situated downstream of a recharge pond. Recharge from water surface bodies can be measured directly by using seepage meter (Kraatz, 1971; Lee, 1977; Lee and Cherry, 1978; Woessner and Sullivan, 1984). This method is inexpensive and easy to apply (Scanlon et al., 2002). The seepage meters provide the point estimates of water flux; measurements may be required at many places to obtain a representative value of seepage (Scanlon et al., 2002). Periodic measurement of change in water level in water bodies is also a simple and direct approach to estimate the recharge from water bodies. In this method, the recorded readings of water level are converted to volume of water by a calculated depth-volume relationship. The volume of water that evaporated from water body is subtracted from the calculated volume of water to get the volume of water that seeps down underneath aquifer. Raju (1985) estimated the ground water recharge from recharge ponds by this method in the southern and western parts of India. Among those, water balance approach is one of the simplest ways to quantify recharge from a water body. The advantages of the water balance approach is that it uses readily available data (rainfall, evaporation), easy to apply, and account for all water component entering and leaving the system. The major disadvantage is that lack of proper consideration each component may lead to error on water balance (Hugo, 2002).

2.2.1 Potential Recharge

Darcy law and continuity equation constitute the basis of physically based potential recharge estimation models through unsaturated soil. Depending on the consideration of dimensions, flow dynamics, hydraulic conductivity, and initial and boundary conditions, numerous physically based infiltration models of varying complexity have been derived, such as: Green-Ampt (1911), Richards' (1931), Philip(1957), Mein and Larson(1971, 1973), Smith (1972), modified Green-Ampt (Morel-Seytoux and Khanji, 1974), Smith and Parlange (1978), and numerical modeling codes such as ; HYDRUS (Simunek et al., 1998), UNSAT-H (Fayer, 2000), TOUGH2 Pruess et al.(1999). Among those, Green-Ampt (GA) (1911) and Richards' equation (1931) are most commonly used model. Between the two, the GA derived from Darcy law for unsaturated zone is most widely used and simple to estimate the length of advancement of wetting front and the potential infiltration. Richards' equation derived from Darcy and continuity equation is usually used for field level studied. Most of the modeling codes have employed the Richards' equation to simulate recharge in unsaturated and variably saturated media (Simunek et al., 1998; Fayer, 2000; Pruess et al.1999). Reeder et al. (1980) reported that the Richards equation (1931) describes satisfactorily the observed flow of soil moisture in a number of laboratory situations, including that of infiltration into well-graded crust dune sand under rapidly varying surface water depth. Warrick et al. (2005) compared the infiltrations estimated by using the solution of Green-Apmt and rigorous numerical solution of Richards equation and noted that the value of cumulative infiltration estimated by Richards flow equation is very close to the value calculated by the Green-Apmt infiltration equation. Govindraraju et al. (1996) reported that the Richards' equation has two disadvantages in present content, namely, analytical solutions are not available for the flow and the numerical solutions are fairly computer intensive. In the present investigation, the GA model is used for the estimation of potential recharge rate.

2.2.1.1 Green-Ampt equation

The Green–Ampt (GA) infiltration model (1911) was the first physically based equation and was developed 98 years ago by the Green and Apmt in 1911 applying the Darcy's law to the wetted zone behind the wetting front(Bouwer, 1978). The GA model assumes one-dimensional vertical flow through homogeneous soil, constant suction head at wetting front, constant saturated hydraulic conductivity behind the wetting front, uniform soil moisture content, initially ponded depth of water and sharp wetting front. It is basically expressed as (Bouwer, 1978):

$$f = k_s\left[1 + \frac{H + \psi_f}{L_f}\right] \tag{2.3}$$

where f is the time dependent potential recharge rate per unit area [LT^{-1}], H is the depth of ponding [L], and L_f is the depth of advancement of wetting front [L].

When H is constant, and replacing f by $\eta\ (dL_f/dt)$, the Eq.(2.3) after integration leads to the well known infiltration equation (Bouwer, 1978):

$$\frac{k_s t}{\eta} = L_f - \left(H + \psi_f\right)\ln\left(1 + \frac{L_f}{H + \psi_f}\right) \tag{2.4}$$

The Eq.(2.4) is an implicit equation of L_f in term of t. Estimation of L_f at a particular time t is a trial and error method and generally obtained using numerical iteration technique, e.g. Newton-Rapson method (Rao et al., 2009) Runge-Kutta method (Enciso-Medina et al., 1998) etc. The GA model has also practical difficulties in application to field conditions, when H is a function of time.

The GA model has been the subject of number of investigations owing to its simplicity and satisfactory performance for a great variety of hydrological problems. The appropriateness of the GA model for predicting water movement in homogeneous unsaturated soil has been studied by Dagan and Bresler (1983) and Govindraraju et al. (1996). Many investigators (Smith, 1972; Bouwer 1978; Freyberg et al., 1980) suggested that GA model is an adequate representation of potential recharge through the porous media particularly when depth of impoundment over an area, riverbed or stream is significant. Analysis of the field data of Bianchi and Haskell (1966) indicated that the Green-Ampt model is adequate to reproduce the field data. Philip (1957) called the GA model as the "delta-function" model.

The GA model was originally developed for idealized conditions (i.e. homogeneous soil and constant ponding depth). Later on the GA model has been extended to take into account more realistic features such as; layered soil, non-uniform moisture, flow of both the water and air. Some important models have been developed based on GA theory by various investigators and are given in Table 2.1.

Table 2.1. Infiltration models based on GA concept.

Investigators	Important features / limitations
Bouwer (1969)	Developed an infiltration model for layered soils. Assumption and limitations of the model are: (1) non-uniform antecedent water content, and (2) constant ponding depth.
Childs and Bybordi (1969)	Proposed an implicit equation for cumulative infiltration in layered soils. Assumption and limitations of the model are : (1) uniform antecedent water content, and (2) constant ponding depth.
Swartzendruber (1974)	Developed infiltration equation for pre-ponding and ponding where, cumulative infiltration is implicitly in time after ponding. Assumption and limitations of the model are: (1) constant surface water flux which is greater than saturated hydraulic conductivity, (2) homogeneous soil, and (3) uniform antecedent water content.
Morel-Seytoux and Khanji (1974)	Modified GA equation by a viscous correction factor β, which is a more complete physically approach to infiltration by the consideration of flow of both air and water. Assumption and limitations of the model are: (1) homogeneous soil, and (3) uniform antecedent water content.

Eagleson (1978)	Developed an infiltration/exfiltration model to estimate the water infiltration during a wetting season and exfiltration during a dry season. Assumption and limitations of the model are: (1) water table depth is much greater than the wetting front depth and root zone depth, (2) soil water content throughout the surface boundary layer is spatially uniform at the start of each storm and at the start of each inter-storm period, (3) vegetation is distributed uniformly and roots extend through the entire volume of soil, and (4) homogeneous soil.
Smith and Parlange (1978)	Developed two parameter models for ponding time and infiltration rate. Assumption and limitations of the model are: (1) arbitrary transient rainfall, (2) homogeneous soil, and (3) uniform antecedent water content.
Philip (1992)	Gave a solution for falling head ponded infiltration. The solution form is the same as GA of constant head infiltration, only the value of constant is changed.
Warrick et al. (2005)	Gave a solution for constant and variable head ponded infiltration. The solution form is the same as GA of constant head infiltration, only the value of constant is changed.

Many other investigators (Salvucci and Entekhabi, 1994; Barry et al., 1995; Serrano, 2003; Chen and Young, 2006; Mailapalli et al., 2009) gave the explicit solution of the GA model in different ways to avoid the trail and error estimation of infiltration. The explicit solution were obtained by rapidly varying power series (Salvucci and Entekhabi, 1994), Lambert W function (Barry et al., 1995), decomposition series (Serrano, 2001, 2003), and nonstandard explicit integration (Ramos, 2007; Mailapalli et al., 2009). A numerous explicit solutions for the GA models have been developed by various authors and given in Table 2.2.

Table 2.2. Explicit solutions of the GA model.

Investigators	Important features / limitations
Li et al. (1976)	Gave an approximate explicit solution for the GA model for calculating infiltration rate and cumulative infiltration as a function of time. Assumption and limitations for the model are: (1) homogeneous soil, (2) uniform antecedent water content, and (3) constant water depth.
Flerchinger et al. (1988)	Developed an implicit equation for cumulative infiltration for layered soils, which is an extension of Li et al. (1976). Assumption and limitations for the model are: (1) constant head at the surface.
Salvucci and Entekhabi (1994)	Gave an explicit solution of GA model for estimating infiltration rate and cumulative infiltration as a function of time. Assumption and limitations for the model are: (1) homogeneous soil, (2) uniform antecedent water content, and (2) constant ponding depth.
Serrano (2001)	Presented an explicit solution of the GA model for the infiltration rate and cumulative infiltration. He noted that a few terms in series provided an accurate estimate. However with any asymptotic series, the decomposition expansion is not universally convergent. Later on, he included more terms in series, new solution improve the result for practical application (Serrano, 2003). Assumption and limitations for the model are: (1) homogeneous soil, (2) uniform antecedent water content, and (3) negligible depth of water on surface.
Chen and Young (2006)	Gave an explicit approximate solution for the GA model to estimate L_f, expending the logarithm term of Eq.(2.9) in power series and retaining the first two terms. Solution has the same mathematical structure as the well known approximation of Philip equation (1957). Assumption and limitations for the model are: (1) homogeneous soil, and (2) uniform antecedent water content, and (3) negligible depth pf water on surface.
Mailapalli et al., (2009)	Developed a procedure which is the explicit approximation of the GA model for cumulative infiltration. Assumption and limitations for the model is: (1) homogeneous soil, (2) uniform antecedent water content, and (3) negligible depth of water on surface.

2.2.2 Actual Groundwater Recharge

Several studies have been carried out in abroad (Baumann, 1952; Bouwer, 1962; Morel-Seytoux, 1984, 1985; Abdulrazzak and Morel-Seytoux, 1983, 1997; Gua, 2001;) and very few in India (Mishra and Ghosh, 2002; Mishra and Fahimuddin, 2005; Fahimmuddin et al., 2009) for quantifying the actual recharge that actually reached to water table. The various analytical and numerical solutions are also available in literature for seepage/recharge estimation from different shapes of a channel (Morel-Seytoux, 1964; Sorman, and Abdulrazzak 1993; Chahar, 2006), canals (Goyal and Chawala, 1997; Swammee et al., 2000; Chahar, 2007) and array of channels/canals (Chaudhary and Chahar, 2007). Numerous analytical solutions based on the Boussinesq equation with various assumed initial and boundary conditions have been derived to predict the rise and fall of groundwater mound due to constant (Baumann, 1952; Glover, 1960; Hantush, 1967; Hunt, 1971; Sharma and Rao 1980; Molden et al. 1984) and variable artificial recharge (Latinopoulos, 1984; Rai and Singh, 1992, 1995; Abdulrazzak and Morel-Seytoux, 1983; Morel-Seytoux, 1984; Rai and Manglik, 1999; Morel-Seytoux et al., 1990; Sarkar et al., 2007) from recharge basin of circular or rectangular in shape. Most of these, analytical solutions have not been used for practical applications because the solutions often involve complex integral functions, which are poorly behaved and also computationally extensive (Molden et al. 1984). Of those, Hantush (1967) approximate solution to predict the rise and fall of groundwater mound due to constant recharge through rectangular and circular basins has been found used extensively.

Baumann (1952) gave an expression for estimating the volume of recharge water underneath the recharge mound of a circular recharge basin. Bouwer (1962) developed an equation for transmitted flux of water at the water table. Morel-Seytoux (1984) presented a simple expression based on the flow of water in unsaturated soil for conversion of infiltration rate (potential recharge) to the actual recharge rate. Abdulrazzak and Morel-

Seytoux (1983) developed an analytical solution based on the Darcy's law for one dimensional recharge rate from the recharge basin (recharge stream). They reported that observations from laboratory experimental and theoretical results showed excellent match for as long as the ratio of the width of recharge basin (river bed) over the depth to water table exceeds 2.5, and as long as the ratio of the initial saturated thickness over the depth to water table exceeds 2.5. Morel-Seytoux et al., (1990) also proposed an expression using the flow net approach for the both constant and variable recharge rate from a circular basin through unsaturated zone. The mathematical formulation gave an integro-differential equation whose solution was obtained numerically using the discrete kernel approach. Mishra and Ghosh (2002) have given a model to compute variable recharge rate from a rectangular and trapezoidal water body for varying surface water depth developing kernel coefficients by Duhamel's principle on the Hantush's analytical equation (1967). Gua (2001) derived an axially symmetric potential flow model to estimate the location of wetting front, volume of water recharge and mounding depth through the unsaturated zone under a circular infiltration basin. He reported that the application of the model for prediction of seepage rate and saturation depth below the circular basin agreed with the MODFLOW model.

2.3 RAINFALL-RUNOFF MODELING

Surface runoff is the excess rainfall that can not be absorbed by the ground surface as infiltration and depression storage. It depends on the climatologic and hydrologic variability viz. intensity and duration of rainfall, evapotranspiration and watershed's geomorphologic properties viz. topology, soil type, vegetation, slope, antecedent soil moisture (Istok and Boersma, 1986; Garg, 1987). The involvement of these factors and many of their combinations make the rainfall-runoff process very complex, dynamic, and non-linear process (Jain and Indurthy, 2003; Wang et al., 2007). The origin of the rainfall-runoff (RR) modeling dates back to the rational method developed by Mulvany (1850) and an event model by Imbeau (1892) relating peak runoff to rainfall intensity. About four decade later, Sherman (1932) introduced the hydrograph concept relating the direct runoff response to the rainfall excess. About the same time, Horton (1933) developed a theory of infiltration to estimate rainfall excess and improved the hydrograph separation technique. Later on, many investigators have studied rainfall-runoff (RR) modeling (SCS 1956; Boughton, 1968, 1984; Haan, 1972; Knudsen et al., 1986; Wilcon et al., 1990; Haan et al. 1995; Mishra and Singh, 1999; Mishra et al., 2005; Jain et al., 2006; Ali et al., 2009). The common methods for determining the runoff are based on the statistical, physical process and /or combined approaches. These modeling approaches differ in terms of mathematical representation of physical process, complexity, applicability, spatial descritization of the watersheds and data requirements. Statistical methods are the black box model, which includes simple linear (Mockus, 1949) and multiple linear and non-linear multiple regression (Chiew et al., 1993; Tsykin, 1985; Basha, 2000; Jain and Indurthy, 2003), autoregressive moving average (ARMA) model, and ARMAX models with periodic parameters and transfer function (Haltiner and Salas, 1988). Physically based processes level RR models involve the use of partial differential equation representing various physical process, and equation of continuity for surface and soil water flow (Boughton, 1968; Freeze and Harlan, 1969; Abbott et al., 1986; Beven et al., 1987). Process based approach of the RR modeling has wide application being based on the fundamental physical relationship and distributed parameters (Wang et al., 2007). Several conceptual RR models have been developed in the past and used by many investigators (Amorocho and Hart, 1964, Haan, 1972; Sorooshian, 1983; Boughton, 1984; Knudsen et al., 1986). The last decade witnessed usages of artificial neural networks (ANNs) approach that has proven a promising tool for modeling rainfall-runoff process as a black box model (Bishop 1994; ASCE 2000). Several ANN, and RR models developed in recent years (Lorrai and Sechi 1995; Dawson and Wibly, 1998; Sajikumar and Thadaveswara, 1999, Tokar and Johnson, 1999, Hsu et al., 2007) had shown encouraging results (Campolo et al., 1999; Jain et al., 1999). Many investigators (Weeks and Hebbert, 1980; Chiew et al., 1993; Jain, and Indurthy, 2003) compared the rainfall-runoff models, varying in complexity with the ANN modeling approaches.

The processes based and conceptual RR models require a large amount of data for calibration and validation purposes, and they are computationally extensive (Chiew et al. 1993; Jain and Indurthy, 2003). These data types are commonly found missing particularly for small and un-gauged watersheds. As a result, most of these models have restricted uses (Grayson et al., 1992). To this end, several less data driven and simple RR models have been developed and used (SCS, 1993, Heggen, 2001; Mishra et al., 2005). Among those, Soil Conservation Service-Curve Number (SCS-CN), and antecedent precipitation index (API) based model are widely used models for practical applications.

2.3.1 Soil Conservation Service-Curve Number (SCS-CN)

The SCS-CN model is one of the most widely used models for computing runoff from a given rainfall event in small agricultural watersheds (Ponce and Hawkins 1996). This method was developed by Soil Conservation Service (SCS) of USDA (United State Department of Agriculture) (now Natural Resources Conservation Service, NRCS) for estimating runoff volume and peak rate of runoff in the un-gauged watersheds based on the measured rainfall and physical features of the watershed. Since its development in 1954, the SCS method has undergone numerous refinements including extension from agricultural to urban areas (Rallison 1980). Rallison and Cronshey (1979) have given some historical insight into its development. Ponce and Hawkins (1996) have provided a critical review of the method, its limitation and usefulness. The reason for its wide application includes simplicity, ease of use and widespread acceptance (Garen and Moore, 2005).

The SCS-CN model is based on the water balance equation and two hypotheses. The water balance relating rainfall and losses is given by (SCS, 1956, 1985; 1993):

$$Q = P - I_a - F \tag{2.5}$$

The SCS-CN model employs the hypothesis of proportional equality (Mishra and Singh, 2004):

$$\frac{Q}{P - I_a} = \frac{F}{S} \tag{2.6}$$

and hypothesis of relation between initial abstraction and potential maximum retention:

$$I_a = \lambda S \tag{2.7}$$

where Q is the direct runoff, P is the precipitation, I_a is the initial abstraction F is the cumulative infiltration, S is the maximum potential retention, and λ is the initial abstraction coefficient. The P, Q, and S are in depth dimension, while λ is dimensionless.

Combination of Eqs. (2.6) and (2.7) into Eq.(2.5) leads to the popular form of the existing SCS-CN model (SCS, 1986):

$$Q = \frac{(P - \lambda S)^2}{P + (1 - \lambda)S} \tag{2.8}$$

The parameter S depends on land use, land treatment, hydrological soil group, hydrologic condition and AMC and it varies as, $0 \leq S \leq \infty$. The λ is viewed as a regional parameter depending on geologic and climatic factors (Boszany, 1989), and usually varies in between 0 and 0.3 (Bosznay, 1989), whereas $\lambda = 0.2$ is a standard value for practical application (SCS, 1985; Schneider and McCuen, 2005). For each combination of land use, land treatment, hydrological soil group, and hydrologic condition, a number is assigned which is known as curve number. Curve number (CN) is an index of runoff producing potential. The parameter 'S' is mapped on to CN as (SCS, 1986):

$$S = \frac{25400}{CN} - 254 \tag{2.9}$$

where S is in mm, and CN is dimensionless that varies in range of $0 \leq CN \leq 100$. The CN has no intrinsic meaning; it is only a convenient transformation of S to establish a 0-100 scale (Hawkins, 1978).

The CN = 100 represents a condition of zero maximum potential retention (S = 0), that is, an impermeable watershed; on the contrary, CN = 0 represents a theoretical upper bound to maximum potential retention ($S = \infty$), that is, an infinitely abstracting watershed. However, the practical values lie in the range (40, 98) (Van and Mullem, 1989). Combination of the value of S and λ into Eq.(2.8) yields:

$$Q = \frac{25.4\left[\frac{P}{25.4} - \frac{200}{CN} + 2\right]^2}{\left[\frac{P}{25.4} + \frac{800}{CN} - 8\right]} \tag{2.10}$$

It is valid for:

$$P > 0.2S \quad \text{or} \quad P > \frac{5080}{CN} - 50.80 \tag{2.11}$$

The precision of the SCS-CN model depends on the accurate estimation of the curve number 'CN'. The CN value for a given soil series, land use and land treatment can be determined using standard tables developed by the NEH (National Engineering Handbook, NEH-4) through analysis of watershed data (SCS 1985). The Curve number values reported in the NEH-4 (SCS 1985) are for the antecedent soil moisture condition-II (AMC-II), which is one of the three conditions established to account for the generation of runoff at the time of occurrence of a storm event. The CN values for AMC-I and AMC-III are calculated as (Lewis et al. 2000):

$$CN(I) = \frac{4.2\, CN(II)}{10 - 0.058\, CN(II)} \tag{2.12}$$

$$CN(III) = \frac{23\, CN(II)}{10 + 0.13\, CN(II)} \tag{2.13}$$

Since its inception, the SCS-CN model has been applied successfully in hydrology, watershed management and environmental engineering such as; long term hydrologic simulation (Knisel, 1980; Young et al., 1985; Leonard et al., 1986), prediction of infiltration and rainfall excess (Mishra and Singh, 2004), sediment yield modeling (Mishra and Singh, 2004, Mishra et al., 2006) and determination of subsurface flow (Yuan et al., 2001). It has also been successfully applied to distributed watershed modeling (White, 1988; Moglen, 2000; Mishra and Singh 2004). Springer et al. (1980) stated that one of the major weaknesses of the SCS-CN model is the absence of calibration using experimental watershed data.

2.3.2 API and NAPI Based Model

Several models based on the concept of antecedent moisture condition (AMC) have been proposed by investigators (Sittner et. al., 1969; Heggen, 2001; Mishra et al., 2005). The AMC is descried using (i) antecedent precipitation index (API), (ii) normalized antecedent precipitation index (NAPI), (3) antecedent base flow index (ABFI), and (4) soil moisture index (SMI) (Heggen, 2001; Mishra et al., 2005; Jain et al., 2006). All these indices are primarily based on the amount of antecedent rainfall. Out of these models, the API based models are simple, easy to use and widely practiced in the field (Mishra et al., 2005; Jain et al, 2006). Many investigators (Xia et al., 1997; Heggen, 2001) reported that the API based models enhanced the efficiency of non-linear forecasting models. The API based models work on limited data but have limitations to represent physical conditions (Fedora and Beschta, 1989; Rose, 1998; Descroix et al., 2002; Dowson and Abrahat, 2007),which restrict their straightforward use to all field conditions.

To overcome the paradoxes of the API based models, Heggen (2001) proposed a NAPI based lumped rainfall-runoff model as improvement to the API based model. Mathematically, the model is expressed as:

$$\frac{Q}{P} = 1 - e^{a + b\,P + c\,NAPI} \tag{2.14}$$

where NAPI is dimensionless; a, b, and c are watershed specific parameters, in which a and c are dimensionless, and b has the dimension of $[L^{-1}]$.

Heggen (2001) suggested that NAPI modifies the conventional API in three aspects: inclusion of antecedent precipitation earlier in the day of the event, normalization to the station mean, and normalization to the antecedent series length. The NAPI suggested by Heggen (2001) is defined as ratio of the API extended to precipitation on the day, but before the storm, to the average daily precipitation multiplied by the weighted sum due to decay constant in respective day. Mathematically, it is given by:

$$NAPI = \frac{\sum_{t=0}^{-i} P_t\, k^{-t}}{\bar{P} \sum_{t=-1}^{-i} k^{-t}} \tag{2.15}$$

where i is an integer number of antecedent days; k is the decay constant; P_t is the rainfall during t day; and $\bar{P}$ is the average rainfall in the antecedent days. 'i' is usually taken as 5, 7 or 14 days (Garg, 1987; Viessman and Lewis, 1996) and k ranges between 0.80 and 0.98 (Viessman and Lewis 1996).

Although the Heggen's model has promising potential for its use, however, lacks in physical explanation to its mathematical structure, and needs verification in the context of widely used SCS-CN model.

2.4 EVAPORATION

Surface water evaporation depends on meteorological viz., solar radiation, temperature, humidity, wind speed and atmospheric pressure, and geometrical factors viz. shape, size, and depth of water. It is difficult to assess quantitatively the relative importance of each of the factors. According to Knapp et al. (1984), evaporation is sensitive to water temperature, and is a significant amount of water that loose by ponds and storage tanks by the process of evaporation (Szumiec, 1979).

The earliest attempts to explain the evaporation process involving the principles of vapor pressure was proposed by Dalton in 1802(Dalton, 1802). Later on, an authentic description and observations on different philosophers and thinkers about evaporation were given by Brutsaert (1982). There exist numerous methods for measurement and estimation of evaporation (Brutsaert, 1982; Benson, 1986; Singh, 1989; Shuttleworth, 1993; Morton, 1990, 1994; Panu and Nguyen, 1994; Winter et al., 1995; Singh and Xu, 1997; Ali et al., 2008). These methods include: (i) empirical (Kohler et al., 1955; Singh and Xu, 1997), (ii) water budget (Guitjens, 1982; Abtew, 2001), (iii) energy budget (Sturrock et al., 1992; Sack et al., 1994), (iv) mass transfer (Harbeck, 1962), (v) combination of energy and mass (Penman, 1948; Priestly and Taylor, 1972) and (vi) measurements (Young, 1947). These methods vary from one to another in terms of: types of data requirement, range of applicability, structural and parametric differences and cost involved in collection of required data. For example, empirical methods although relate pan evaporation, actual evaporation or lysimeter measurements to meteorological factors, but these are site specific as they have been developed based on observations within one region. The water budget methods are considered to be simple in theory, but rarely produce reliable results for short period evaporation estimate (Singh, 1989; Morton, 1990; Singh and Xu, 1997; Abtew, 2001). The energy budget methods are considered to be accurate and reliable (Anderson, 1954; Harbeck, 1962; Gunaji, 1968; Barry and Robertson, 1975; Winter, 1981; Benson, 1986; Stauffer, 1991; Sturrock et al., 1992) up to the accuracy of ±5% of the mean evaporation when all other individual components are measured with care and measurement periods are one week or longer (Anderson, 1954). The energy budget methods are data intensive and hence considered to be very costly. The mass transfer methods have been reported to give satisfactory results in many cases (Thornthwaite and Holzman, 1939; Jensen, 1973). These methods are considered relatively accurate alternatives and less expensive than the energy budget methods (Harbeck, 1962; Hosteler and Bartlein, 1990; Rosenberry et al., 1993). However, the success of these methods depends on the accuracy of the mass transfer coefficient, which is normally determined by calibration against an independent method of measuring evaporation (Rosenberry et al., 1993). The Penman combination methods have similar advantages and problems as of the energy budget methods. Several empirical equations derived based on the mass transfer approach by various authors is given in Table 2.3. Singh and Xu (1997) reported that vapour pressure deficit has been the most dominant factor in the mass transfer approach in estimating monthly evaporation, while wind speed remained an insignificant factor.

Table 2.3. Evaporation estimate methods based on the mass transfer concept.

Investigators	Mass transferred based formulae
Dalton (1802)	$E(in/month) = a(e_s - e_a)$; where E is the rate of evaporation, a =15 for small shallow water, and a = 11 for large deep water.
Fitzgerald (1886)	$E(in/month) = (0.4 + 0.199U)(e_s - e_a)$; where e_s is the saturated vapour pressure at water temperature, e_a is the actual vapour pressure, , and U is the wind speed.
Meyer (1915)	$E(in/month) = 11(1 + 0.1U)(e_s - e_a)$
Horton(1917)	$E(in/month) = 0.4[(2 - \exp(-2U))(e_s - e_a)]$
Rohwer(1931)	$E(in/day) = 0.77(1.465 - 0.0186P_b)(0.44 + 0.118U)(e_s - e_a)$; where P_b is the barometric pressure in inch of Hg

Penman(1948)	$E(in/day)=0.35(1+0.24U_2)(e_s-e_a)$
Harbeck et l.(1954)	$E(in/day)=0.0578U_8\ (e_s-e_a)\ E(in/day)=0.0728U_4\ (e_s-e_a)$
Kuzmin (1957)	$E(in/day)=6.0(1+0.21U_8)(e_s-e_a)$
Harbeck et al. (1958)	$E(in/day)=0.001813U\ (e_s-e_a)(1-0.03(T_a-T_w))$; where T_a and T_w are the average air and water temperature (^{0}C), respectively.
Romanenko (1961)	$E(cm/month)=0.0018(T_a+25)^2\ (100-RH)$; where RH is the relative humidity in percentage.
Papadakis (Winter et al., 1995)	$E(cm/day)=0.5625[e_a(T_{max})-e_a(T_{min})-2]$; where $e_0(T_{max})$ and $e_0(T_{min})$ are actual vapour pressure at maximum and minimum air temperature, respectively [mbars]

The wind speed (monthly mean) U is measured in miles per hour and vapour pressures e_a/e_s in inches of Hg. The subscripts to U refer to height in meters at which the measurements are taken and no subscript refers to measurements near the water surface or the ground.

Energy budget approach is similar to water budget approach, where the conservation equation is applied to energy instead of mass. It is expressed as:

$$R_n + H_a + H_b - H_e - H_s - H_w = G \tag{2.16}$$

where R_n is the net radiation, H_a is the net heat energy advected to the water body by stream flow, groundwater and precipitation, H_b is the heat transfer to the water from the bottom sediments, H_e is the heat energy used for evaporation, H_s is the heat energy conducted from the water body as sensible heat, H_w is the heat energy advected from the water body by the evaporated water, and G is the change in heat energy content of the water body. All units are in MJm^{-2}day^{-1}.

Anderson (1954) derived evaporation equation from the surface energy balance using the relationship among the H_e, H_s and H_w, (Sack et al., 1994; Strurrock et al., 1992; Rosenberry et al., 1993) as:

$$E = \frac{R_n - (G - H_a - H_b)}{\rho_w \lambda(1+\beta) + c_w(T_0 - T_b)} \tag{2.17}$$

where, ρ_w is the density of evaporating water(kg m^{-3}), λ is the latent heat of vaporization, β is the Bowen ratio, c_w is the specific heat of water, T_o is the temperature of evaporating water, and T_b is the arbitrary base temperature (^{0}C).

Later on, many investigators (Simon and Mero, 1985; Assouline and Mahrer, 1993; Reis and Dias, 1998) considered the reduced form of Eq.(2.17) by neglecting H_b and H_a and found their effects below 7% of the annual evaporation. The reduced form of Eq.(2.17) is:

$$E = \frac{R_n - G}{\lambda(1+\beta)} \tag{2.18}$$

Many investigators have derived evaporation estimation models from both the energy budget and mass transfer approach, and called combined approach (Penman, 1948; Abtew, 2001). The concept of combined approach is relatively new. Penman (1948) first utilized the best feature of energy balance and mass transfer approaches. These methods are convenient because they require meteorological information from one level only. Hence, the combination methods are widely used in hydrology (Thom and Oliver, 1977). Many investigators have suggested improvements to the original Penman method; some of the important accepted modified methods are the FAO-24 Penman method (Doorenbos and Pruitt, 1977), the Penman-Montieth method (Montieth, 1965), the Kohler- Nordenson-Fox method (Kohler et al., 1955), Kohler-Parmele (1967), Priestley-Taylor (1972), Morton (1979) .

Priestley-Taylor (1972) has proposed a simplified form of the combined component of radiation and aerodynamics, with a coefficient, α , greater than 1.0, as a multiplier. Stewart et al. (1976) have proposed a simple method to estimate evaporation from temperature and radiation measurements. This modification was done in order to make the equation less sensitive to differences in land and lake based environments. Morton again in 1990 proposed a method known as CRLE, which is very similar to the Priestley-Taylor (PT) method. A brief descriptions of some of the most commonly used evaporation rate estimation methods are presented in Table 2.4.

Table 2.4. Evaporation estimate methods based on combined approach of energy balance and mass transfer concept.

Investigators	Equation
Penman (1948) Abtew (2001)	$E(mm/day)=\frac{1}{\lambda}\left[\frac{\Delta}{\Delta+\gamma}\right](R_n-G)+\frac{1}{\lambda}\left[\frac{\gamma}{\Delta+\gamma}\right][6.43(a_w+b_wU_2)(e_s-e_a)]$; where Δ is the slope of saturated vapour pressure at water temperature verses temperature curve(kpa $^0C^{-1}$), U_2 is the wind speed at 2m height(m/s), a_w and b_w are the empirical wind coefficients.
Priestley-Taylor (1972)	$E(mm/day) = \frac{1}{\lambda}\alpha\left[\frac{\Delta}{\Delta+\gamma}\right](R_n-G)$; where α is the Priestley-Taylor's coefficient, usually consider as 1.26.
Morton (1983)	$E(mm/day) = \frac{b_1}{\lambda}+\frac{b_2}{\lambda}\left[\frac{\Delta}{\Delta+\gamma}\right](R_n-G)$; where b_1 = 13 W m^{-2} and b_2 = 1.12.
deBruin-Keijman (1978)	$E(mm/day)=\frac{1}{\lambda}\left[\frac{\Delta}{0.85\Delta+0.63\gamma}\right](R_n-G)$
deBruin(1979)	$E=\frac{1}{\lambda}\left(\frac{\alpha}{\alpha-1}\right)\left[\frac{\gamma}{\Delta+\gamma}\right](2.9+2.1U_2)(e_s-e_a)$
Brutsaert-Stricker (1979)	$E=\frac{1}{\lambda}(2\alpha-1)\left[\frac{\Delta}{\Delta+\gamma}\right](R_n-G)+\left[\frac{\gamma}{\Delta+\gamma}\right]\{0.26(0.5+0.54U_2)(e_s-e_a)\}$

The Pan Evaporation method is one of the simplest, inexpensive, and most widely used methods for estimating evaporation rate. The use of the pan data involves the application of a pan coefficient to measure pan readings to estimate evaporation from a larger water body. Morton (1990) presented a review of the evaporation measurement methods. The last decade witnessed a new technique for estimate of evaporation, called artificial neural networks (ANN). Some typical studies have been done (Kumar, et al., 2002) by modeling daily evapo-transpiration using ANN.

The number models developed so far for estimation of evaporation rate are so huge; selection of an appropriate model for a particular region is a difficult task. There have been several comparative studies on evaporation estimate models (Winter et al., 1995; Singh and Xu, 1997; Hussein, 1999; Kashyap and Panda, 2001; Abtew 2001). Winter et al.(1995) studied performances of eleven evaporation models in a study of a small lake in the north central United States; Singh and Xu (1997) compared thirteen mass transfer method and suggested seven generalized models for determining the monthly evaporation in Atikkokan, Lansdown, Pickle Lake and Rawson Lake located in north-western Ontario, Canada. Abtew (2001) by evaluating performances of seven evaporation models namely; pan evaporation, energy balance, water budget, Penman combination, modified Turc, Priestly-Taylor and Mass transfer methods based on solar radiation and maximum air temperature suggested a simple model.

A critical appraisal of different evaporation estimate methods/models indicated that each method has its own merits and limitations. The method that has been found giving precise estimation of evaporation for most cases needs huge databases which are difficult and expensive to monitor. On the other hand, the method that requires relatively less data, which can be monitored on routine basis with less effort, has been performed weakly to produce desired results to many other cases. Thus, selection an appropriate evaporation model largely depends on the data availability, quality of data and the purpose for which it is to be used. As such, no definite guidelines have been derived for selecting an area specific evaporation model.

2.5 WATER BALANCE STUDY OF POND

Many investigators have used the water balance method for estimation of groundwater recharge from lake (Winter, 1981; Pennequien and Anderson, 1983; Goyal et al., 2003), reservoirs (Sharma, 1985; Al-Muttair and Al-Turbak 1989), and percolation ponds (Raju, 1985; Sharma, 1985; Sukhija et al., 1997; Shinogi et al., 1998; Sharda et al., 2006). Quinn (1978) modeled the hydrological response of the unregulated parts of the North American Great Lake by using water balance concept. Stuff and Dale (1978) used water balance methods for prediction of soil moisture and rise in groundwater level. Pennequin and Anderson (1983) studied the groundwater budget of Lake Wingra, Wisconsin, by measuring groundwater inflow to and out from the lake using in-lake and onshore piezometers. Nath and Bolte (1998) developed a water balance simulation model for forecasting water requirement in an aquaculture pond at Asian institute of Technology, Bangkong. Panigrahi and Panda (2001) carried out the water balance study of a rice field and reported that seepage is an extremely variable factor depending on soil texture, water head variation, soil hydraulic conductivity, cultural and water management practice. Goyal et al. (2003) estimated the groundwater contribution to the Mansar lake system in Jammu and Kasmir, India using the water balance approach. Kebede et al. (2006), in their study on the water balance study of Lake Tana in Ethiopia, estimated all the water balance components separately and then integrated to simulate the lake depth variation on monthly basis. Pandey et al. (2006) developed a water balance model to study the availability of rainwater in a pond for irrigation and picsiculture purposes. de Silva and Rushton (2007) estimated the groundwater recharge using the water balance approach based on single soil layer. Sivaprgasam et al. (2009) have studied the water balance of a reservoir using genetic programming technique, and reported that seepage and evaporation formed the vital components of the water balance study. Many investigators (Sharma, 1984; Al-Muttair and Al-Turbak, 1989; Sharda et al., 2006; Ganji et al., 2008) used only the evaporation term in the water balance equation for estimating the recharge. A quantitative analysis of recharge from a pond has also been studied by Yadav and Keshari (2006) using water balance approach.

2.6 CONCLUSIONS

From the literature review, following conclusions are drawn.

1) Literature has been reviewed in the context of the hydrological and hydrogeological components of an artificial recharge scheme focusing mainly towards previous investigations on groundwater recharge estimation modeling, rainfall-runoff modeling, and evaporation modeling.

2) The Green-Ampt (GA) infiltration model is extensively used, because of its computational simplicity, for estimation of the potential groundwater recharge from surface water storage of constant depth. The GA model has the difficulty to estimate of length of wetting front even for the constant depth of water. For time variant depth of water, its computation becomes more complicated.

3) The Hantush's approximate analytical solution for rise and fall of groundwater table due to constant recharge from rectangular basin is found to be successfully used to estimate the actual recharge for time variant depth of water. It has the potential to be used for variable recharge areas also.

4) The normalized antecedent precipitation index (NAPI) based model proposed by Heggen as an improvement over the API based model, for estimation of runoff yields from rainfall events, has promising potential for its use to limited databases as compares to other widely used rainfall-runoff models. The Heggen's lumped model lacks in physical explanation to its parameters, and needs verification in the context of the widely accepted model to establish its credibility.

5) The selection of a suitable and reliable model for estimation of evaporation, particularly for semi-arid region, needs a rigorous analysis in the context of their data requirement, range of applicability, structural and parametric differences and cost involved in collection of the required data.

6) Studies related to estimate of artificial groundwater recharge integrating process based hydrological models to the comprehensive water balance equation are scarcely available in literature.

CHAPTER-3

PROBLEM CONCEPTUALIZATION

3.1 GENERAL

Groundwater recharge process is primarily governed by the soil moisture movement in the unsaturated zone, and the Darcy's law is the basis to describe its physical connotation. Mechanics of groundwater recharge is a two-fold infiltration process: the first phase of infiltration process begins with the advancement of wetting front through the unsaturated zone in the form of vertical percolation of water, and continues till it reaches the underneath water table, known as potential recharge. The potential recharge rate at a given time depends on the difference of heads of water above the recharge pond *(herein after referred to as pond)* and the depth of wetting front below the bed of the pond at that time, and the underneath soil properties, namely; saturated hydraulic conductivity and porosity. The second phase begins just immediately after the wetting front touches the water table and its continuance due to the subsequent recharges, known as actual recharge. During this process because of subsequent recharges, the groundwater table may evolve. The actual recharge rate, in such case, depends on the potential difference of heads of water between the pond and the increased water table position below the bed, and the underneath soil properties. The potential difference of heads in both the cases being time varying, the potential recharge and the actual recharge rates are also time-variant.

The head of water in a pond is exhibited by the inflows it receives in the form of surface runoffs and direct rainfalls, and the outflows release from its storage in the form of the water surface evaporation, excess surface runoff and the groundwater recharge. The surface runoffs into the pond depend on the climatologic and hydrologic variability viz. intensity and duration of rainfall, evapotranspiration and watershed's geomorphologic properties viz. topology, soil type, vegetation, slope, antecedent soil moisture. The water surface evaporation depends on meteorological viz., solar radiation, temperature, humidity, wind speed and atmospheric pressure and geometrical factors viz. shape, size, and depth of water of the pond. The outflows of surplus runoffs and rainfalls from the pond depend on its capacity (shape, size and depth) and the quantity of runoffs and rainfalls it receives. The surface runoffs, water surface evaporation, and rainfalls being time variant and continuous simultaneous process; the depth of water in the pond is also a time variant. Even after the recession of runoffs and rainfalls, groundwater recharge and evaporation take place as a continuous simultaneous process.

3.2 STATEMENT OF THE PROBLEM

Let a recharge pond be of trapezoidal in shape, as shown in Fig. 3.1, has its own watershed area. Let the pond be initially empty; and the groundwater table located in an unconfined condition over an impervious stratum at a large depth below the pond's bed is also initially under static condition. Let the soil below the pond be homogeneous and isotropic. A schematic diagram of the components involved in the water balance of the pond and conceptualization of the variables are shown in Fig. 3.1. Let the runoff rate per unit area of the catchment into the recharge pond be Q [LT^{-1}], the rainfall rate over the pond be P [LT^{-1}], the evaporation rate from the water surface of the pond be E [LT^{-1}], the volumetric rate of outflow of surplus water from the pond be Q_o [LT^{-3}], the groundwater recharge rate through the pond's wetted surface area *be* R [LT^{-1}], the depth to water table below the pond's bed be D_w [L], and the depth of impervious stratum below the groundwater table be h_0 [L].

Let consequent to the surface runoffs, Q into and rainfalls, P onto the pond, the depth of water instantaneously be increased to H_1 at time t = 0. Due to which, the infiltration and thereby the recharge, and the water surface evaporation continued as a simultaneous process. Let H_2 be the reduced depth of water in the pond at time, 't +Δt' and ΔH be the change in the water level in the pond at time, $\{(t+\Delta t)-t = \Delta t\}$. Let s be the rise in the static groundwater table consequent to the continuance of Q, P, E and R, after the wetting front touches it. It is required to be derived expressions for determining the potential and the actual recharge rates resulting from the time varying continuance of Q, P, E and Q_0.

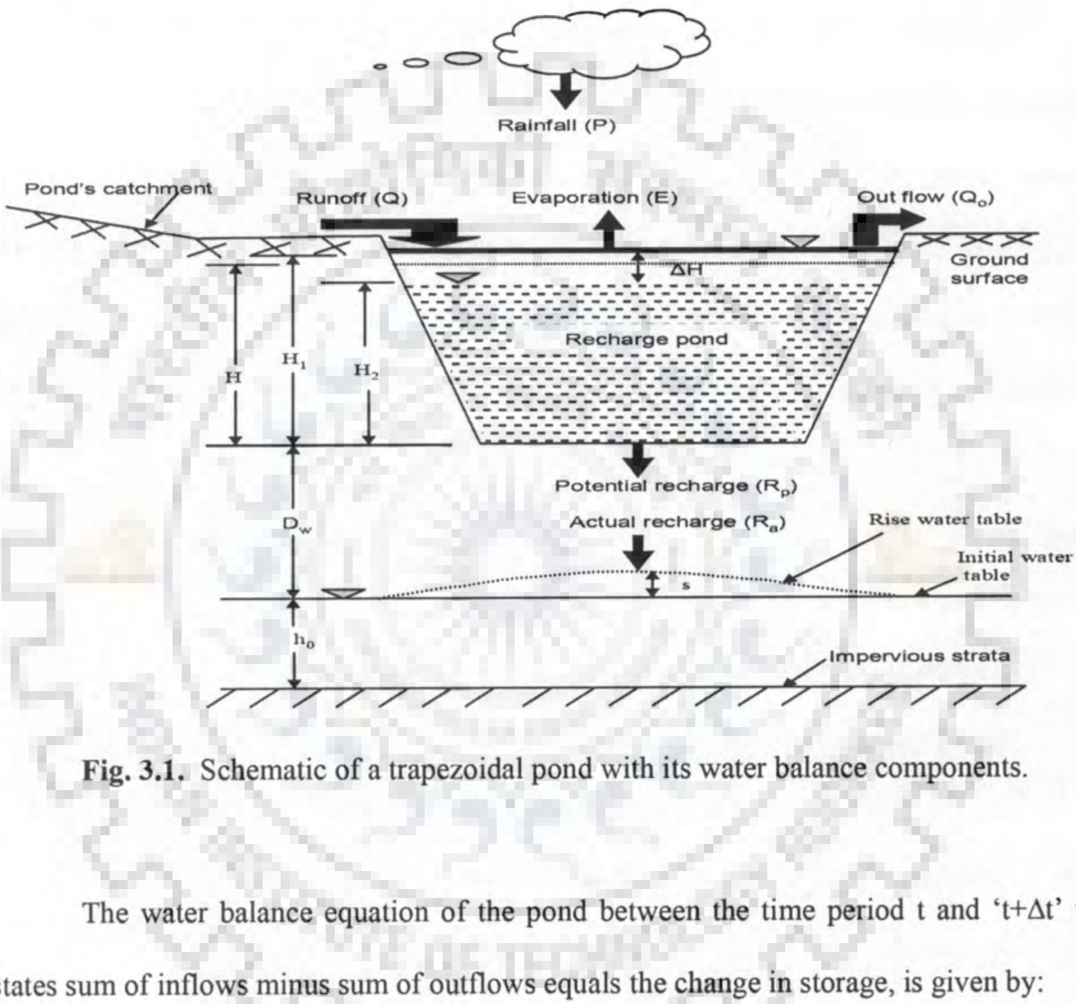

Fig. 3.1. Schematic of a trapezoidal pond with its water balance components.

The water balance equation of the pond between the time period t and 't+Δt' that states sum of inflows minus sum of outflows equals the change in storage, is given by:

$$\overline{A}_{ws}\ \Delta H + H\ \Delta A_{ws} = Q\ A_w\ \Delta t + P\ A_s\ \Delta t - E\ \overline{A}_{ws}\ \ \Delta t\ - Q_0\ \Delta t - R\ \overline{A}_{rs}\ \Delta t \tag{3.1}$$

where ΔH is the change in head of water in the pond between t and 't+Δt', [L], in this case it is = H_1 - H_2; ΔA_{ws} is the change in water surface area of the pond between t and 't+Δt', [L^2] = [$A_{ws}(1)$ - $A_{ws}(2)$]; A_w is the area of the pond's catchment [L^2]; A_s is the surface area of the pond at the top [L^2]; $\overline{A}_{ws}$ is the average water surface area between t and 't+Δt', [L^2], = $0.5[A_{ws}(1)+ A_{ws}(2)]$; $\overline{A}_{rs}$ is the average wetted surface area of the pond between t and 't+Δt', [L^2] = $0.5[A_{rs}(1)+ A_{rs}(2)]$; and all other terms are time varying components of variables defined earlier.

Incorporating functional relationships of Q(t) from rainfall-runoff processes, E(t) from water surface evaporation processes in Eq.(3.1); the expression for the change in heads of water, ΔH(t) and the corresponding recharge rate, R(t) can be derived in terms of P(t) and $Q_0(t)$. Knowing geometrical dimensions of the recharge pond, initial conditions of the state variables and using measured values of P(t) and $Q_0(t)$ in the integrated expressions, the equations for estimate time varying heads of water and the corresponding recharge rates can be found.

The investigations are thus envisaged to:

(i) develop the rainfall-runoff model to compute Q(t),

(ii) identify suitable water surface evaporation model to compute E(t),

(iii) develop models for computing the potential and the actual recharge rates, and finally

(iv) develop the integrated model by incorporating the above three models in Eq.(3.1), for computation of the time varying potential and actual recharge rates.

CHAPTER-4

DERIVATION FOR POTENTIAL AND ACTUAL GROUNDWATER RECHARGE

4.1 GENERAL

In a recharge pond, as water starts accumulating it infiltrates immediately and moves gradually downward creating a wetting front. Continuous process of infiltration and percolation advances the wetting front till it reaches the groundwater table. After the wetting front reaches the groundwater table, the recharge to the groundwater starts. The rate of advancement of wetting front and recharge mainly depends on the unsaturated zone soil properties, and the potential difference of heads between the pond and the saturated front. Numerous models describing the moisture movement in the unsaturated zone are available to estimate the advancement of wetting front, the potential and actual recharge. Amongst those, the Green-Ampt (GA) (1911) and the Richards' equation (1931) are well recognized and widely used. The Richards' equation contains two highly non-linear functions related to the soil water potential, the unsaturated hydraulic conductivity, and the soil water content. The analytical solutions of the Richards' equation are limited to simplified descriptions of the unsaturated hydraulic properties that require verification. It is postulated by many investigators (Chapter-**2.2.1.1**) that the GA model is adequate for estimate of the potential recharge through the porous media particularly when the depth of impoundment over an area is significant.

The potential recharge at a given time is the product of derivate of wetting front length and porosity, and the actual recharge rate is the same as given by the Darcy's equation under saturated condition. Estimation of the length of the wetting front by the GA model is a trial and error method, and its estimation becomes more cumbersome and complicated when head varies. It thus necessitates requirement of an explicit equation for estimation of time varying length of the wetting front, which is simple to use and also preserves the characteristics of the GA model.

4.2 STATEMENT OF THE PROBLEM

Let us consider a rectangular recharge pond of significant size initially with no water. The soils below the pond bed are homogeneous and isotropic, and their textural properties are known. The groundwater table is at a large depth below the pond bed and is horizontal. The pond suddenly receives water and its level rises to a steady state condition. Consequent to that the infiltration process begins simultaneously. The infiltration from the pond to the subsurface takes place through its bed along the vertical direction only. As the wetting front advances and reaches the groundwater table the aquifer becomes hydraulically connected and its level starts evolving. The aquifer is assumed to be unconfined. The time is reckoned since the onset of the infiltration process.

It is required to be derived expressions for estimating the advancement of wetting front, time varying potential recharge, time for the wetting front to reach the water table, and the time varying actual recharge consequent to the rise in the ground levels.

4.3 DERIVATION FOR POTENTIAL RECHARGE

The infiltration process through a soil column as conceptualized in the Green-Ampt model is shown in Fig. 4.1. Let H be the depth of ponding [L]; ψ_f be the suction head at the wetting front (negative pressure head) [L]; L_f be the length of the advancement of wetting front [L]; θ_i be the initial volumetric moisture content [dimensionless]; and θ_s be the volumetric moisture content at near saturation [dimensionless]. The wetting front is the interface between the wetted and non-wetted zone. The infiltration process is, thus considered to be a piston flow and the Darcy's law is applicable.

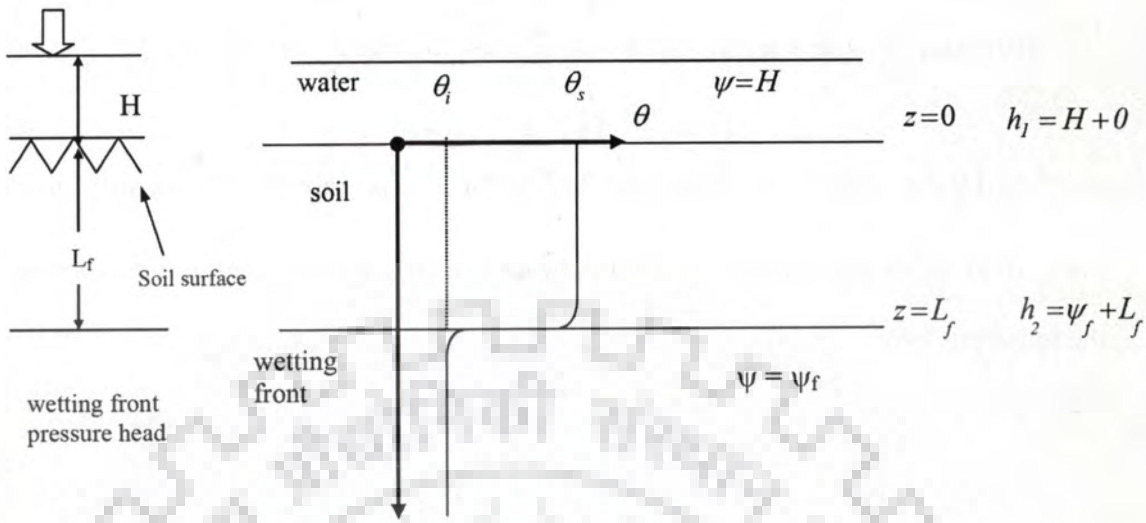

Fig. 4.1. Parametric and volumetric water content profile as conceptualized in the Green-Ampt model.

The GA model with the above parametric descriptions in terms of length of advancement of the wetting front, L_f can be written as:

$$\frac{K_s}{\eta} t = L_f - \left(H + \psi_f\right) ln\left[1 + \frac{L_f}{H + \psi_f}\right] \tag{4.1}$$

in which, K_s is the saturated hydraulic conductivity of the transmission zone, $\lfloor LT^{-1} \rfloor$; and η is the porosity = θ_s - θ_i . Eq. (4.1) clearly indicates that for known value of H, K_s, η, and ψ_f, it requires a hit and trial to calculate L_f for any time, t.

The potential recharge rate, R_p in terms of L_f is given by:

$$R_p = \eta \left(dL_f / dt\right) \tag{4.2}$$

The logarithm term in Eq.(4.1) for $\left|\left\{L_f / \left(H + \psi_f\right)\right\}\right| \leq 1$ can be expressed as:

$$ln\left[1+\left(\frac{L_f}{H+\psi_f}\right)\right]=\left(\frac{L_f}{H+\psi_f}\right)-\frac{1}{2}\left(\frac{L_f}{H+\psi_f}\right)^2+\frac{1}{3}\left(\frac{L_f}{H+\psi_f}\right)^3-\frac{1}{4}\left(\frac{L_f}{H+\psi_f}\right)^4+\ldots.. \quad (4.3)$$

For $\left|\{L_f/(H+\psi_f)\}\right|>1$, the series described by Eq.(4.3) is not valid. The logarithmic term in Eq. (4.1) for all practical purposes can be approximated by a second order polynomial of the following form:

$$ln\left[1+\left(\frac{L_f}{H+\psi_f}\right)\right] \approx A_i+B_i\left(\frac{L_f}{H+\psi_f}\right)+C_i\left(\frac{L_f}{H+\psi_f}\right)^2 \quad (4.4)$$

where, A_i, B_i and C_i are the coefficients of the polynomial whose value depend on the logarithmic distribution of the operating variable $\left|\{L_f/(H+\psi_f)\}\right|$, and are to be determined; suffix *'i'* refers an integer number.

Substituting Eq. (4.4) into Eq.(4.1) leads to:

$$L_f^{\,2}-\left[\frac{(1-B_i)(H+\psi_f)}{C_i}\right]L_f+\left[\frac{K_s\,(H+\psi_f)}{C_i\eta}\,t+\frac{A_i\,(H+\psi_f)^2}{C_i}\right]=0 \quad (4.5)$$

Eq.(4.5) is a quadratic equation of L_f, whose roots are:

$$L_f=\frac{\left[\frac{(1-B_i)(H+\psi_f)}{C_i}\right]\pm\sqrt{-\frac{4K_s\,(H+\psi_f)}{C_i\eta}\,t+(H+\psi_f)^2\left[\left(\frac{1-B_i}{C_i}\right)^2-\frac{4A_i}{C_i}\right]}}{2} \quad (4.6)$$

Taking the positive root, and simplifying:

$$L_f=\sqrt{-\frac{K_S\,(H+\psi_f)}{C_i\eta}\,t+(H+\psi_f)^2\left[\left(\frac{1-B_i}{2C_i}\right)^2-\frac{A_i}{C_i}\right]}+\left[\frac{(1-B_i)(H+\psi_f)}{2\,C_i}\right] \quad (4.7)$$

The rate of advancement of the wetting front, $\left(\frac{dL_f}{dt}\right)$, which is the seepage rate, R_s, is given by:

$$R_s = \frac{dL_f}{dt} = \frac{\left[-\dfrac{K_s\left(H+\psi_f\right)}{2C_i\eta}\right]}{\sqrt{-\dfrac{K_s\left(H+\psi_f\right)}{C_i\eta}\ t+\left(H+\psi_f\right)^2\left[\left(\dfrac{1-B_i}{2C_i}\right)^2-\dfrac{A_i}{C_i}\right]}} \tag{4.8}$$

The potential recharge rate, R_p is given by:

$$R_p = \eta\, R_s = \frac{\left[-\dfrac{K_s\left(H+\psi_f\right)}{2C_i}\right]}{\sqrt{-\dfrac{K_s\left(H+\psi_f\right)}{C_i\eta}\ t+\left(H+\psi_f\right)^2\left[\left(\dfrac{1-B_i}{2C_i}\right)^2-\dfrac{A_i}{C_i}\right]}} \tag{4.9}$$

The depth of ponding, H may vary due to variable inflows and outflows. The change in H with respect to time, will change the magnitude of L_f, in turn, R_s and R_P. The derivation of L_f, Rs and R_P for variable $H(t)$, for such cases, are given by:

$$L_f(t) = \sqrt{-\frac{K_s\left[H(t)+\psi_f\right]}{C_i\eta}\ t+\left[H(t)+\psi_f\right]^2\left[\left(\frac{1-B_i}{2C_i}\right)^2-\frac{A_i}{C_i}\right]} + \left[\frac{(1-B_i)\left[H(t)+\psi_f\right]}{2\,C_i}\right] \tag{4.10}$$

$$R_s(t) = \frac{\left[-\dfrac{K_s\left[H(t)+\psi_f\right]}{2C_i\eta}\right]}{\sqrt{-\dfrac{K_s\left[H(t)+\psi_f\right]}{C_i\eta}\ t+\left[H(t)+\psi_f\right]^2\left[\left(\dfrac{1-B_i}{2C_i}\right)^2-\dfrac{A_i}{C_i}\right]}} \tag{4.11}$$

and,

$$R_p(t) = \frac{\left[-\dfrac{K_s\left[H(t)+\psi_f\right]}{2C_i}\right]}{\sqrt{-\dfrac{K_s\left[H(t)+\psi_f\right]}{C_i\eta}\ t+\left[H(t)+\psi_f\right]^2\left[\left(\dfrac{1-B_i}{2C_i}\right)^2-\dfrac{A_i}{C_i}\right]}} \tag{4.12}$$

where $L_f(t)$, $R_s(t)$ and $R_P(t)$ are the time varying component of L_f, R_s and R_p, respectively.

Discretizing t by n number of integer time step size, Δt, such that $t = n\Delta t$, where $n = 1, 2, 3, 4......$; Eqs. (4.10), (4.11) and (4.12) can, respectively be written as:

$$L_f(n\Delta t) = \sqrt{-\frac{K_s\left[H(n\Delta t)+\psi_f\right](n\Delta t)}{C_i\eta} + \left[H(n\Delta t)+\psi_f\right]^2\left[\left(\frac{1-B_i}{2C_i}\right)^2-\frac{A_i}{C_i}\right]} + \left[\frac{(1-B_i)\left[H(n\Delta t)+\psi_f\right]}{2\,C_i}\right] \quad (4.13)$$

$$R_s(n\Delta t) = \frac{\left[-\frac{K_s\left[H(n\Delta t)+\psi_f\right]}{2C_i\eta}\right]}{\sqrt{-\frac{K_s\left[H(n\Delta t)+\psi_f\right](n\Delta t)}{C_i\eta} + \left[H(n\Delta t)+\psi_f\right]^2\left[\left(\frac{1-B_i}{2C_i}\right)^2-\frac{A_i}{C_i}\right]}} \quad (4.14)$$

and,

$$R_p(n\Delta t) = \frac{\left[-\frac{K_s\left[H(n\Delta t)+\psi_f\right]}{2C_i}\right]}{\sqrt{-\frac{K_s\left[H(n\Delta t)+\psi_f\right](n\Delta t)}{C_i\eta} + \left[H(n\Delta t)+\psi_f\right]^2\left[\left(\frac{1-B_i}{2C_i}\right)^2-\frac{A_i}{C_i}\right]}} \quad (4.15)$$

In Eqs. (4.13), (4.14) and (4.15); $H(n\Delta t)$ is a time variable unknown at which $L_f(n\Delta t)$, $R_s(n\Delta t)$ and $R_P(n\Delta t)$ are to be determined. $H(n\Delta t)$ can be obtained by solving the water balance equation in succession of time interval.

4.3.1 Derivation of Time for Wetting Front to Reach Water Table

Let T_d be the time delay for the wetting front, L_f to reach the water table, and D_w be the depth to water table below the pond. T_d can be obtained by substituting $L_f = D_w$ and $t = T_d$ in Eq. (4.7). Rearranging Eq. (4.7) with the substituted parameters, T_d is given by:

$$T_d = \frac{\eta}{K_s}C_i\left(H+\psi_f\right)\left[\left(\frac{1-B_i}{2C_i}\right)^2-\frac{A_i}{C_i}\right] - \frac{\eta}{K_s}C_i\left(H+\psi_f\right)\left[\frac{D_w}{H+\psi_f}-\frac{1-B_i}{2C_i}\right]^2 \quad (4.16)$$

where A_i, B_i and C_i are the coefficients of the second order polynomial.

4.4 DERIVATION FOR ACTUAL RECHARGE

The derivation given by Eq.(4.9) for estimation of R_p is valid till the wetting front reaches the water table. As the wetting front reaches the water table, the suction head, ψ_f becomes zero, and the potential recharge becomes the actual recharge. For a constant head and with no rise in the underneath groundwater table, the actual recharge per unit area, R_a is given by:

$$R_a = K_s\left(1 + \frac{H}{D_w}\right) \text{, where } D_w = \text{depth to groundwater table.} \tag{4.17}$$

In real life problems, as the wetting front reaches the water table and if the recharge process continued, the groundwater level evolves, creating mound with its peak below the centre of the recharge pond. The rate of evolving of groundwater level depends on the soil properties above the groundwater level. Rise in the groundwater level reduces the potential difference of heads that governs the recharge rate. Further, the variation of H would also change the recharge rate.

A schematic of a rectangular recharge pond hydraulically connected to the underneath unconfined aquifer is shown in Fig.4.2. Let 'L' be the half of the length, and 'W' be the half of the width of the recharge pond, H_L be the depth of impervious strata measured below the pond bed, h_0 be the initial groundwater level measured from the impervious strata, h be the rise in groundwater level measured from the impervious strata and s be the rise in groundwater level above the initial position.

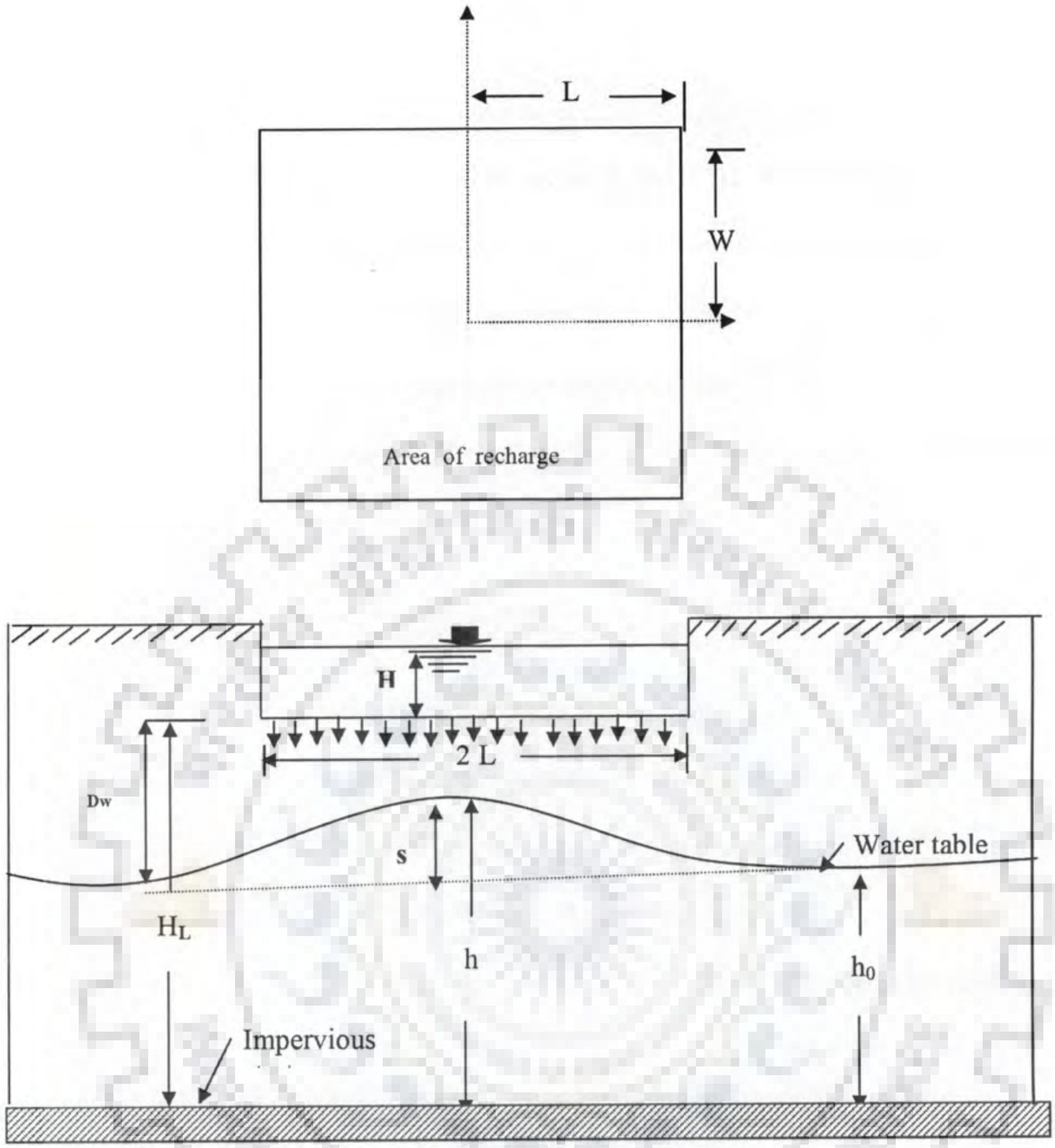

Fig. 4.2. Schematic plan and section of a rectangular recharge pond.

The head difference between the height of water above the pond bed and the depth of groundwater level below the pond's bed, Δh_a, is:

$$\Delta h_a = [H_L + H] - [h_0 + s] = D_w + H - s \tag{4.18}$$

Applying the Darcy's law, the recharge rate is given by:

$$q_a = K_s A_{rs} \left[\frac{D_w + H - s}{D_w} \right] \tag{4.19}$$

where q_a is the volumetric recharge rate from the pond [L^3 T^{-1}); and A_{rs} is the recharge area of the pond [L^2] $= 2L \, x \, 2W$; and s is the rise in the water table to be determined.

Hantush (1967) has given the following approximate analytical expression for the rise and fall of water table underneath an infinite unconfined aquifer in response to uniform percolation from a rectangular spreading basin:

$$h^2 = h_0^2 + \left(\frac{w\bar{h}\,t}{2\phi}\right)\left\{\begin{array}{l} F\left[\dfrac{L+x}{\sqrt{4K\bar{h}\,t/\phi}},\dfrac{W+y}{\sqrt{4K\bar{h}\,t/\phi}}\right]+F\left[\dfrac{L+x}{\sqrt{4K\bar{h}\,t/\phi}},\dfrac{W-y}{\sqrt{4K\bar{h}\,t/\phi}}\right] \\ +F\left[\dfrac{L-x}{\sqrt{4K\bar{h}\,t/\phi}},\dfrac{W+y}{\sqrt{4K\bar{h}\,t/\phi}}\right]+F\left[\dfrac{L-x}{\sqrt{4K\bar{h}\,t/\phi}},\dfrac{W-y}{\sqrt{4K\bar{h}\,t/\phi}}\right]\end{array}\right\} \tag{4.20}$$

or

$$h^2 = h_0^2 + \left(\frac{w\bar{h}\,t}{2\phi}\right) f(x,\ y,\ t) \tag{4.21}$$

in which, $\bar{h}$ = weighted mean of the depth of saturation during the period of flow[L]; w = constant rate of recharge/percolation [LT^{-1}]; ϕ = storage coefficient of the aquifer[dimensionless]; K = hydraulic conductivity or coefficient of permeability of the aquifer material[LT^{-1}]; time, t is reckoned since wetting front touches the water table, i.e., $t = 0$ at $L_f = D_w$, and $F(p,q) = \int_0^1 erf(p/\sqrt{z}).erf(q/\sqrt{z})\,dz$; and $erf(x) = \frac{2}{\sqrt{\pi}}\int_0^x e^{-u^2}du$.

Assuming $\bar{h} \approx \frac{h_0 + h}{2}$, Eq.(4.21) yields:

$$h - h_0 = \left(\frac{w\,t}{4\phi}\right) f(x,\ y,\ t) \tag{4.22}$$

The rise in the water table, s is given by:

$$s(x,y,t) = \left(\frac{w\,t}{4\,\phi}\right) f(x,\ y,\ t) \tag{4.23}$$

The average rise in the water table, $\bar{s}$, under the recharge pond consequent to uniform recharge from its bed that has the water spread area [$2L \times 2W$], can be written as:

$$\bar{s} = \frac{1}{2}\left[\left(\frac{w\,t}{4\phi}\right) f\,(0,\,0,\,t) + \left(\frac{w\,t}{4\phi}\right) f(L,\,W,\,t)\right] \tag{4.24}$$

Let $U(t)$ be the unit step response function for the rise in water table corresponding to unit recharge rate per unit area per unit time, i.e., $w = 1$ [LT^{-1}]. The unit step response function is given by:

$$U(t) = \left(\frac{t}{8\phi}\right)[f\,(0,\,0,\,t) + f\,(L,\,W,\,t)] \tag{4.25}$$

Let δ_s (t) be the unit pulse response function. The unit pulse response function due to unit recharge rate per unit area per unit time, which takes place during the first time period, Δt, and no recharge afterwards, is given by:

$$\delta_s(\Delta t) = \frac{1}{\Delta t}[U(t) - U(t - \Delta t]] \tag{4.26}$$

where $\delta_s(\Delta t)$ is the unit pulse response function for rise in water table.

Let the time domain be descritised by time step, Δt; $t = \gamma\,\Delta t$; and $\gamma = 1, 2, 3 \ldots\ldots n$; and n is the number of integer time step. Let the recharge from the bed of the pond be approximately equal to a train of pulses. Let $q_a(\gamma)$ be the recharge rate from the pond during $(\gamma - 1)\,\Delta t$ to $(\gamma\,\Delta t)$.

The average rise in water table height consequence to a train of pulse recharge can be derived using Duhamel's principle as:

$$s(n\Delta t) = \sum_{\gamma=1}^{n} \frac{q_a(\gamma)\Delta t}{(4\,L\,W)}\ \ \delta_s\,[\,n - \gamma + 1,\ \ \Delta t] \tag{4.27}$$

The Hantush's discrete kernel coefficients are given by:

$$\delta_s(m,\ \Delta t)=\frac{1}{\Delta t}\left\{\begin{array}{l}\frac{m\,\Delta t}{8\phi}\ [\,f(0,\ 0, m\,\Delta t)+f(L,\ W, m\,\Delta t)\,] \\ -\frac{(m-1)\,\Delta t}{8\phi}[\,f(0,\ 0,(m-1)\Delta t)+f(L,W,(m-1)\Delta t)\,]\end{array}\right\} \tag{4.28}$$

From Eq.(4.19), the recharge rate from the pond during time, Δt is:

$$q_a(n\Delta t)\ =\ (4\,L\ W)K_s\left[\frac{D_w\ +\ H\ -\ s(n\Delta t)}{D_w}\right] \tag{4.29}$$

Substituting Eq.(4.27) in Eq.(4.29), yields:

$$q_a(n\Delta t)\ =(4\,L\,W)\,K_s\left\{\frac{D_w+H\ -\sum_{\gamma=1}^{n}\frac{q_a(\gamma\Delta t)}{(4\,L\,W)}\ \delta_s\,[\,n-\gamma+1,\Delta t\,]\,\Delta t}{D_w}\right\} \tag{4.30}$$

Eq.(4.30) can be re-written as:

$$\frac{q_a(n\Delta t)}{(4LW)\,K_s}D_w=D_w+H-\left[\sum_{\gamma=1}^{n-1}\frac{q_a(\gamma\Delta t)\,\Delta t}{(4LW)}\ \delta_s[\,n-\gamma+1,\Delta t]+\frac{q_a(n\Delta t)\,\Delta t}{(4LW)}\ \delta_s[\,1,\ \Delta t]\right] \tag{4.31}$$

Rearranging Eq.(4.31) yields:

$$q_a(n\Delta t)=\frac{(4\,L\,W)\,K_s\ \left[D_w+H\ -\sum_{\gamma=1}^{n-1}\frac{q_a(\gamma)\,\Delta t}{(4\,L\,W)}\ \delta_s[\,n-\gamma+1,\ \Delta t]\right]}{D_w\ +\ K_s\ \Delta t\ \delta_s\,[\,1,\ \Delta t\,]} \tag{4.32}$$

Rate of recharge per unit area, R_a is obtained as:

$$R_a(n\Delta t)=\frac{K_s\left[D_w+H\ -\sum_{\gamma=1}^{n-1}\frac{q_a(\gamma\Delta t)\,\Delta t}{(4\,L\,W)}\ \delta_s[\,n-\gamma+1,\ \Delta t]\right]}{\left[D_w\ +\ K_s\ \Delta t\ \delta_s\,[\ 1,\ \Delta t\ ]\right]} \tag{4.33}$$

Knowing $L,\ W,\ K_s, D_w,\ K,\ \phi$ and h_0, the recharge rate from a rectangular pond for constant H can be computed using Eq.(4.33).

4.4.1 Recharge from Variable Recharge Area

The water spread area may change with time due to fluctuation of water depth in the recharge pond, such as, for trapezoidal pond. The derivation given in Eq.(4.33) can also be extended for variable recharge area.

Let 2L (γ), and 2W (γ) be the length and the width respectively corresponding to the variable head, H (γ), where $\gamma = 1, 2, 3......n$. The length and the width of the water spread area during 1st, 2nd and nth unit time period would respectively be (2L(1), 2W(1)), (2L(2), 2W(2)) ......(2L (n), 2W(n)). Let δ_s(L(1), W(1), m), δ_s(L(2), W(2), m) ......δ_s(L(n), W(n), m); m = 1, 2, ...n be the unit pulse response coefficients, which can be generated using Eq.(4.27).

The water table rise below the recharge pond can also be expressed as:

$$s(n\Delta t) = \sum_{\gamma=1}^{n} \frac{q_a(\gamma\Delta t)\Delta t}{[4L(\gamma)W(\gamma)]} \delta_s[L(\gamma), W(\gamma), n-\gamma+1, \Delta t] \tag{4.34}$$

and, recharge rate from the pond is given by:

$$q_a(n\Delta t) = \frac{[4L(n)W(n)]K_s\left[D_w + H(n\Delta t) - \sum_{\gamma=1}^{n-1} \frac{q_a(\gamma\Delta t)\Delta t}{[4L(\gamma)W(\gamma)]} \delta_s[L(\gamma), W(\gamma), n-\gamma+1, \Delta t]\right]}{D_w + K_s \Delta t\, \delta_s[L(n), W(n), 1, \Delta t]} \tag{4.35}$$

And, recharge rate per unit area of the pond is,

$$R_a(n\Delta t) = \frac{K_s\left[D_w + H(n\Delta t) - \sum_{\gamma=1}^{n-1} \frac{q_a(\gamma\Delta t)\Delta t}{[4L(\gamma)W(\gamma)]} \delta_s[L(\gamma), W(\gamma), n-\gamma+1, \Delta t]\right]}{[D_w + K_s \Delta t\, \delta_s[L(n), W(n), 1, \Delta t]]} \tag{4.36}$$

Knowing K_s, D_w, K and h_0, ϕ, and by computing $L(n)$ and $W(n)$ corresponding to $H(n)$, the rate of recharge from water spread area that changes with time can be estimated using Eqs (4.35) and (4.36).

4.5 RESULTS AND DISCUSSION

4.5.1 Potential Recharge

The derivation of L_f, R_s, and R_p is given by Eqs. (4.7), (4.8) and (4.9) respectively, contains three external coefficients, A_i, B_i, and C_i of the second order polynomial (Eq.4.4) approximated in place of the logarithmic term representing $ln(1+x)$, where $|x| = \left|\left\{L_f/\left(H+\psi_f\right)\right\}\right|$. The values of the coefficients A_i, B_i, and C_i (i represents segment number) are obtained by numerical experiments. For numerical experiment, synthetic values of $ln(1+x)$ for different x, $/x/> 0$, are generated. These generated data represent the distribution of $/x/$ versus $ln(1 + x)$. These data are thereafter utilized to fit to the second-order polynomial. The values of the coefficients corresponding to the best-fit are considered to be the value of A_i, B_i, and C_i. The coefficient of determination, R^2, and the standard error of estimate, *SE*, are chosen as the decision variables, i.e., higher the value of R^2 (close to 1) and lower the value of SE (close to zero), better is the approximation. Equation for R^2 and SE is given in the Appendix-A. It is found that the logarithmic distribution is fitted closely to the second order polynomial(Eq.4.4) in five segments; for operating variable, (i) $/x/\leq 1$; (ii) $1 < /x/ \leq 5$; (iii) $5 < /x/ \leq 15$; (iv) $15 < /x/ \leq 50$; *and* (v) $/x/ \geq 50$. The estimated values of A_i, B_i, and C_i corresponding to the fitted segments for different $|x|$ and the values of the decision variables are given in Table 4.1. It can be seen from Table 4.1 that for all the five cases, $R^2 \geq 0.9986$ and SE $\leq$ 0.015; that indicates a close agreement between the logarithmic distribution and the derived polynomials. Responses of the estimated A_i, B_i, and C_i of the respective segment as given in Table 4.1, for different ranges of $|x|$ are compared with corresponding responses of $ln(1+x)$, and the comparison is shown in Fig.4.3. It is evident from Fig.(4.3) that both the distributions match closely. To assess the agreement and the biasness between the two distributions, the index of agreement (D) and the relative biasness (RB) are calculated and their values are given in Table 4.2.

The equation of D and RB is given in the Appendix-A. Higher the value of D (close to 1), and lesser the value of RB (close to zero), superior is the agreement. Table 4.2 indicates D $\approx$ 1, and RB $\leq \pm 0.0128$ for different ranges of $/x/$. It can also be seen from Table 4.2 that the derived polynomials slightly underestimate (RB<0) the values for $1< /x/ \leq 50$ and slightly overestimate for $/x/ \leq 1$ and $|x| \geq 50$ than the values described by $ln(1+x)$. The profile of the percentage relative errors (PRE) between the two series showing the deviation of the second order polynomials with respect to the logarithmic distribution for different ranges of $/x/$ is given in Fig. 4.4. The PRE (Fig. 4.4) shows a maximum error of ±1% between the values of the polynomials and the logarithmic distribution. These five segmental polynomials can be considered as approximated derivations of $ln\{1+L_f/(H+\psi_f)\}$ of the GA model for all ranges of $|\{L_f/(H+\psi_f)\}| > 0$.

Table 4.1. Estimated values of the coefficients of the second order polynomials (Eq.4.4) fitted to the $ln(1+x)$ of the GA model for different ranges of operating variable, $/x/ = |\{L_f/(H+\psi_f)\}|$ and their statistical values.

Segment range	Coefficient of polynomial			R^2	SE
	A_i	B_i	C_i		
$\vert x\vert \leq 1$	0.0047	0.9277	-0.2403	0.9999	0.0015
$1 < \vert x\vert \leq 5$	0.2505	0.4919	-0.0371	0.9986	0.0142
$5 < \vert x\vert \leq 15$	0.9778	0.1884	-0.0046	0.9996	0.0053
$15 < \vert x\vert \leq 50$	1.9395	0.0651	-0.0005	0.9992	0.0089
$\vert x\vert \geq 50$	3.0197	0.0215	-0.00006	0.9997	0.0044

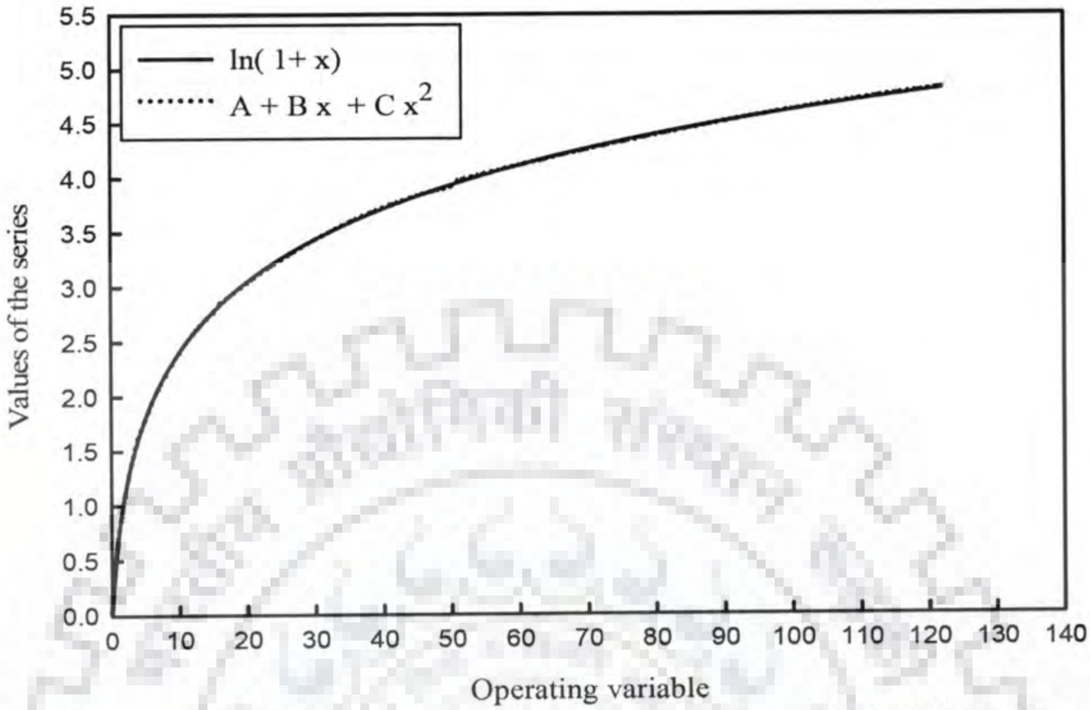

Fig. 4.3. Comparison of the responses of the second order polynomial (Eq.4.4) and the logarithm term of the GA model for operating variable, $/x/ = \left|\{L_f/(H+\psi_f)\}\right| > 0$.

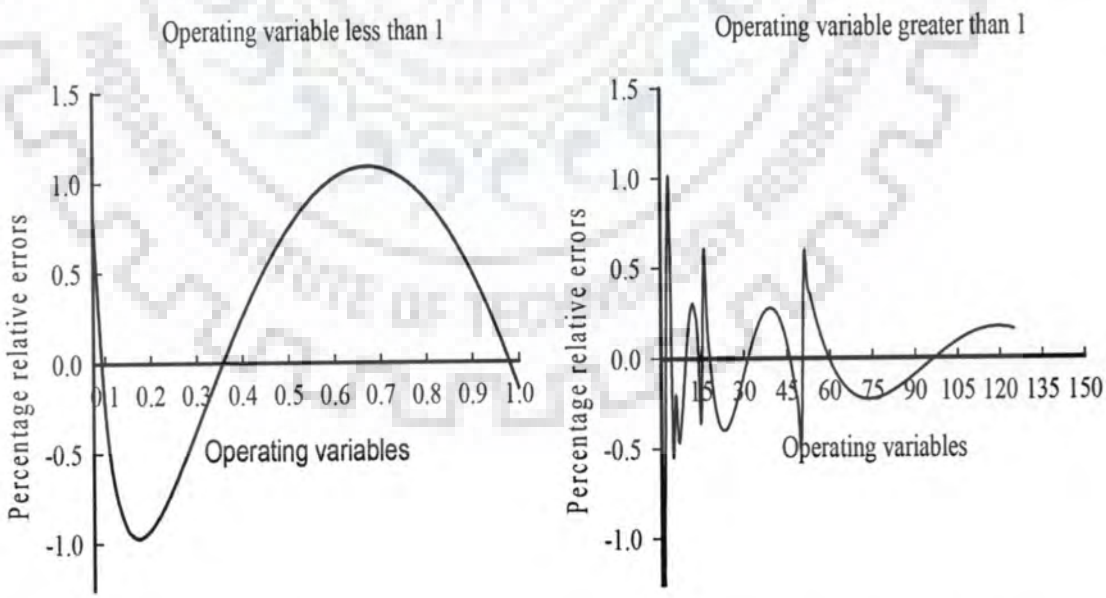

Fig. 4.4. Relative errors of the second order polynomial (Eq.4.4) with respect to $ln(1+x)$; $|x|$ is the operating variable

Table 4.2. Goodness-of-fit values of different statistical parameters, estimated by comparing responses of the second order polynomial (Eq.4.4) for value of coefficients as given in Table (4.1) with the distribution of $ln(1+x)$, $/x/ = \left|\{L_f/(H+\psi_f)\}\right|$.

Range	D	RB
$\|x\| \leq 1$	0.9970	0.0128
$1 < \|x\| \leq 5$	0.9998	-0.0004
$5 < \|x\| \leq 15$	0.9999	-0.0013
$15 < \|x\| \leq 50$	0.9998	-0.0008
$\|x\| \geq 50$	0.9998	0.0002

4.5.1.1 Comparison of the proposed derivations with the Green-Ampt model

Making use of the estimated values of A_i, B_i, and C_i as given in Table (4.1) for different ranges of $L_f/(H+\psi_f)$ in Eq. (4.7), the generalized expression for L_f, can be written as:

$$L_f = \sqrt{\frac{F_1 K_s (H+\psi_f)}{\eta} t + F_2 (H+\psi_f)^2} - F_3 (H+\psi_f) \tag{4.37}$$

in which F_1, F_2 and F_3 are the numerical factors of the five segments. The values of these factors are given in Table 4.3.

Table 4.3. Segmental values of the numerical factors F_1, F_2, and F_3 as given in Eq.(4.37).

Segments	F_1	F_2	F_3
$\left\|L_f/(H+\psi_f)\right\| \leq 1$	4.16	0.04	0.15
$1 < \left\|L_f/(H+\psi_f)\right\| \leq 5$	26.96	53.68	6.85
$5 < \left\|L_f/(H+\psi_f)\right\| \leq 15$	216.18	7906.76	87.72
$15 < \left\|L_f/(H+\psi_f)\right\| \leq 50$	1955.96	839845.55	914.36
$\left\|L_f/(H+\psi_f)\right\| > 50$	18137.87	78804363.26	8874.10

To investigate the performances of Eq.(4.37) with respect to the corresponding segment of the GA model, (Eq.4.1); a constant H = 2.0 m and the soil properties as complied by Rawls et al. (1982) [given in Appendix -B] are considered. The higher values of $\left|\left\{L_f/\left(H+\psi_f\right)\right\}\right| \geq 1$, which represent depth to water table, $D_w > H$, are chosen by allowing the wetting front to move for a longer time. For known D_w, H and the soil properties, the time required for the wetting front to reach the water table can be ascertained using $L_f = D_w$ in Eq.(4.1). To investigate the characteristic behaviors of Eq.(4.37) for its different segmental values with respect to the corresponding part of the GA model, four textural classes of soils, namely; sand, loam, clay loam and sandy clay as given in Appendix-B are considered. The initial moisture condition, θi, is assumed to be on its residual saturation, that gives $\eta = \theta_s$. Using the values of K_s, ψ_f, η and H of the respective soil groups in the GA model (Eq.4.1) the time varying L_f is computed. Extending the same value of variables, K_s, ψ_f, η and H to the respective segmental equation [Eq.(4.37)] chosen based on the criterion of $\left|\left\{L_f/\left(H+\psi_f\right)\right\}\right|$, the time varying L_f is also computed for each segment. The computed values by Eq. (4.37) for the four textural classes of soils and those by the GA model are shown in Fig.4.5. It can be seen from Fig. 4.5 that the values given by Eq.(4.37) are closely matched with that of the values by the GA model, for all the four textural classes of soils. The statistical parameters (Table 4.4), which show $R^2 \approx 1$, $D \approx 1$, and $RB \leq -0.2027$, also conforms agreement between the responses depicted by proposed derived Eq. (4.37) and the GA model. Thus, the Eq. (4.37) can be used as the alternate derivation to the logarithmic term of the GA model for estimating time varying Lf. These generalized segmental equations help estimation of L_f explicitly and can be used for all ranges of $\left|\left\{L_f/\left(H+\psi_f\right)\right\}\right|$.

Table 4.4. Goodness-of-fit for different statistical parameters estimated from the values of L_f, computed by the proposed models and the Green-Ampt model

Textural classes of soils	R^2	D	RB
Sand	0.9999	0.9995	-0.2037
Loam	1.0000	1.0000	-0.0269
Clay loam	1.0000	1.0000	-0.0088
Sandy clay	1.0000	1.0000	-0.0056

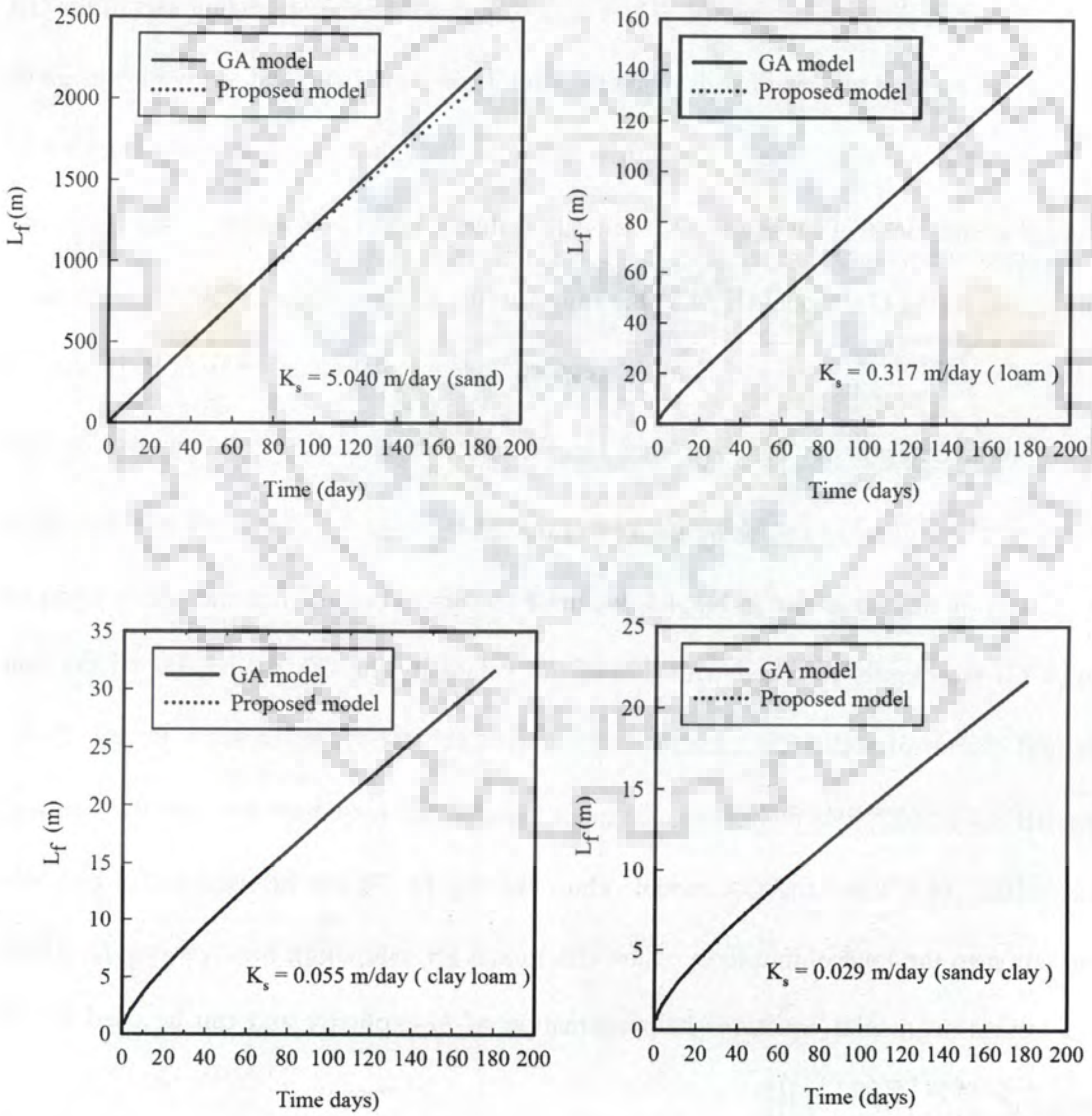

Fig.4.5. Comparison of the responses of L_f, depicted by the proposed model (Eq. 4.37) and the Green–Ampt model.

4.5.1.2 Characteristic behaviors of R_P

Using the estimated values of A_i, B_i, and C_i of the corresponding segment [as given in Table (4.1)] in Eq. (4.9), the generalized expression of the potential recharge, R_P is given by:

$$R_P = \frac{G_1 K_s (H+\psi_f)}{\sqrt{\frac{G_2 K_s (H+\psi_f)}{\eta} t + G_3 (H+\psi_f)^2}} \quad (4.38)$$

in which G_1, G_2 and G_3 are the numerical factors of the five segmental equation. The values of G_1, G_2 and G_3 are given in Table 4.5.

Table 4.5. Segmental values of the numerical factors G_1, G_2, and G_3 as given in Eq.(4.38).

Segments	G_1	G_2	G_3
$\lvert L_f/(H+\psi_f)\rvert \le 1$	2.28	4.16	0.04
$1 < \lvert L_f/(H+\psi_f)\rvert \le 5$	13.48	26.96	53.68
$5 < \lvert L_f/(H+\psi_f)\rvert \le 15$	108.09	216.18	7906.76
$15 < \lvert L_f/(H+\psi_f)\rvert \le 50$	977.98	1955.96	839845.55
$\lvert L_f/(H+\psi_f)\rvert > 50$	9068.94	18137.87	78804363.26

The dimensionless form of Eq. (4.38) is given as:

$$\frac{R_p}{K_s} = \frac{G_1\left(\frac{H+\psi_f}{K_s\, t}\right)}{\sqrt{\frac{G_2}{\eta}\left(\frac{H+\psi_f}{K_s\, t}\right) + G_3\left(\frac{H+\psi_f}{K_s\, t}\right)^2}} \quad (4.39)$$

For a given value of H, K_s, ψ_f and η, using Eq.(4.39) with its respective segmental values of the numerical factors, the dimensionless quantity, (R_p/K_s) for different time varying $((H + \psi_f) / K_s\, t)$ can be computed. The characteristic graphs of R_P

for the four soil texture classes given in the Appendix-B are generated for varying time, t using $H = 2$m and are shown in Fig. 4.6 (a, b). It can be seen from Fig. 4.6 (a, b) that for a particular K_S, η and ψ_f: R_p is high on the onset of the recharge process and reduces gradually with time and reaches nearly to a steady state at large time. It can also be seen that as the value of K_s increases, R_p also increases. These characteristics are on the expected lines.

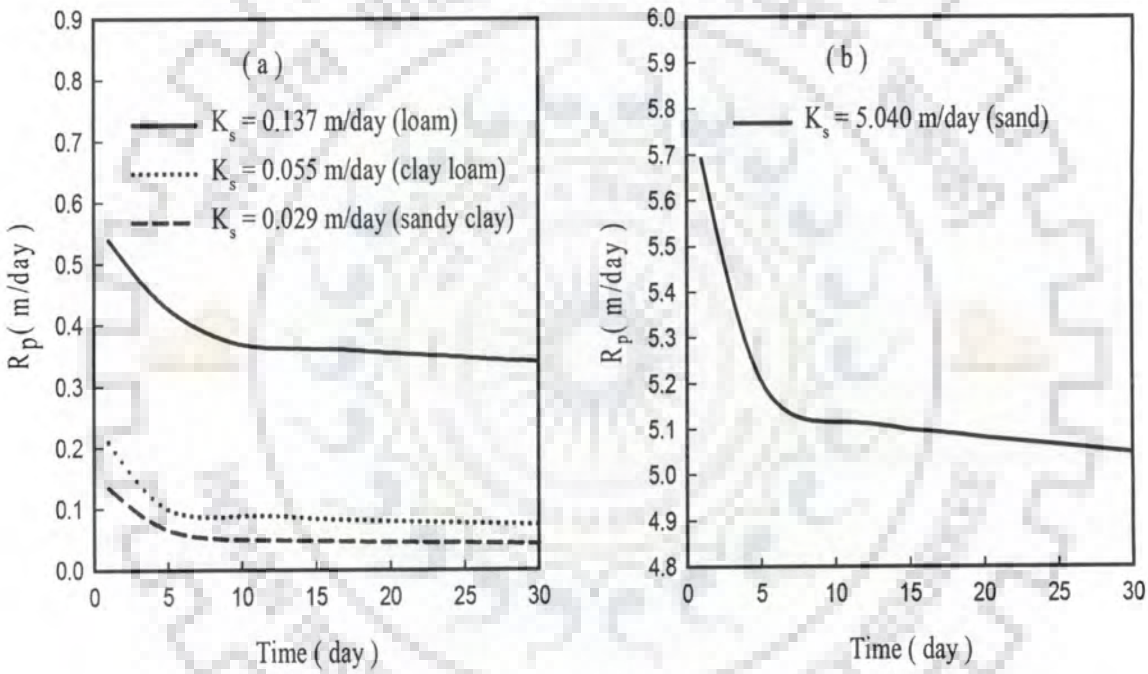

Fig. 4.6. Variation of potential recharge rate, R_P with time for different textural classes of soils

The generalized characteristic graphs of (R_p/K_s) versus $((H + \psi_f) / K_s\, t)$ generated for the four textural classes of soils using $H = 2.0$ m and the respective values of G_1, G_2, and G_3 in Eq. (4.39) are shown in Fig. 4.7. As t increases, the term $((H + \psi_f) / K_s\, t)$ reduces, for other factors remaining unaltered. In other words, for smaller value of t, the term $((H + \psi_f) / K_s\, t)$ gets magnified. Thus, these graphs (Fig. 4.7) demonstrate clearly a significant variation of (R_p/K_s) in the initial period for all the soil textural classes. As 't'

increases, indicating smaller value of $((H + \psi_f) / K_s t)$, the differences of (R_p/K_s) between different soil textural classes reduce. These characteristics are in the expected line. The proposed model has all promising potential to estimate the seepage rate and the potential recharge, and hence can be considered a generalized model that can successfully be used to all field conditions to estimate the seepage rate and the potential recharge rate.

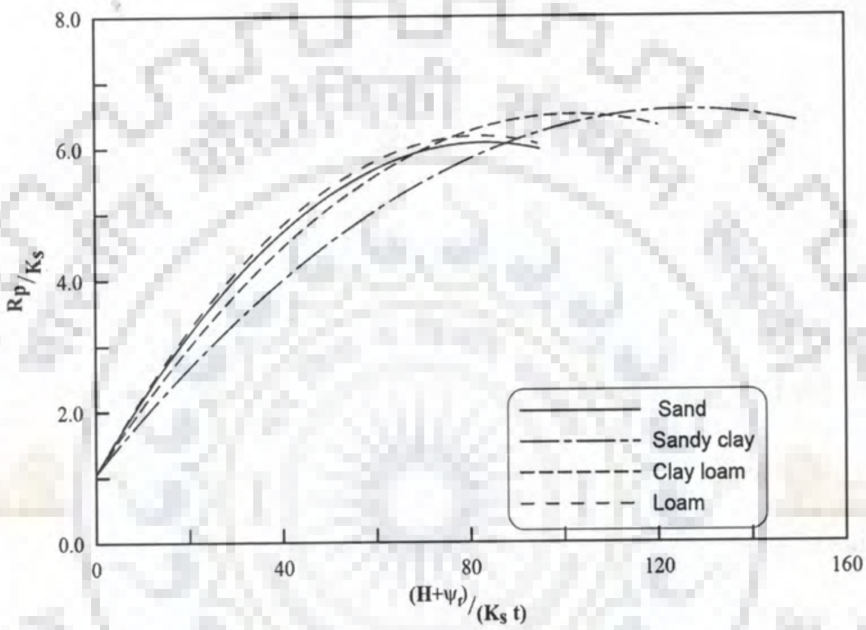

Fig. 4.7. Dimensionless plot of (R_p/K_s) versus $(H+\psi_f)/K_s t$ for different textural classes of soils

4.5.1.3 Estimation of T_d

The expression of T_d by putting different segmental values of A_i, B_i, and C_i in Eq.(4.16), satisfying the conditions of $L_f/(H+\psi_f)$, can be written as:

$$T_d = -\frac{J_1 \eta}{K_s}\left(H+\psi_f\right) + \frac{J_2 \eta}{K_s}\left(H+\psi_f\right)\left[\frac{D_w}{H+\psi_f} + J_3\right]^2 \tag{4.40}$$

where J_1, J_2 and J_3 are the numerical factors of Eq. (4.40).

The numerical factors J_1, J_2, and J_3 for the five segments are given in Table 4.6.

Table 4.6. Numerical factors J_1, J_2, and J_3 of different segments for estimation of T_d.

Segments	J_1	J_2	J_3
$\lvert L_f/(H+\psi_f)\rvert \le 1$	0.01	0.240300	0.15
$1 < \lvert L_f/(H+\psi_f)\rvert \le 5$	2.00	0.037090	6.85
$5 < \lvert L_f/(H+\psi_f)\rvert \le 15$	36.58	0.004630	87.22
$15 < \lvert L_f/(H+\psi_f)\rvert \le 50$	429.38	0.000510	914.36
$\lvert L_f/(H+\psi_f)\rvert > 50$	4344.79	0.000061	8874.10

For a given H, D_w and textural class of soil; T_d can be estimated using Eqs. (4.40) sequentially based on the criterion of $L_f/(H+\psi_f)$. For example, T_d for $D_w = n\,H$, where n is an integer, say n > 50, can be calculated as follows: $L_f/(H+\psi_f)$ is first calculated, based on which the segmental equation of T_d is chosen, and thereafter each segmental T_d is calculated substituting segmental L_f in place of D_w. Summation of each segmental T_d satisfying D_w = n H is taken as the actual T_d.

4.5.2 Actual Recharge

Results are presented for a case in which the water spread area does not change with time, i.e., for a constant H. The following input values are used: H = 2.0 m; length of the pond, $2L$ = 500 m; width of the pond, $2W$ = 400 m; depth to water table from the pond bottom, D_w = 20 m; hydraulic conductivity of the aquifer material, K = 1 m/day; hydraulic conductivity of the soil layer below pond bed, K_s = 1, 0.5, and 0.25 m/day; and the initial position of water table, h_0 = 30 m.

Corresponding the above data, the variation of dimensionless recharge, $\frac{q_a(n\Delta t)}{[4LW K_s)]}$,

with dimensionless time, $\frac{K h_0 n \Delta t}{LWb\phi}$, is shown in Fig. 4.8. It can be seen from Fig. 4.8 that recharge is high in the beginning and decreases monotonically for low value of K_s/K as the potential difference between the pond bed and the aquifer decreases with time. As K_s/K increases the non-dimensional recharge decreases and the potential difference between the pond bed and the aquifer reduces more rapidly with time. However, the dimensional recharge rate is more for higher value of K_s/K.

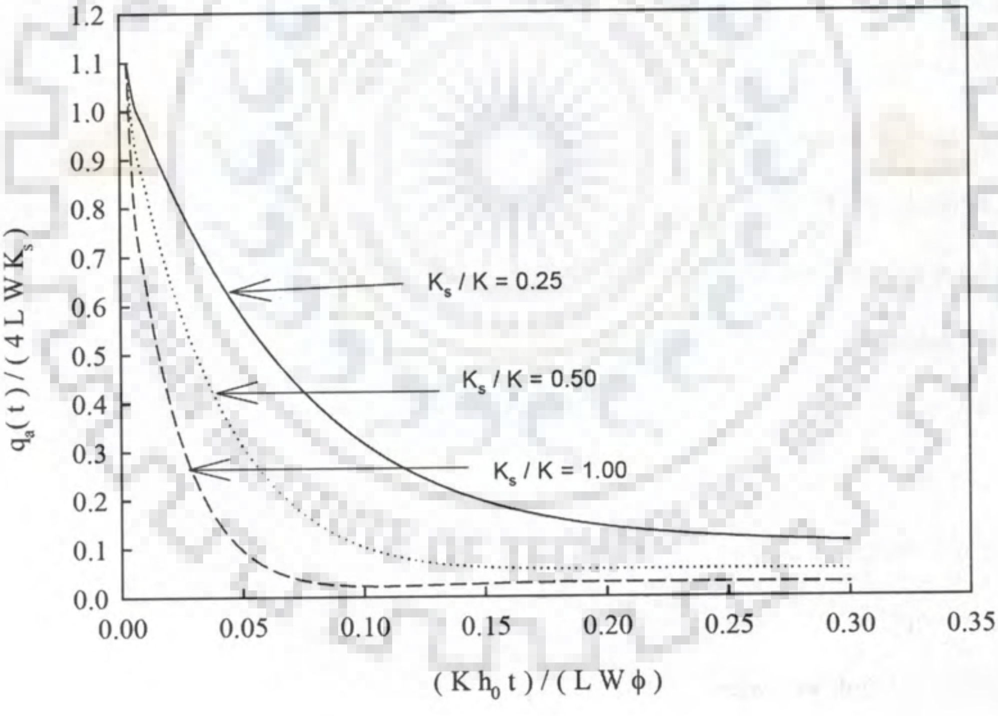

Fig.4.8. Variation of non-dimensional recharge rate versus non-dimensional time for constant head and water spread area.

4.6 CONCLUSIONS

1. The logarithm term, $ln\{1+L_f/(H+\psi_f)\}$of the Green-Ampt (GA) model has been approximated by a second order polynomial in segments. Five segmental polynomials could describe the algorithmic term for all ranges of $\{L_f/(H+\psi_f)\}$ within the error bound maximum of ± 1%.
2. The replacement of the logarithmic term of the GA model by the second order polynomial could derive explicit expression for estimate of the time varying length of the advancement of wetting front.
3. The performance comparison of the proposed segmental polynomial with that of the GA model has shown a robust agreement with $R^2 \approx 1$, D ≈1, and RB ≤ ± 0.2027.
4. The generalized models along with their segmental values of the respective numerical factors for estimation of the length of advancement of wetting front, the seepage rate and the potential recharge rates have been derived.
5. The characteristic behaviors of the generalized models have been studied for four textural classes of soils, and found promising for application to all field conditions.
6. The generalized model for estimation of the time for the wetting front to reach water table has also been derived.
7. Using the Hantush's approximate analytical expression for the rise and fall of water table for uniform percolation of water from a rectangular pond, the models for estimation of the actual recharge both for constant and time varying water spread area have been derived considering the Duhamel's principle. Performances of the derived model for different soil textural classes have been studied .

CHAPTER-5

RAINFALL-RUNOFF MODELING OF A WATERSHED

5.1 GENERAL

In rural areas, ponds are located in such a way that they can have adequate water to take into storage. Each pond thus constitutes a specific drainage area that represents a watershed. This type of watershed is small in size and normally is a part of larger catchment. Runoff originates from rainfall on such watershed forms the main source of water for the pond. In addition to that, the direct rainfall on the pond also constitutes a part of the pond's water. Being small in size, runoffs generate from these watersheds remain un-gauged. Numerous models are available to estimate runoff yields from an un-gauged watershed. Those models are either empirical in nature or required good database for estimation of runoff yields. Even the most widely used Soil Conservation Service-Curve Number (SCS-CN) model, which can also be used for computation of runoff from un-gauged watersheds, also requires a good database related to land use, land treatment practice, hydrological condition, hydrological soil group and antecedent moisture condition (AMC) for estimation of its parameter CN. These types of data are generally found either missing or sparsely available for a small watershed.

The antecedent precipitation index (API) based models, which work on limited data, have limitations to represent physical conditions (Descroix et al., 2002; Dowson and Abrahat, 2007), those restrict their straightforward use. The normalized antecedent precipitation index (NAPI) based model proposed by Heggen (2001), as improvement over the API based model, has promising potential for its use to limited databases. However, the Heggen's model lacks in physical explanation to its mathematical structure and also needs verification in the context of the widely used models, such as the SCS-CN model. Keeping the above in view, it is envisaged to verify the physical and analytical description of the Heggen's NAPI-model including its further simplification and performance evaluation.

5.2 DERIVATION FOR RUNOFF

A schematic diagram depicting the primary components of rainfall-runoff processes and their conceptualized graphs of the characteristic behavior for gradually varying rainfall events are shown in Figs.5.1 (a, b and c). Figure 5.1(b) shows a qualitative graphical representation of the variation of runoffs and losses for varying rainfall events, and Fig. 5.1(c) describes the variations of ratios of runoff and losses to the corresponding rainfall with varying rainfall events.

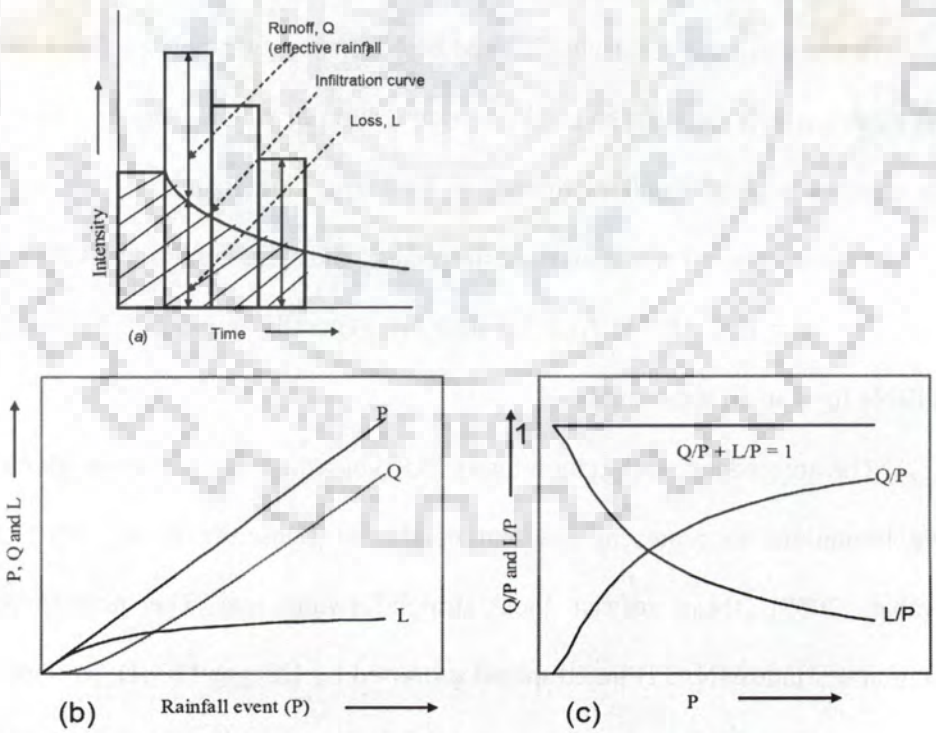

Fig.5.1.Qualitative characteristic graphs of rainfall-runoff variables: (a) figure showing different components of rainfall-runoff process; (b) graph showing variation of runoff, Q and Losses, L for varying rainfall event, P; and (c) graph showing variation of Q/P and L/P versus P.

Let P be the rainfall event over a watershed on a specific time period; Q be the surface runoff corresponding to that rainfall event; L be the loss of rainfall due to interception, initial abstractions and infiltration; I_a be the initial abstractions] from that rainfall event; and F be the infiltration. All these variables are in unit of length.

The water balance equation relating runoff, rainfall and losses due to infiltration and initial abstraction on a specific period of time can be expressed as:

$$Q = P - L \tag{5.1}$$

Eq. (5.1) can be written as:

$$\frac{Q}{P} = \left(1 - \frac{L}{P}\right) \tag{5.2}$$

Derivative of Eq.(5.2) w.r.t. P is:

$$\frac{d\left(Q/P\right)}{dP} = -\frac{d\left(L/P\right)}{dP} \tag{5.3}$$

Eq. (5.2) suggests that the ratio of Q over P is equal to the excess of ratio of L over P. It also indicates and can be seen from Fig. 5.1(c) that for *(Q/P)* to increase for increasing *P*, *(L/P)* has to be decreased to satisfy the condition, $(Q/P + L/P) = 1$. That means, the slope of the graph of *(Q/P)* with respect to *P*, *i.e.* $(d(Q/P)/dP)$, will be positive, and that of the slope of graph of *(L/P)* versus *P* i.e., $(d(L/P)/dP)$, will be negative, which are also clearly evident from Eq. (5.3). If losses from a rainfall event exist till the rainfall event continue, then a derivative of *(L/P)* with respect to that rainfall event, *P* will also exist, and is assumed to follow a linear hypothesis obeying the following logistic equation, as,

$$\frac{d(L/P)}{dP} = -b\,(L/P) \qquad : \mathrm{P} > 0 \tag{5.4}$$

where *b* is a proportionality constant of dimension in inverse of unit of length, and *(L/P)* is a dimensionless quantity.

Let $\left(L/_P\right) = r$. Integrating Eq.(5.3):

$$ln[r] = -bP + I_c \tag{5.5}$$

The integration constant, I_c in Eq. (5.5) describes the boundary value of *'r'* prior to the occurrence of the rainfall event, which is to be derived from the soil moisture condition i.e., from the API.

Let *'I_L'* be an index of losses in the watershed. The status of *'I_L'* shall be governed by interceptions, initial abstractions, and antecedent soil moisture condition (AMC). The interception and initial abstraction mainly occur at the initial period of time, while the soil moisture condition is a continuous process over time. Assuming that API is an index of AMC, and the change in the 'API' will change the status of I_L proportionality. With this hypothesis, the derivative of *'I_L'* with respect to the 'API' is considered proportional to 'I_L', which can mathematically be expressed as:

$$\frac{dI_L}{d[API]} = C\, I_L \tag{5.6}$$

where '*C*' is a proportionality coefficient having a dimension inverse of length .

Integrating Eq. (5.6):

$$ln[I_L] = C(API) + a \tag{5.7}$$

where *a* is an integration constant (dimensionless). The value of *a* is watershed specific, and shall be the minimum threshold value of *'I_L'* for that watershed.

From Eq. (5.7), I_L is given by:

$$I_L = e^{C(API) + a} \tag{5.8}$$

Replacing 'API' by 'NAPI', and *'C'* a dimensional term by *'c'* a dimensionless term; Eq. (5.8) yields to:

$$I_L = e^{c(NAPI) + a} \tag{5.9}$$

The 'NAPI' as described by Heggen (2001) is:

$$NAPI = \frac{\sum_{t=0}^{-i} P_t k^{-t}}{\bar{P} \sum_{t=-1}^{-i} k^{-t}} \tag{5.10}$$

where, i is the number of antecedent days, usually taken 5, 7 or 14 days; k is a decay constant, the value ranges between 0.80 and 0.98; and $\bar{P}$ is the average rainfall for antecedent days.

Now referring to Eq. (5.5), the integration constant, I_c is obtained from the limit as, $P \rightarrow 0$, $r \rightarrow I_L$, i.e., when $P \rightarrow 0$, $\left(L/P\right)$ is characterized by the 'AMC' just prior to the occurrence of rainfall. Substituting these along with I_L as given by Eq. (5.9), in Eq. (5.5), the solution for $\left(L/P\right)$ is given by:

$$r = L/P = e^{-bP + c(NAPI) + a} \tag{5.11}$$

Combining Eq. (5.11) with Eq. (5.2) leads to:

$$\frac{Q}{P} = \left(1 - e^{(-bP + c\,NAPI + a)}\right) \tag{5.12}$$

Eq. (5.12) is same to the equation as proposed by Heggen (2001), except sign of 'b'. The constant 'a' represents a minimum threshold value of the soil moisture condition in a watershed, 'b' represents the value of per unit rainfall that converts to losses, and 'c' is linked to the soil moisture content.

It now intended to bring out a mathematical structure of Eq.(5.12) that is comparable with the SCS-CN model. An expansion of the right hand side of Eq. (5.12) leads to:

$$\frac{Q}{P} = 1 - \left[1 + (-bP + cNAPI + a) + \frac{(-bP + cNAPI + a)^2}{2!} + \frac{(-bP + cNAPI + a)^3}{3!} + \ldots + \frac{(-bP + cNAPI + a)^n}{n!}\right] \tag{5.13}$$

where n is an integer. For $(-b\,P + c\,NAPI + a) << 1$, Eq.(5.13) can be reasonably approximated as:

$$\frac{Q}{P} = 1 - \left[1 + (-bP + cNAPI + a) + (-bP + cNAPI + a)^2 + (-bP + cNAPI + a)^3 + \ldots\ldots + (-bP + cNAPI + a)^n\right] \quad (5.14)$$

Or, $$\frac{Q}{P} = (-bP + c\,NAPI + a)\left[(-bP + c\,NAPI + a) - 1\right]^{-1} \quad (5.15)$$

Eq. (5.15) can be written alternatively, as:

$$Q = \frac{P(-bP + c\,NAPI + a)}{\left[(-bP + c\,NAPI + a) - 1\right]} \quad : \text{for } P > 0 \quad (5.16)$$

Eq. (5.16) is the transformed rational form of Eq. (5.12) and represents a mathematical structure comparable to the SCS-CN model.

5.3 SCS-CN MODEL

The runoff yields by the SCS-CN model is given (SCS, 1985; SCS, 1993; Mishra and Singh, 1999) by:

$$Q = \frac{(P - \lambda S)^2}{P + (1 - \lambda)S} \qquad for \quad P > \lambda S \quad (5.17)$$

$$Q = 0 \qquad for \;\; P \leq \lambda S$$

$$S = \frac{25400}{CN} - 254 \quad (5.18)$$

in which, S is the maximum potential retention (mm); λ is the initial abstraction weight as a fraction of S, normally, $0 \leq \lambda \leq 0.3$, conventionally taken as 0.2; 25400 and 254 in Eq. (5.18) are arbitrary constants in units of S; and CN is the Curve Number (dimensionless). Theoretically, S varies between 0 to ∞ for CN ranges from 100 to 0.

Substituting S as given by Eq.(5.18), and λ=0.2, Eq. (5.17), yields to:

$$Q = \frac{25.4\left[\dfrac{P}{25.4} - \dfrac{200}{CN} + 2\right]^2}{\left[\dfrac{P}{25.4} + \dfrac{800}{CN} - 8\right]} \quad ; \quad valid\ for\ P > 0.2S \tag{5.19}$$

The watershed specific-CNs relating to the antecedent moisture condition (AMC) is:

$$CN_I = \frac{4.2\,CN_{II}}{10 - 0.058\,CN_{II}} \tag{5.20}$$

$$CN_{III} = \frac{23\ CN_{II}}{10 - 0.13\ CN_{II}} \tag{5.21}$$

where subscripts indicate the AMC, I being dry, II normal, and III wet.

5.4 RESULTS AND DISCUSSION

Eq.(5.12) represents the Heggen's model except the negative sign of 'b', and Eq.(5.16) represents a simplified rational form of Eq.(5.12). To investigate the errors between an exponential series, Eq.(5.12) and a rational form as given by Eq.(5.16) when the former one is replaced by the later case, the synthetic values of Q/P for different values of $|(-bP + c\ NAPI + a)| < 1$, are generated using the same arbitrary value of a, b, and c in Eqs.(5.12) and (5.16), and the generated profiles are given in Fig. 5.2. It can be seen from Fig. 5.2 that the generated profiles of Q/P by Eq. (5.16) closely matched with that of the profiles generated by Eq.(5.12) for operating variable, $|(-bP + c\ NAPI + a)| \leq 0.256$. The profiles diverge from one from another as $|(-bP + c\ NAPI + a)|$ increases over 0.256. To assess the agreement and biasness quantitatively between the profiles generated by Eq.(5.12) and (5.16), the index of agreement (D), the relative biasness (RB) and the percentage relative errors (PRE) are calculated and given in (Table 5.1). Equations of D, RB, and PRE are given in Appendix-A. Table 5.1 indicates D ≥ 0.7963, and RB ≤ - 0.0433 for different ranges of $/(- bP + c\ NAPI + a)/ \leq 0.485$; D = 0.6406, and RB ≤ - 0.0923 for $/(-bP + c$

$NAPI + a) /$ ranges between 0.485 and 0.880. The relationship between the two series shows a meager agreement $(D = 0.1254)$ when $/(- bP + c\ NAPI + a) / \geq 0.88$. It can also be seen from Table 5.1 that the rational form (Eq.5.16) underestimates Q/P (RB<0) for all the values of $/(-bP + c\ NAPI + a) / > 0.256$ than the values described by the exponential form (Eq. 5.12). Table 5.1 also shows that the errors between the two series are below 20% for $/(-bP + c\ NAPI + a) / \leq 0.88$. As the value of $/(-bP + c\ NAPI + a) /$ reduces below 0.88, the errors between the two profiles decrease and they tend to match one another .

The characteristic behaviors of Eq. (5.12) and (5.16) showing Q/P as a function of P and NAPI, for an arbitrary value of a, b, and c, are shown in Fig.5.3. It can be seen from Fig. 5.3 that as NAPI increases, which increases the magnitude of (-b P + c NAPI +a), (Q/P) also increases for the value of a, b, and c remaining unchanged. The deviation between the two graphs increases with the increase of NAPI. In other words, for the same P and NAPI, the responses (Q/P) of Eq. (5.12) and (5.16) to become alike, the value of a, b, and c of Eq. (5.16) has to be different than that of Eq.(5.12).

Table 5.1. Goodness-of-fit between the profiles of Q/P computed using Heggen model (Eq.5.12) and the proposed model (Eq. 5.16) for different ranges of $/(-bP + c\ NAPI + a) /$.

Range of $\lvert -bP + cNAPI + a \rvert$	D	RB	PRE
< 0.115	0.9988	-0.0019	<5
0.115 to 0.265	0.9511	-0.0158	5 -10
0.265 to 0.485	0.7963	-0.0433	10 - 15
0.485 to 0.880	0.6406	-0.0923	15 - 20
> 0.880	0.1254	-0.1254	> 20

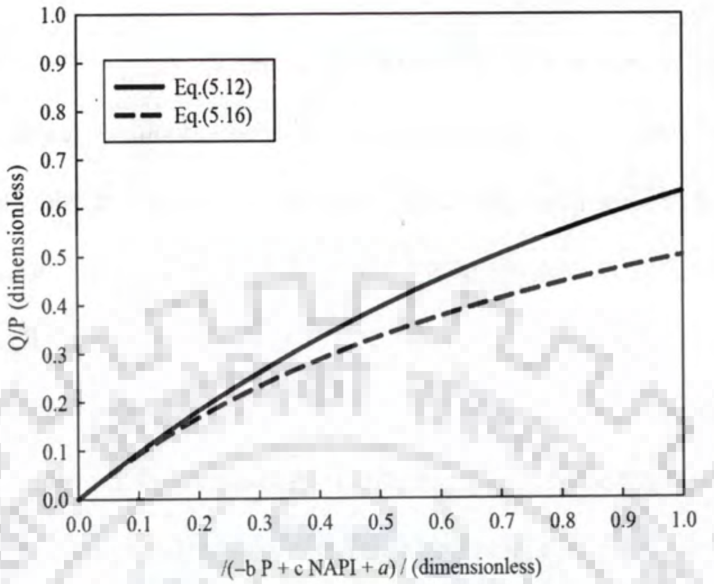

Fig. 5.2. Comparison of Q/P profile generated by Heggen model (Eq. 5.12) and the proposed model (Eq. 5.16) for different values of $/(-bP + c\,NAPI + a)/$.

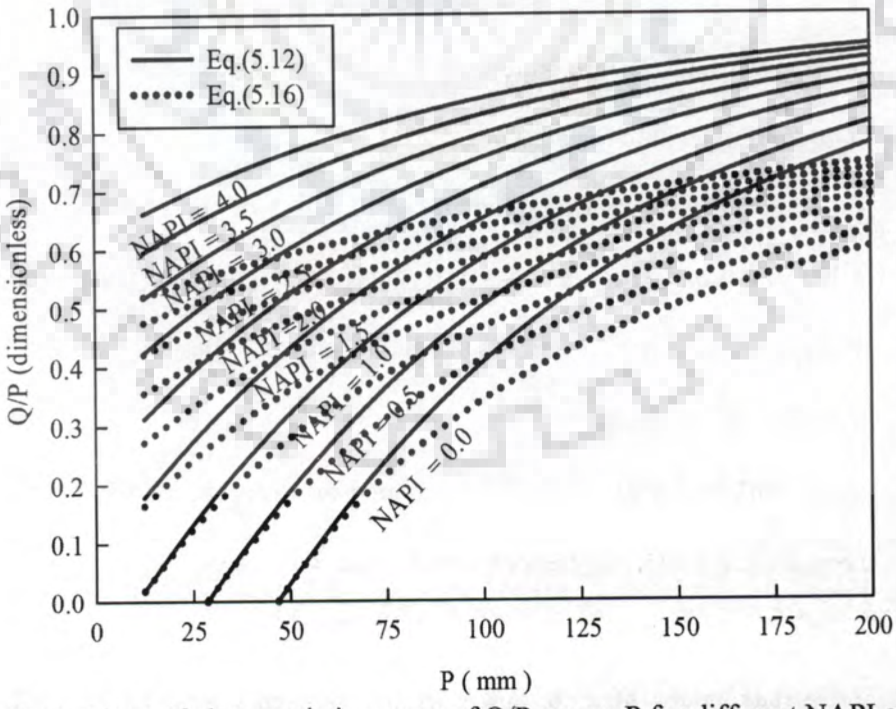

Fig. 5.3. Comparison of characteristic curves of Q/P versus P for different NAPI generated using the Heggen's model (Eq. 5.12) and the proposed model (Eq.5.16) for an arbitrary value of model parameters, b = 0.0098, c = -0.3550, and a = 0.4585.

5.4.1 Comparison of the Heggen Model and the Proposed Model with the SCS-CN Model

The SCS-CN model is a well-established model. Any new model is said to be acceptable, if its performance supersedes or, at least equalizes responses of the well-established model. To compare the performance of the Heggen model (Eq. 5.12) and the proposed model (Eq. 5.16) with the SCS-CN model, the following procedure is adopted:

(i) responses of the SCS-CN model (Eq. 5.19) for CN_{II} (AMC-II) of 30, 40, 50, 60, 70, 80 and 90 as prescribed in NEH-4 (SCS, 1985) based on five antecedent days are generated for gradually increasing rainfall events. These generated values are error free and considered as the synthetic observed runoffs data.

(ii) Considering these rainfall events, P, the antecedent days as five day and decay constant, $k = 0.9$; NAPI for each CN profile is estimated using Eq.(5.10).

(iii) making use of these Ps, estimated NAPIs and the respective synthetic runoff data in Eqs (5.12) and (5.16), the parameters a, b, and c of the proposed model and the Heggen's model are estimated using least squares optimization employing Marquardt algorithm (Marquardt, 1963).

(iv) responses of each set of estimated a, b, and c of the respective model, Eqs. (5.12) and Eq.(5.16), for different values of P and NAPI are computed and compared with that of the (Q/P) profile generated using the SCS-CN model for different CN_{II} values.

(v) visual comparison of the profiles depicted by different models is considered as the guiding criterion for performance evaluation.

The estimated values of *a*, b, and c of the Heggen's model (Eq. 5.12), and the proposed model (Eq. 5.16) for different CN based (Q/P) profiles are given in Table-5.2. NAPI is function of P and the antecedent days, therefore, its value remains same irrespective of CN values. From Table 5.2, it can be seen that for a particular CN based Q/P profile, the value of a, b, and c of the Heggen's model (Eq. 5.12) is different from that of the proposed model (Eq. 5.16), and they are different for different CN based Q/P profiles. The estimated values of a, b, and c of the Heggen's model and the proposed model for different CN values are graphically shown in Fig.5.5. Table-5.2 and Fig. 5.5 reveal that the parameter 'b' consistently increases as CN value increases, for both the models; whereas 'a' and 'c' are found complementary to one another as CN varies, i.e., when 'a' increases the magnitude of 'c' reduces and vice-versa. The values of 'a' and 'c' for all ranges of CN are found to have opposite sign for both the models, while 'a' and 'c' in the case of the Heggen's model change their sign respectively from (+ve) to (-ve) and (-ve) to (+ve) nearly at CN = 60 giving the intersected value as zero for both the parameters, but the same is not true for the proposed model. The values of 'a' and 'c' in case of the proposed model, for all ranges of CN are found to have consistently following the same sign, i.e., a is found (+ve), and c is (–ve) and tend towards zero as CN approaches to 100. The zero value of 'a' and 'c' implies no change in the soil moisture condition and the runoff in such case is governed by the parameter 'b' associated with P. The parameter 'a' and 'c' represent index of soil moisture condition and 'b' represents rate coefficient of losses from precipitation. Physically for all ranges of CN, the parameters 'a'has to be (+ve) and 'c' has to be (-ve) and both will tend to zero as CN approaches to 100. These conditions are found holding in the proposed model, and thus proves better scientific connotation of the physical conditions than the Heggen's model.

Making use of the estimated values of a, b, and c of the respective model, as given in Table 5.2, the responses of the Heggen's model and the proposed model are generated utilizing the same data set of P and NAPI. These profiles of Q/P are compared with the corresponding Q/P profile of the SCS-CN model. The comparison is shown in Figs.5.4 (a, b). It can be seen from Figs. 5.4 (a, b) that the profiles of Q/P depicted by the proposed model show superior match than that of the profiles depicted by the Heggen's model with the corresponding profiles of the SCS-CN model for all the cases. The proposed model shows a better physical explanation of its parameter and also gives improved agreement in the context of the SCS-CN model.

The estimated value of a, b, and c represents response of the error free data for a particular CN_{II}. Field observations may contain errors. Random error, in terms of percentage, on standard deviation of the error free synthetic data keeping the mean of the data unchanged (Mishra and Jain, 1999) is applied on these error free data. This random error based data represent runoff values corresponding to the considered rainfall events and NAPI. Using these random error based data, the model coefficients a, b, and c are estimated using Eq. (5.16). Different percentages of random error are considered to investigate the flexibility of the model in estimation of its parameters. Fig.5.6 compares the synthetic runoff data generated by the SCS-CN model for CN_{II} = 50, and 70, and the corresponding simulated runoff values estimated by the proposed model for data containing no error, and with 5% and 10% error. It can be seen (Fig. 5.6) that the profiles generated based on parameters estimated from the profile containing the errors match closely with the respective profiles; and hence, prove that the parameters of the proposed model can be successfully estimated from rainfall-runoff events. It can be pointed out that the SCS-CN model has one parameter, CN to fit the runoff data whereas the proposed model has three watershed specific parameters, in addition to a derived variable NAPI. If these parameters are known from a particular set of rainfall-runoff data of a gauged watershed, the proposed model then turns to a single input model.

Table 5.2. Values of parameters a, b, and c of the Heggen's model and the proposed model estimated from different CN based Q/P profiles.

CN values	Haggen model(Eq. 5.12)			Proposed simplified model(Eq. 5.16)		
	a	b	c	a	b	c
30	0.2973	0.0001	-0.1889	0.3066	0.0001	-0.1954
40	0.4854	0.0006	-0.3046	0.5632	0.0006	-0.3552
50	0.3655	0.0017	-0.1944	0.6046	0.0019	-0.3469
60	0.0475	0.0032	0.0437	0.5590	0.0039	-0.2765
70	-0.4223	0.0050	0.3578	0.5053	0.0069	-0.2056
80	-1.1109	0.0070	0.7666	0.4565	0.0126	-0.1476
90	-2.3082	0.0098	1.3784	0.3979	0.0293	-0.0838

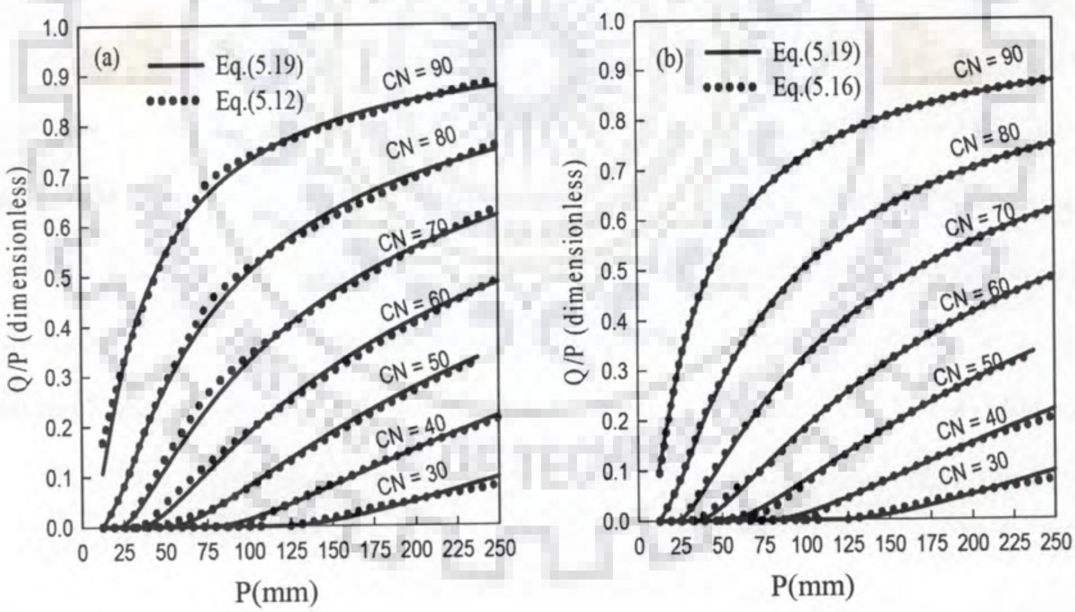

Fig. 5.4. Figure showing comparison of Q/P profiles by the SCS-CN model for different P and CN values generated by the SCS model with that of the responses of; (a) the Heggen's model (Eq. 5.12), and (b) the proposed model (Eq. 5.16).

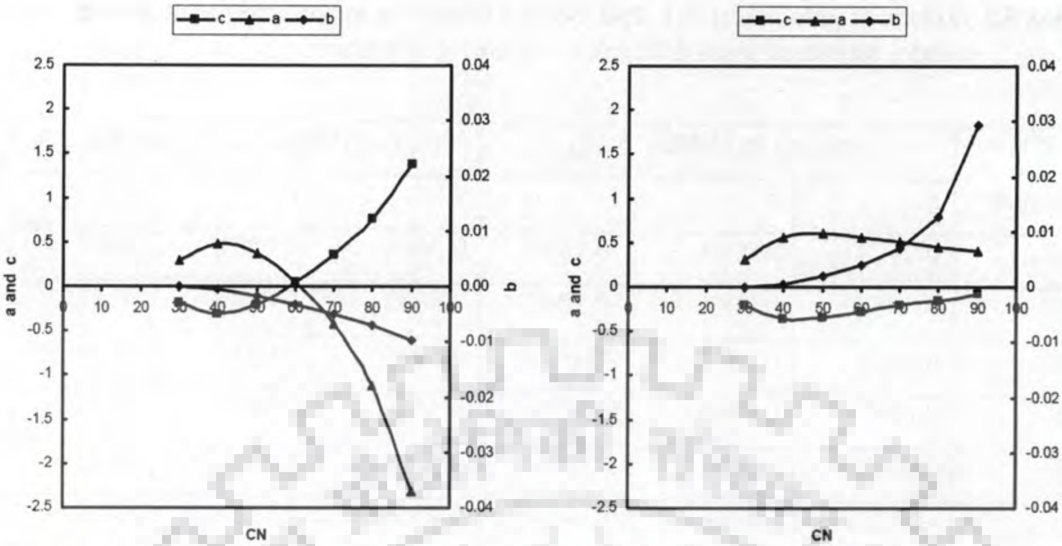

Fig. 5.5. Variation of parameters, a, b, and c with CN values: (a) the Heggen's model, and (b) the proposed model.

5.5.2 Field Application of the Proposed Model

The proposed model is applied to three different watersheds of sizes range from 0.4 to 29.2 ha, located in the Kota and the Bundi districts of Rajasthan (India). The details about the watershed, data collection procedure and data availability are given in Appendix-C. The salient features of the watersheds are given in Table 5.3.The watersheds are locally known as the agricultural watersheds (AG), the Badakhera watersheds (BK), and the ravenous watersheds (RAV). From the total datasets of rainfall events and observed runoffs; 73 of the AG, 23 of the BK and 42 of the RAV; first 50, 14 and 28 of the respective watersheds are utilized for model calibration, and the remaining for the model validation. The NAPIs corresponding to the observed Ps and based on the consideration of antecedent days to be 5 for each of the watershed are estimated externally taking k = 0.9. The NAPI and P remaining unchanged, the parameters a, b, and c for each of the watershed are determined extending least squares optimization technique to Eq. (5.16) (SYSTAT, 2006). The estimated values of a, b, and c along with the statistics of dependent and independent variables are given in Table-5.4. The t-test reveals that the estimated values of the parameters are highly significant at 1% probability level.

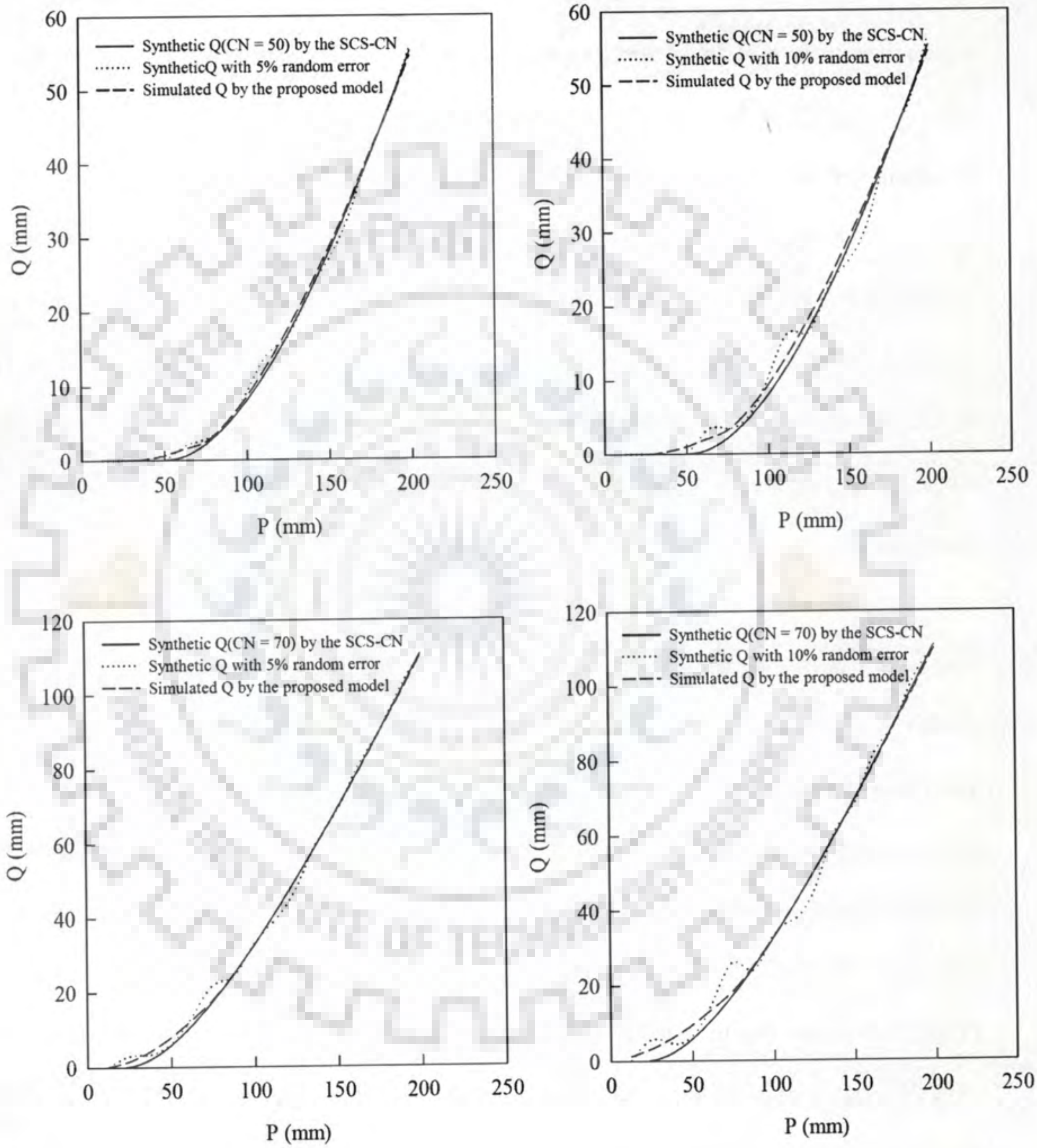

Fig. 5.6. Figure showing comparison between the synthetic runoffs by the SCS-CN model for CN_{II} = 50 and 70 and the corresponding simulated runoffs by the proposed model(estimated parameters for error free dataset representing CN_{II} = 50, are : a = 0.6115, b = 0.0019 mm^{-1}, c = - 0.3523; and for dataset CN_{II} = 70 are : a = 0.5078, b = 0.00692 mm^{-1}, c = - 0.2091).

This is also recognized for the BK and RAV watersheds from the coefficient of determination ($R^2 \geq 0.908$) and standard error ($SE \leq 3.49$). However, the AG watershed exhibit a low R^2 (= 0.374) and a high SE (=17.54) value. Validation of the model by the remaining datasets of the respective watersheds for the corresponding Ps and NAPIs is shown in Fig.5.7 by the plot of 1:1 line of the observed and the predicted runoff values. The statistical values of the correlation obtained by the F-test and the student t-test are shown in Table 5.5. The high values of F-test at 0.01% significance level suggest a closer correlation between the observed and predicted runoffs. The student t-test is used to evaluate the hypothesis that the slope of regression line between the observed and predicted runoffs equals to one, and intercept equals to zero. The results (Table 5.5) show that neither the slope nor the intercept significantly differ from one and zero, respectively for all the watersheds.

Mean values of the CNs for each of the watershed are also estimated from the observed data of P-Q using lognormal frequency method as described by Ali and Sharda (2008). The CN values are estimated to be 79, 87 and 84 for the AG, BK and RAV watershed, respectively. Making use of the respective CN and observed P, the runoffs are also computed by the SCS-CN model. The estimated runoffs by the proposed model and the SCS-CN model are compared with the observed runoffs using the statistical properties, viz. 'D' and 'RB' (Table 5.6). The *'D'* and the 'RB' determined from the respective datasets (Table 5.6) reveal that the runoffs computed by the proposed model are in close agreement with the observed values than the SCS-CN model; 'D' being higher and 'RB' being lower for the proposed model than the SCS-CN model. The performance of the proposed model over the SCS-CN model is also examined by their chronological ranking for each of the watershed (Table 5.6). The proposed model for all the three watersheds shows first rank; D being higher (≥ 0.805), and RB being lower (≤ 5.52 mm) compared to the SCS-CN model (Table 5.6) except the small deviation in 'RB' for the RAV watershed. The overall performance of the proposed model is found promising in terms of data requirement and simplicity in estimation of its parameters.

Table 5.3. Salient features of the watersheds in the semi-arid region of Rajasthan in India.

Water sheds	Location	No of events	Area (ha)	Average Slope (%)	Hydrological soil group	Land use cover	Hydrologic condition	Treat ment
AG	Kota	73	0.4	1.1	D	Single	Good	Inter cropping
BK	Bundi	23	29.2	6.5	C	Mixed	Poor	No treatment
RAV	Kota	42	1.4	8.4	D	Single	Poor	No treatment

Table 5.4. Values of the proposed model parameters, coefficient of determination (R^2), standard error (SE), and Student's t-test statistical values of the dependent and independent variables estimated from the datasets of watershed in Rajasthan

Watershed	Sampling size	Model parameters		R^2	SE	t-test$_{[\dagger]}$
		Parameters	Value			
AG	50	b	-0.0022	0.374	17.54	-1.34
		c	0.0241			0.89
		a	-0.8681			-3.39
BK	14	b	0.0046	0.979	3.49	6.12
		c	-0.0169			-0.30
		a	-0.1625			0.89
RAV	28	b	0.0034	0.908	1.79	5.20
		c	0.0035			0.15
		a	-0.1335			-2.04

† indicates 1% probability level of 1%.

Table 5.5. Estimated regression coefficients, F-test and t-test values for the observed and predicted runoffs of the watersheds.

Watersheds	Regression coefficients		F-test$_{[a]}$	t- test$_{[b]}$
	Parameters	Value		
AG	Slope	1.06	34.49	0.33
	Intercept	6.06		1.54
BK	Slope	0.53	386.55	2.25
	Intercept	1.77		3.25
RAV	Slope	0.93	80.35	0.68
	Intercept	3.53		3.12

[a] and [b] at 0.01 and 0.001% significance level, respectively.

Table 5.6. Statistics of different goodness- of- fit measures of the observed and predicted runoff by the proposed and SCS-CN model for the watersheds.

Goodness- of- fit measures	Watersheds		
	AG	BK	RAV
Index of Agreement (D)			
Observed verses proposed model	0.805 (I)	0.889 (I)	0.956 (I)
Observed verses SCS-CN model	0.523 (II)	0.627 (II)	0.863 (II)
Relative Bias (RB)			
Observed verses proposed model	5.66 (I)	-2.69 (I)	-0.59 (II)
Observed verses SCS-CN model	-6.91 (II)	-4.03 (II)	-0.54 (I)

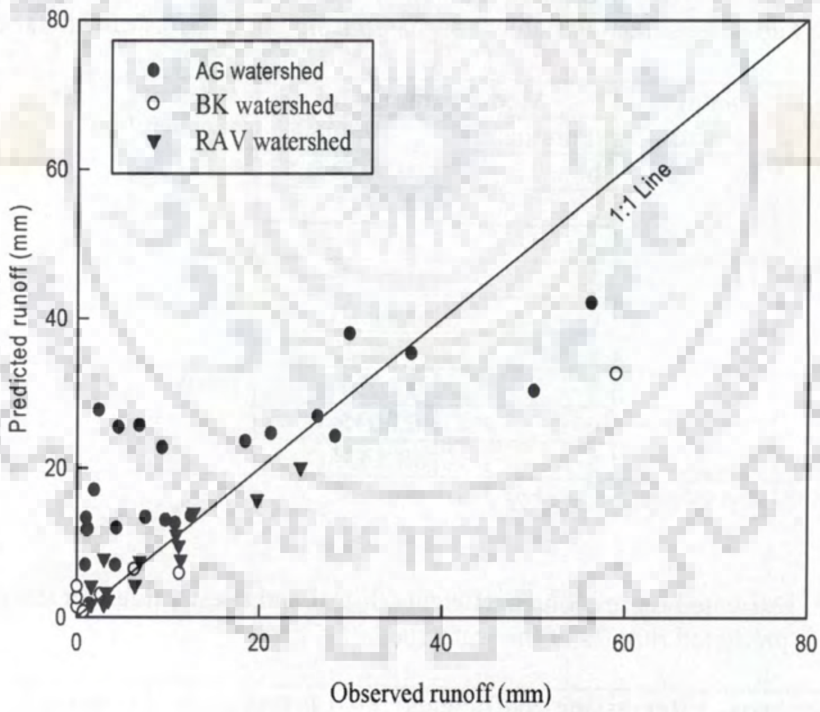

Fig. 5.7. Comparison of observed and predicted runoffs by the proposed model

5.6 CONCLUSIONS

1. The normalized antecedent precipitation index (NAPI) model proposed by Heggen (2001) for prediction of runoff yield has been analytically derived from the water balance equation. The model has further been simplified to a rational form. The proposed model has three watershed specific parameters, and requires two inputs; one is rainfall and the other one is rainfall derived variable "NAPI".
2. The performance of the Heggen's model and the proposed model has been verified with the SCS-CN model. The proposed model showed superior match with the SCS-CN model than the Heggen's model. The characteristic behavior of the parameters of the proposed and the Heggen's model have been studied in the context of CN of the SCS-CN model. The parameters of the proposed model explained the physical processes more realistically than the Hagen's model.
3. The parameters of the proposed model can be estimated with reasonable accuracy using least squares optimization technique from the observed rainfall-runoff data.
4. The model has been tested with the field data of the three watersheds located in semi-arid region of Rajasthan.
5. The proposed model has advantages of: (i) minimal data requirement, and (ii) relatively simple to use.

CHAPTER-6

ESTIMATION OF WATER SURFACE EVAPORATION

6.1 GENERAL

Water surface evaporation is a significant component of water loss from a pond's storage. Significance of this component and its accurate estimation increases when the problems are associated with the arid and semi-arid regions. Surface water evaporation from a pond is a continuous process like recharge to the groundwater. It depends on many factors namely, solar radiation, temperature, wind speed, vapour pressure deficit, atmospheric pressure, water surface area and the surrounding environment.

Several methods (discussed in the review of literature) exist for estimation of evaporation. Most commonly used methods whose degree of reliability has been reported within a desired limit, are: (i) Bowen ratio energy balance (BREB), (ii) Mass transfer (MT), (iii) Priestley-Taylor (PT) and (iv) Pan evaporation (PE) method. These methods vary from one to another in terms of: types of data requirement, range of applicability, structural and parametric differences and cost involved in collection of required data. A method that holds good for a specific meteorological region may or may not perform satisfactorily for other regions. Among the above methods, the energy balance method has been reported the most accurate and reliable, but the data required by this method is very expensive to generate on routine basis, and hence often remain missing. Singh and Xu (1997) suggested that although structural and parametric differences exist in many evaporation models, yet under certain considerations, they complement each other in terms of performance and parametric similarity.

Keeping the above in view, it is intended to identify and derive a reliable and promising method for estimation of evaporation by comparing performances of the four most commonly used methods, and to evolve and establish appropriate technique for parameters estimation of the proposed method from limited data.

6.2 EVAPORATION ESTIMATION METHODS

6.2.1 The Bowen Ratio Energy Balance (BREB) Method

The BREB method derived from the principle of energy budget considering surface energy balance and flux gradient relationship between latent heat of water evaporation and sensible heat conducted and convected from water surface to atmosphere is given by (Ikebughi, *et al.*, 1988; Stannard and Rosenberry, 1991):

$$E_{BR} = \frac{R_n - (G + H_b + H_a)}{\lambda_h (1+\beta)} \tag{6.1}$$

where E_{BR} is the evaporation rate [mm/day]; R_n is the net radiation on the water surface[MJm^{-2} /day]; G is the heat gained or lost by the upper layer of water body [MJm^{-2}/day]; H_b is the heat flux into bottom of water body [MJm^{-2}/day]; H_a is the heat energy advection into water body [MJm^{-2}/day]; λ_h is the latent heat of evaporation of water [= 2.45MJ/kg]; and β is the Bowen ratio[dimensionless].

The reduced form of the BREB equation neglecting H_b *and* H_a is given by (Simon and Mero, 1985; Assouline and Mahrer, 1993):

$$E_{BR} = \frac{R_n - G}{\lambda_h (1+\beta)} \tag{6.2}$$

To compute E_{BR} using Eq.(6.2), one requires measurements of each component in the R.H.S. In absence of on-site data or when quality of data is poor, these components can be determined from empirical relationships of each parameter with allied meteorological variables (WHO, 1985). The empirical relationships for estimation of R_n, G and β are given in the Appendix-C.

6.2.2 The Mass Transfer (MT) Method

The MT method is based on the Dalton equation, and it assumes that the evaporation rate is linearly proportional to the wind speed, and the difference between the vapour pressure of the water face and the atmosphere. Mathematically it is given by:

$$E_{MT} = \mu U_2 (e_s - e_a) \tag{6.3}$$

where E_{MT} is the evaporation rate [mm/day]; μ is the mass transfer coefficient [mm s m^{-1} kpa^{-1}]; U_2 is the wind speed at 2 m above the water surface [ms^{-1}]; e_s is the saturated vapour pressure at water temperature [kpa]; and e_a is the actual vapour pressure [pa].

Equations for estimation of μ, U_2, e_s and e_a Eq.(6.3) is given in the Appendix-C.

6.2.3 The Priestley-Taylor (PT) Method

The PT method is a simplified form of the combined component of radiation and aerodynamics with the aerodynamic component dropped, but a coefficient, α, greater than 1.0 is included as a multiplier. The PT model is given by (Priestley-Taylor, 1972):

$$E_{PT} = \frac{1}{\lambda_h} \alpha \left[\frac{\Delta}{\Delta + \gamma_c} \right] (R_n - G) \tag{6.4}$$

where E_{PT} is the evaporation rate [mm/day]; α is the dimensionless proportionality parameter or Priestley-Taylor's coefficient, usually considered as 1.26; Δ is the slope of saturated vapour pressure at water temperature verses temperature curve [kpa $^0C^{-1}$]; and γ_c is the psychometric constant [kpa$^0C^{-1}$].

Equations for estimation of α, Δ and γ_c is given in the Appendix-C.

6.2.4 The Pan Evaporation (PE) Method

The standard PE method is given by (Abtew, 2001):

$$E_P = K_p E_{pan} \tag{6.5}$$

where E_P is the evaporation rate [mm/day)]; K_p is the pan coefficient, which is defined as the ratio of the theoretically free surface evaporation to the pan evaporation; E_{pan} is the Class A pan evaporation [mm/day]. K_p is normally calculated from the ratio of evaporation rate determined from the energy balance method, to the measured pan evaporation rate.

6.3 RESULTS AND DISCUSSION

Eqs.(6.2), (6.3), (6.4) and (6.5) represent respectively; the Bowen ratio energy balance, mass transfer, Priestley-Taylor and pan evaporation method. Data required for estimating evaporation rate by each of the method are as follows:

BREB method: Air temperature, water temperature, relative humidity, sunshine duration.

MT method : Air temperature, water temperature, relative humidity, wind speed.

PT method : Air temperature, water temperature, sunshine duration.

PE method : Pan evaporation rate.

These data were collected from the agricultural meteorological observatory (AMO) of the Central Soil and Water Conservation Research and Training Institute, Research Centre (CSWCRTI, RC) located in Kota district and from an experimental site located in BK watershed in Bundi district, both district in Rajasthan. Two stations are nearly 65 km apart. Daily data of all the variables for 729 days in four years (2002-2005) from July to December in every year were available.

6.3.1 Air -Water Temperature Model

To fill up the gap of the unrecorded water temperature data, a regression model using the recorded data of the mean daily air temperature and the corresponding water temperature is first established. Three regression models; linear, logarithm and power are employed to select the best-fitted one. The statistics of the three different models are summarized in Table 6.1. Among the three, the linear model is found to be the best as it has higher coefficient of determination, R^2, index of agreement, D and the lesser relative bias, RB compared to the other two models (Table 6.1). The plot of the measured and the simulated water temperatures obtained from the linear model exhibits a good agreement with the 1:1 line (Fig 6.1). In mathematical notation, the derived linear regression model is given by:

$$T_w = 1.04\ T_a + 0.22 \tag{6.6}$$

where T_w and T_a are the surface water temperature(^{0}C) and the air temperature(^{0}C), respectively.

Eq.(6.6) can be used to find the water temperature corresponding to a air temperature of that area.

Table 6.1. Regression coefficients (m and c), coefficient of determination (R^2) and standard error of estimates(SE) of the air and the water temperature relationship, and their performance statistics.

Conceived Models	Values of the regression analysis between air and water temperature				Statistics of the measured and the simulated water temperature		
	Slope (m)	Intercept (c)	R^2	SE (^{0}C)	R^2	D	RB (^{0}C)
$T_w = mT_a + c$	1.04	0.22	0.9618	1.55	0.9518	0.9802	-0.000013
$T_w = m \ln(T_a) + c$	22.42	-39.34	0.9508	1.65	0.9508	0.9742	-0.000023
$T_w = cT_a{}^m$	1.13	0.98	0.9595	1.58	0.9517	0.9797	-0.071226

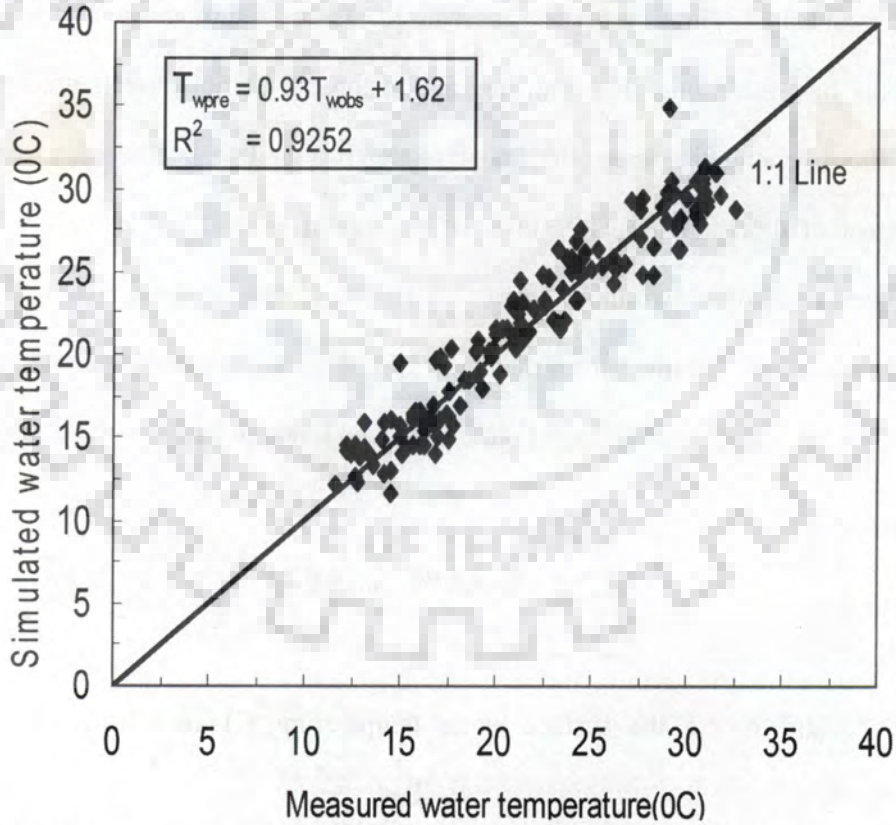

Fig.6.1. Plot of measured and simulated water temperature data fitted to 1: 1 line.

6.3.2 Estimation of Evaporation Rate

To estimate the evaporation rate from the Bowen ratio energy balance (BREB) method (Eq. 6.2), one requires the parameters R_n, G and β. These parameters are calculated using the required observed data in equations [(C.1) through (C.9), (C.10) and (C.11)] given in the Appendix-C. For example, R_n is calculated using Eqs. (C.1) through (C.10) one after anther, G is by Eq.(C.10), and β *is* by Eq.(C.11). The values of R_n and G computed from the daily data series range from 1.93 to 16.03MJ m^{-2}/day and 0.01 to 1.81MJ m^{-2}/day, respectively while β ranges between 0.06 and 0.08 with a mean of 0.07. Utilizing the daily values of R_n, G and β in Eq. (6.2), the daily evaporation rate is calculated.

To estimate the evaporation rate using the mass transfer (MT) method (Eq. 6.3) the parameters e_s, e_a, μ and U_2 are required. Using the required observed data, the daily value of e_s, e_a and U_2, is calculated employing Eqs.(C.13), (C.14) and (C.16), respectively (Appendix-C). The mass transfer coefficient, μ is determined in two ways: one from the relationship between the daily evaporation rate computed by the BREB model and daily the mass transfer product $(U_2\ (e_s - e_a)\ )$, and the other one, from the water surface area relationship using Eq. (C.15). The linear fitting (Fig. 6.2) describing relationship between the evaporation rates by the BREB method and $(U_2\ (e_s - e_a)\ )$ show a meager correlation $(R^2 = 0.49)$, which indicates that the MT method is not in agreement with the response of the BREB method. The values of μ vary between 2.21 and 2.81 with a mean of 2.35. The value of $\mu = 3.80$ determined from the water surface area relationship is found to be 61.70% higher than the value computed from the BREB method. Using the value of $\mu = 2.35$ *and* 3.80 and the computed daily values of e_s, e_a and U_2 in Eq.(6.3), the daily evaporation rate is calculated. This gives two sets of evaporation rate data; one for $\mu = 2.35$ termed as MT1, and another for $\mu = 3.80$ termed as MT2.

For estimation of the evaporation rate by the PT model, the parameters α, Δ and γ are required. These parameters are determined using the required observed data in Eqs.(C.17), (C.18) and (C.14), respectively (Appendix-C). The estimated values of α for the given period (2002-2005) vary between 1.29 and 1.32 with a mean of 1.31 against the normal value of 1.26. This small variation in the magnitude of α has negligible effect on the evaporation rate. Using both the values of α = 1.31 and 1.26, and the calculated daily value of Δ, γ, R_n, and G in Eq.(6.4), the daily evaporation rate is computed. It also gives two sets of evaporation rate data; one for α = *1.31* termed as PT1, and another for α = *1.26* termed as PT2.

For estimation of the evaporation rate by the PE method, the coefficient, K_p is to be known. It is determined from the ratio of daily evaporation rate computed by the BREB method to the daily observed Class A pan evaporation rate data. The estimated value of K_p ranges from 0.65 to 0.72. The average value of K_p = 0.65 is thus considered for computation of the pan evaporation rate. Using K_p = 0.65 and the daily data of Class A evaporation rate in Eq.(6.5), the actual daily evaporation rate is calculated.

The statistical properties, *viz.* range, mean, standard deviation, coefficient of variation and skewness of the daily evaporation rate estimated by each of the method for the period 2002-2005 are given in Table 6.2. It can be seen from Table 6.2 that the mean of the daily evaporation rate estimated by the BREB, PT, and PE method is in close agreement, while the MT method for both MT1 and MT2 deviates from other three. The coefficient of variation, C_v which is lowest for the BREB method, is also higher in case of the MT1 and MT2 than the other three methods (Table 6.2). A similar trend is also seen in the skewness of daily evaporation rate data series. While, the performances of the BREB, PT and PE method is comparable.

Table 6.2. Statistical values of the daily evaporation rates of the various evaporation methods computed using their average value of coefficient for the study period 2002 to 2005. [Std. is the standard deviation; and C_v is the coefficient of variation].

Model	Statistical parameters			
	Range	Mean ±Std.	C_v	Skewness
	mm/day	mm/day		
BREB	0.67-6.56	2.86 ±1.29	0.45	0.57
MT1	0.18-18.74	3.04 ±2.79	0.92	1.98
MT2	0.11-11.54	1.86 ±1.72	0.92	1.98
PT1	0.72-6.44	2.76 ±1.31	0.48	0.61
PT2	0.75-6.68	2.86 ±1.36	0.48	0.61
PE	0.52-7.39	2.86 ±1.17	0.49	0.84

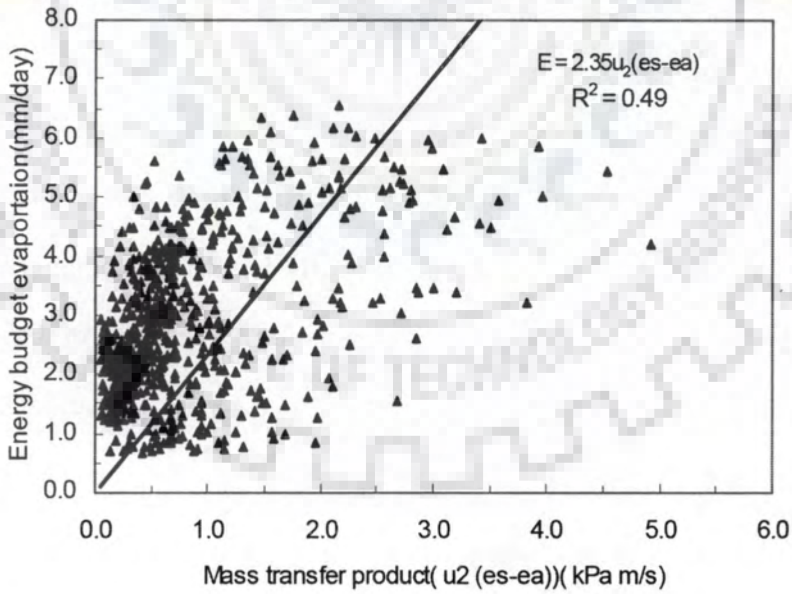

Fig. 6.2. Plot of daily evaporation rates by BREB versus mass transfer product during the period 2002 -2005

6.3.3 Comparison of Performances

To investigate the performance of all the four methods, coefficient of determination, R^2, index of agreement, D and relative bias, RB are considered as guiding factors. The values of these statistical properties, which are calculated from the evaporation rates exhibited by the BREB, MT (for μ=2.35 and 3.80), PE, PT (for $\alpha = 1.26$ and $\alpha = 1.31$) methods, are given in Table 6.3. Table 6.3 represents matrices of statistical possession obtained from the inter-comparison of different methods with respect to the BREB method. The column represents the targeted series, and the row describes the series being compared with the targeted one. The performance of one method over another for each of the statistical property is also ranked chronologically.

Table 6.3 reveals that there is a close agreement among the values estimated by the BREB, PE and PT methods. Both PT1 and PT2 are by and large in conformity with the BREB followed by the PE in all the four goodness-of-fit measures. The statistical performances of the PT1 and PT2 with respect to the BREB are: (i) R^2 = 0.9892 and 0.9893, (ii) D = 0.9928 and 0.9938, and (iii) RB = - 0.1065 and -0.0011. The PE method rank second in correlation with the BREB method (R^2 = 0.6805, D = 0.8200 and RB = 0.0002), while both MT1 and MT2 of the MT methods are poorly correlated with the BREB and the PT method, and show an improved correlation with the PE method (Table 6.3). The variation of the relative bias, RB for both PT1 and PT2 in comparison to the BREB method is insignificant (Table 6.3). The variation of the statistical properties, such as, R^2, D and RB of the PE for K_p = 0.65 in comparison to the BREB and the PT is marginal (Table 6.3), while the skewness and the coefficient of variation (Table 6.2) are higher than the BREB and the PT method. This indicates that the BREB and the PT method are superior to the PE method. In between the PT and the BREB method, the PT method is a simplified form of the BREB method with similarity in parameters, but the input data requirement for the PT method is less than the BREB method. If, the Bowen ratio, β of a specific region is known a

priori or determined externally, the PT method would prove more economic as well as promising than the BREB method.

Table 6.3. Statistics of different goodness of fit measures for different combination of methods (column: targeted series; row: series being compared)

Methods	BREB	PE	PT1	PT2	MT1	MT2
a) Coefficient of determination, R^2						
BREB	1.0000					
PE	0.6805 (4)	1.0000				
PT1	0.9892 (1)	0.7074 (2)	1.0000			
PT2	0.9893 (1)	0.7074 (2)	1.0000	1.0000		
MT1	0.4933	0.7034 (3)	0.5181	0.5181	1.0000	
MT2	0.4934	0.7034 (3)	0.5182	0.5182	1.0000	1.0000
b) Index of agreement, D						
BREB	1.0000					
PE	0.8200 (3)	1.0000				
PT1	0.9928 (1)	0.8343 (2)	1.0000			
PT2	0.9938 (1)	0.8333 (2)	0.9981	1.0000		
MT1	0.5924	0.6841	0.6127	0.6231	1.0000	
MT2	0.6320	0.7361 (4)	0.6576	0.6519	0.8867	1.0000
c) Relative bias, RB(mm)						
BREB	0					
PE	0.0002 (1)	0				
PT1	-0.1065 (4)	0.1067	0			
PT2	-0.0011 (2)	0.0013 (3)	0.1054	0		
MT1	0.1643	-0.1641	-0.2708	-0.1654	0	
MT2	-0.9937	0.9930	0.8873	0.9926	-1.1580	0

(*): represents rank.

6.4 CONCLUSIONS

1 Performances of the Bowen ratio energy balance (BERB), Mass transfer (MT), Priestley-Taylor (PT) and Pan evaporation (PE) method have been analyzed using measured meteorological data from the semi-arid region in Rajasthan. The PT method has been found superior and effective than the other three methods for estimation of evaporation rate for semi-arid region. The limited data requirement has qualified the PT model to supersede the BREB model.

2 The performances of the BREB, the PT and the PE method have been found nearly complementary to each other while the MT method deviated.

3 The Bowen ratio, β and the Priestley-Taylor coefficient, α has been estimated to be 0.07 and 1.31, respectively.

CHAPTER-7

INTEGRATION OF RUNOFF, EVAPORATION AND RECHARGE MODELS, AND FIELD APPLICATION

7.1 GENERAL

The water balance equation of the pond incorporating the time varying recharge, runoff, evaporation and rainfall components is given by Eq.(3.1) in Chapter-3. The derivations for estimation of the potential and the actual recharge rate for a constant depth of water in the pond are given by Eqs.(4.15) and (4.33), respectively in Chapter-4. The expression for estimating the surface runoff yield from rainfall is given by Eq.(5.16) in Chapter-5. The surface water evaporation estimation method identifying the Bowen ratio energy balance model as the superior one is described in Chapter-6. It is required to integrate the expression of each component into the water balance equation to derive a single equation for determining the unknown variable of interest such as; rate of recharge. The rate of recharge is a function of depth of water in the recharge pond, and is characterized by the simultaneous processes of runoff, rainfall, and evaporation in a specified period of time. The solution can therefore be sought in two ways; (i) by determining the time varying depth of water and then compute the corresponding recharge rate, and (ii) by straightway deriving the expression in terms of recharge rate. In either case, we have to derive the expression for two different sets of condition: one till the wetting front touches the water table, i.e., till the pond is hydraulically connected with the underneath aquifer, and the other one as the water table rises due to subsequent recharges after the pond is hydraulically connected to the aquifer.

7.2 TIME VARYING DEPTH OF WATER AND POTENTIAL RECHARGE RATE

Discretizing the time, t into n number of integer time step size, Δt, such that $t = n\Delta t$, and the water balance equation [Eq.(3.1)] in discrete form between the time domain (n-1)Δt and nΔt , can be written as:

$$\begin{aligned} &H(n\Delta t)\, A_{ws}(n\Delta t) - H(n\Delta t - \Delta t)\, A_{ws}(n\Delta t - \Delta t) \\ &= Q(n\Delta t)\, A_w\, \Delta t + P(n\Delta t) A_s\, \Delta t - E(n\Delta t)\overline{A}_{ws}\, \Delta t - Q_0(n\Delta t)\,\Delta t - R(n\Delta t)\overline{A}_{rs}\, \Delta t \end{aligned} \tag{7.1}$$

Notions are same as explained in Eq.(3.1). In Eq. (7.1),

$\overline{A}_{sw} = 0.5[A_{ws}(n\Delta t) + A_{ws}(n\Delta t - \Delta t)]$ and $\overline{A}_{rs} = 0.5[A_{rs}(n\Delta t) + A_{rs}(n\Delta t - \Delta t)]$.

Rearranging Eq.(7.1):

$$\begin{aligned} H(n\Delta t) \;=\; & H(n\Delta t - \Delta t)\, \frac{A_{ws}(n\Delta t - \Delta t)}{A_{ws}(n\Delta t)} \\ & + \frac{1}{A_{ws}(n\Delta t)}\left[Q(n\Delta t)\, A_w + P(n\Delta t) A_s - E(n\Delta t)\overline{A}_{ws} - Q_0(n\Delta t) \right]\Delta t \\ & - \frac{\overline{A}_{rs}}{A_{ws}(n\Delta t)}\, R(n\Delta t)\,\Delta t \end{aligned} \tag{7.2}$$

Substituting the recharge component, $R(n\Delta t)$ in Eq.(7.2) by Eq.(4.15) [Chapter-4], Eq.(7.2) yields to:

$$\begin{aligned} H(n\Delta t) = \;& H(n\Delta t - \Delta t)\, \frac{A_{ws}(n\Delta t - \Delta t)}{A_{ws}(n\Delta t)} \\ & + \frac{1}{A_{ws}(n\Delta t)}\left[Q(n\Delta t)\, A_w + P(n\Delta t) A_s - E(n\Delta t)\overline{A}_{ws} - Q_0(n\Delta t) \right]\Delta t \\ & - \frac{\overline{A}_{rs}}{A_{ws}(n\Delta t)} \left[\frac{ -\dfrac{K_s\left[H(n\Delta t) + \psi_f\right]}{2C_i} }{ \sqrt{ -\dfrac{K_s\left[H(n\Delta t) + \psi_f\right](n\Delta t)}{C_i \eta} + \left[H(n\Delta t) + \psi_f\right]^2 \left[\left(\dfrac{1 - B_i}{2C_i}\right)^2 - \dfrac{A_i}{C_i} \right] } } \right]\Delta t \end{aligned} \tag{7.3}$$

Eq.(7.3) has single unknown $H(n\Delta t)$ and several other $H(n\Delta t)$ dependent variables, viz. $A_{ws}(n\Delta t), A_{rs}(n\Delta t)$, A_i, B_i, and C_i. As the variable $H(n\Delta t)$ and its dependent variables appeared in different mathematical forms at the R.H.S of Eq.(7.3), therefore, separation of H(nΔt) in explicit form is a difficult task. $H(n\Delta t)$ from Eq.(7.3) can be solved by iteration. On the other hand, to determine H at the current time step $n\Delta t$, H at the previous time step $(n-1)\Delta t$ and its related components are to be known. Thus, $H(n\Delta t)$ from one time step to another can be solved in succession of time step as given in Appendix-D. Having $H(n\Delta t)$ computed, $R_p(n\Delta t)$ can be determined using Eq.(4.15).

$H(n\Delta t)$, in terms of $R_p(n\Delta t)$, from Eq. (4.15) [Chapter-4] can be written as:

$$H(n\Delta t) = \frac{\left[\dfrac{K_s\, t}{C_i\, \eta}\right] R_P^2(n\Delta t)}{\left[\left(\dfrac{1-B_i}{2C_i}\right)^2 - \dfrac{A_i}{C_i}\right] R_P^2(n\Delta t) - \left[\dfrac{K_s}{2C_i}\right]^2} - \psi_f \tag{7.4}$$

Substituting $H(n\Delta t)$ from Eq.(7.4) in the L.H.S. of Eq.(7.2), the expression in term of $R_p(n\Delta t)$ is given by:

$$R_P(n\Delta t) = \frac{\left\{\begin{array}{l} H(n\Delta t-\Delta t)A_{ws}(n\Delta t-\Delta t) + \psi_f A_{ws}(n\Delta t) \\ + \left[\, Q(n\Delta t)\, A_w + P(n\Delta t) A_s - E(n\Delta t)\overline{A}_{ws} - Q_0(n\Delta t) \right]\Delta t \end{array}\right\}}{\left\{\dfrac{\left(\dfrac{K_s\, t}{C_i \eta}\right)\overline{A}_{ws}\, R_P(n\Delta t)}{\left[\left[\left(\dfrac{1-B_i}{2C_i}\right)^2 - \dfrac{A_i}{C_i}\right] R_P^2(n\Delta t) - \left[\dfrac{K_s}{2C_i}\right]^2\right]} + \overline{A}_{rs}\, \Delta t\right\}} \tag{7.5}$$

In Eq.(7.5), the variable, $R_p(n\Delta t)$, which is to be determined, is also appeared both in the L.H.S and R.H.S. Further, to determine R_p at the current time step, $n\Delta t$, H at the previous time step $(n-1)\Delta t$ and its related components are to be known. Thus, for determining $R_p(n\Delta t)$; Eq.(7.5) is to be solved in succession of time step, following iteration in each time step.

Eqs.(7.3) and (7.5) are the required derivations to estimate the time varying depth of water and the potential recharge rate, respectively, which are valid till the wetting front touches the groundwater table.

7.3 TIME VARYING DEPTH OF WATER AND ACTUAL RECHARGE RATE

Substituting recharge component, *R(nΔt)* from Eq.(4.33) [Chapter-4] in Eq.(7.2); the expression for time varying H is given by:

$$\begin{aligned} H(n\Delta t) = {} & H(n\Delta t-\Delta t)\,\frac{A_{ws}(n\Delta t-\Delta t)}{A_{ws}(n\Delta t)} \\ & + \frac{1}{A_{ws}(n\Delta t)}\left[Q(n\Delta t)\,A_w + P(n\Delta t)A_s - E(n\Delta t)\overline{A}_{ws} - Q_0(n\Delta t)\right]\Delta t \\ & - \frac{\overline{A}_{rs}}{A_{ws}(n\Delta t)}\left[\frac{K_s\left[D_w + H(n\Delta t) - \sum_{\gamma=1}^{n-1}\frac{q_a(\gamma)\Delta t}{[4L(\gamma)W(\gamma)]}\,\delta_s[L(\gamma),W(\gamma),n-\gamma+1,\Delta t]\right]}{\left[D_w + K_s\,\Delta t\,\delta_s\left[L(n),W(n),1,\Delta t\right]\right]}\right]\Delta t \end{aligned} \tag{7.6}$$

In Eq.(7.6), the time is reckoned since the wetting front touches the water table. Eq.(7.6) has single unknown *H(nΔt)* and several other H(nΔt) dependent variables. The unknown *H(nΔt)* and dependent variables, $A_{ws}(n\Delta t)$ and $A_{rs}(n\Delta t)$ are appeared in different mathematical forms at the R.H.S of Eq.(7.6). *H(nΔt)* in such case, can be solved by iteration for each time step following the procedure given in Appendix-D, and in succession of time from one time step to another.

Separating *H(nΔt)* from Eq.(4.43) and replacing it in the L.H.S of Eq.(7.2), the expression the time varying actual recharge rate is given by:

$$R_a(n\Delta t) = \frac{H(n\Delta t-\Delta t)\,\dfrac{A_{ws}(n\Delta t-\Delta t)}{A_{ws}(n\Delta t)} + \dfrac{1}{A_{ws}(n\Delta t)}\left[Q(n\Delta t)\;A_w + P(n\Delta t)A_S - E(n\Delta t)\overline{A}_{ws} \;-Q_0(n\Delta t)\right]\Delta t + \left[D_w - \displaystyle\sum_{\gamma=1}^{n-1}\frac{q_a(\gamma)\Delta t}{[4L(\gamma)W(\gamma)]}\;\delta_s[L(\gamma),W(\gamma),n-\gamma+1,\;\Delta t]\right]}{\left[D_w/K_s + \Delta t\,\delta_s\left[L(n),\,W(n),\,1,\;\Delta t\right]\right] \;+\; \dfrac{\overline{A}_{rs}}{A_{ws}(n\Delta t)}\Delta t} \tag{7.7}$$

In Eq.(7.7), $A_{ws}(n\Delta t)$, $\overline{A}_{ws}(n\Delta t), \overline{A}_{rs}(n\Delta t)$, $\delta_s[L(n),\ W(n),\ 1,\ \Delta t]$ are $H(n\Delta t)$ dependent variable. Therefore i.e. $L(n) = L$ and $W(n) = W$. To determine R_a at the current time step, $n\Delta t$, H at the current $(n\Delta t)$ and the previous time step $(n-1)\Delta t$ and its related components are to be known.

Eqs.(7.6) and (7.7) are the required derivations for determining the time varying depth of water and the actual recharge rate, respectively for the rise in water table due to subsequent recharge after the pond is hydraulically connected to the aquifer.

Particular case: For a rectangular pond

For a rectangular pond, the water surface area and the recharge area will remain same during the recharge period, $n\Delta t$; *i e.,; and* $A_{ws}(n\Delta t) = A_{ws}(n\Delta t - \Delta t) = A_{rs}(n\Delta t) = A_s$; and $L(n)$ $W(n)$ will also remain same. In such case, Eqs.(7.4) through (7.7) will, respectively, reduce to:

$$H(n\Delta t) \;=\; H(n\Delta t-\Delta t) + \left[\frac{Q(n\Delta t)\,A_w}{A_s} + P(n\Delta t) - E(n\Delta t) \;-\; \frac{Q_0(n\Delta t)}{A_s}\right]\Delta t - \left[\frac{-\dfrac{K_s\left[H(n\Delta t)+\psi_f\right]}{2C_i}}{\sqrt{-\dfrac{K_s\left[H(n\Delta t)+\psi_f\right]\,(n\Delta t)}{C_i\eta} + \left[H(n\Delta t)+\psi_f\right]^2\left[\left(\dfrac{1-B_i}{2C_i}\right)^2 - \dfrac{A_i}{C_i}\right]}}\right]\Delta t \tag{7.8}$$

$$R_P(n\Delta t) = \frac{\left\{ \begin{array}{l} H(n\Delta t - \Delta t) + \psi_f \\ + \left[\dfrac{Q(n\Delta t) A_w}{A_s} + P(n\Delta t) - E(n\Delta t) - \dfrac{Q_0(n\Delta t)}{A_s} \right] \Delta t \end{array} \right\}}{\left\{ \dfrac{\left(\dfrac{K_s(n\Delta t)}{C_i \eta} \right) R_P(n\Delta t)}{\sqrt{\left[\left(\dfrac{1-B_i}{2C_i} \right)^2 - \dfrac{A_i}{C_i} \right] R_P^2(n\Delta t) - \left[\dfrac{K_s}{2C_i} \right]^2}} + \Delta t \right\}} \tag{7.9}$$

$$H(n\Delta t) = H(n\Delta t - \Delta t) + \left[\frac{Q(n\Delta t) A_w}{A_s} + P(n\Delta t) - E(n\Delta t) - \frac{Q_0(n\Delta t)}{A_s} \right] \Delta t - \left[\frac{K_s \left[D_w + H(n\Delta t) - \sum_{\gamma=1}^{n-1} \dfrac{q_a(\gamma)\Delta t}{[4 L W]} \delta_s[L, W, n-\gamma+1, \Delta t] \right]}{\left[D_w + K_s \Delta t\, \delta_s [L, W, 1, \Delta t] \right]} \right] \Delta t \tag{7.10}$$

and

$$R_a(n\Delta t) = \frac{H(n\Delta t - \Delta t) + \left[\dfrac{Q(n\Delta t) A_w}{A_s} + P(n\Delta t) - E(n\Delta t) - \dfrac{Q_0(n\Delta t)}{A_s} \right] \Delta t + \left[D_w - \sum_{\gamma=1}^{n-1} \dfrac{q_a(\gamma)\Delta t}{[4 L W]} \delta_s[L, W, n-\gamma+1, \Delta t] \right]}{\left[D_w / K_s + \Delta t\, \delta_s [L, W, 1, \Delta t] \right] + \Delta t} \tag{7.11}$$

A flow chart to determine the variable of an equation by iterative method when it appears both in the L.H.S. and R.H.S. of the equation is given in Appendix-D.

7.4 DATA REQUIREMENT

Application of Eqs.(7.4) and (7.7) to simulate the time varying depth of water and the corresponding recharge rate from a watershed dependent recharge pond will require the following data:

Components	Input parameters
Inflow rate, Q(t)	Rainfall- runoff data, area of watershed.
Evaporation rate, E(t)	Air temperature, water temperature, relative humidity, sunshine duration.
Potential recharge rate, $R_p(t)$	Geometry of the pond (shape, size and depth), saturated hydraulic conductivity (K_s), initial soil moisture content (θ_i), volumetric moisture content at near saturation(θ_s), fillable porosity (η), suction head (ψ_f).
Actual recharge rate, $R_a(t)$	Initial depth to groundwater table (D_w), storage coefficient of aquifer material(φ), saturated hydraulic conductivity (K_s)
Outflow from pond, $Q_o(t)$.	As per measurement
Pond data	Geometrical dimension of the pond such as; shape, length, width, side slope etc.

The relationships of geometrical variables for a trapezoidal pond are given in Appendix-E.

7.5 FIELD APPLICATION

To investigate the effectiveness of the derived mathematical models [Eqs. (7.4) and (7.7)], data collected during the years 2006 and 2007 from an experimental watershed in the semi-arid region of south-eastern, Rajasthan are used.

7.5.1 Study Area

The study area known by Badakhera (BK) watershed is located in the Bundi district of south-eastern Rajasthan, India, (Fig.7.1). It is a part of the Mej catchment, which is one of the catchments of the Chambal river basin. The Cambial River is one of the thirteen rivers of Rajasthan state. Geographically, it is located at 25^0 36' N latitude and 75^0 15' E longitudes with an average elevation of about 252m above the mean sea level. The total area of the watershed is 682.5 ha. The area is characterized mainly by dry semi-arid climate with an average annual rainfall of 574 mm (1997-2008), out of which about 90% is received during mid June through mid September. The summer (March through June) is characterized by high temperature of mean daily temperature of about 35^0C. The winter (November through February) normally remains cool and dry of mean daily temperature of about 15^0C. The depth to groundwater table varies considerably within the watershed: normally between 25m and 30m in the upper reach and 12-18m in the lower reach. And the monsoon runoffs generated from the watershed flow quickly out of the watershed leaving not much scope for aquifer recharge. In order to retain monsoon runoffs within the watershed and to recharge the runoffs to the underneath aquifer for augmentation of groundwater resource, the Central Soil and Water Conservation Research and Training Institute, Research Centre (CSWCRTI, RC), Kota (Rajasthan) under the Integrated Waste Land development Project had constructed a total of 36 small check dams of height ranges 2 to 3m across the gullies and 3 ponds at different locations in the Badakhera watershed. This watershed is under the pilot study of the CSWCRTI, RC. One of the three recharge pond having catchment area of 15.32 ha, as shown in Fig. (7.1), is selected for the experimental study.

The catchment area of the experimental pond has different land uses: about 9.20 ha (66% of 15.32 ha) is comprised of wasteland covered by sparse and thorny vegetation of *Ziziphus zuzuba and Prosopis juliflora,* and grasses of *Cencharus ciliaris* and *Dicanthium anulatum;* about 4.01 ha (26%) is agricultural land, and remaining 2.11 ha encompasses the rural residential and road areas, etc.. The soils in the watershed are black in color of recent alluvial origin, which belong to hyperthemic family of Chromusterts and Pellusterts under the vertisols. The spatial distribution of soils is clay loam at the upper reach and silty-clay loam at the lower reach of the watershed (Singh et al. 2004).

7. 5. 2 The Experimental Pond

The pond is of trapezoidal shape having side slope 1V: 0.5H, bottom dimension of 75m ×45m and maximum depth of 2.75m (Fig.7.1). The maximum storage capacity of the pond is 0.65 ha m. The embankment enclosing the pond is about 1.5 m above the normal ground surface. The monsoon runoff is the main source of water for the pond. The harvested monsoon runoffs in the pond are normally available for a short period (mid June through December). The inlet of the pond is equipped with a silt retention basin to prevent entry of silt from the catchment to the pond. To let off excess runoff, a rectangular weir has been installed as an outlet device. A photograph of the experimental pond can be seen in Fig.2.1(a) [chapter-2].

7.5.3 Measurements and Collection of Data

Although the pond was developed under a specific project of the CSWCRTI, RC, Kota, yet no databases about the pond and hydrological and hydrogeological measurements are available, except hydrometeorological data from an agricultural meteorological observatory located nearly 65km from the experimental pond. These hydro-meteorological data recorded twice a day at 07:00 hours and 14:30 hours at IST (Indian standard time) as per the guidelines prescribed by the India Meteorological Department (IMD) are namely; air temperature, relative humidity, wind speed and sunshine duration. The requirement of other data was fulfilled by field measurements and collections of relevant data under a special derive for this research study during different spells of the year 2006 and 2007. The data related to the hydrological characteristics of the pond's catchment, rainfall, pond's geometry, water temperature and water leveling the pond, soil samples below the pond's bed and the underneath aquifer, depth to groundwater level, etc. were collected by devising instrumentations and measurements.

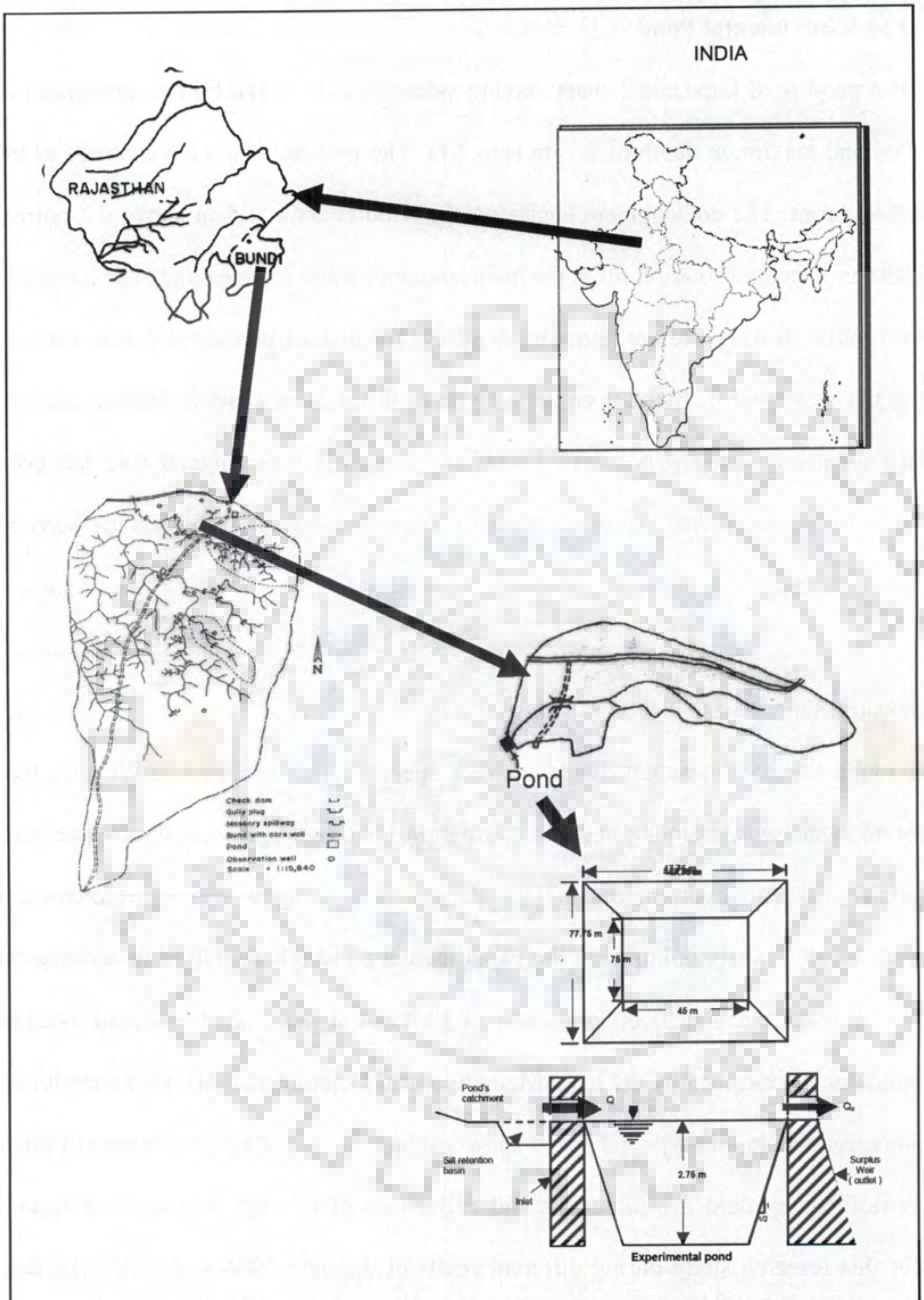

Fig. 7.1. Geographical location of the Badakhera watershed and the experimental pond.

For measuring rainfall a Tipping bucket type rain gauge was installed in the vicinity of the experimental pond site. The water temperature of the pond at 10 mm below the water surface was measured by water thermometer. For measurement of time-varying water levels in the recharge pond, a graduated staff gauge (with precision of 0.1cm) was installed at the centre of the pond. The staff gauge reading was observed manually from time to time. For monitoring groundwater level, two rotary drilled observation wells were installed at the down steam side of the recharge pond. First observation well was located at 2 m away from the edge of the pond, while second one is located at 30m away from the edge of the pond. Each observation well was cased with 150mm diameter and 4 kg/cm^2 pressure polyvinyl chloride (PVC) casing pipe. A 3.2 m long and 2.5mm slotted PVC screen was positioned at the lowest end of each well. The wells were penetrated up to 10m below the groundwater table to bracket the highest and lowest position of the water table in the wells. The groundwater levels from these observation wells were measured manually using a dip meter attached to an electrical sensor device that makes a sound on contact with water. The laboratory analysis of the soil samples collected during the drilling of the observation wells indicated that the aquifer material is of recent unconsolidated alluvial deposits consisting of mixture of clay, silt, sand, and pebbles. The thickness of this mixed deposit varies from 20-25m and represents an aquifer of unconfined type. Below 25 m, the formation is comprised of sandstone layer. The water level and the water temperature in the pond were monitored for the period since onset of the runoff accumulation and till depth of water in the pond reduced to a minimal height (about 10 to 30 cm). The water level in the pond and depth to water table in the observation wells were measured once daily at 7.00 hours, while the water temperature was measured twice a day at 07:00 hours and 14:30 hours. Thus, daily data of all the variables for 329 days in two consecutive years (2006-2007) were available.

To determine the saturated hydraulic conductivity, K_s of the bed material below the pond, infiltration tests were conducted when the pond remained completely emptied using standard double ring constant head infiltrometer. Infiltration tests were conducted at five places in the pond, one at the center of the pond and other four at the four middle edges of the pond. All necessary precautions generally required for a perfect infiltration test had been followed. The duration of the infiltration tests varied between 5 h and 9.5 h.

For determining the physical properties of the bed material below the pond such as; total porosity, initial moisture content and bulk density, undisturbed soil cores, each of 6 cm in diameter and 7.6cm in length collected from the upper soil layer (0-15cm) were analyzed in the laboratory. The bulk density was ascertained from the ratio of air-dried soil core mass to the core volume of that soil, while the initial moisture content was determined by the gravitational method that describes the ratio of mass of water in a soil sample to the dried mass of that soil sample. The total porosity was calculated using the relationship between the bulk density and particle density (Parker et al., 1999) as: $\phi = 1 - \rho_b / \rho_s$, where ρ_b is the dry bulk density of a sample; and ρ_s is the particle density of the sample and is considered to be 2.65gcm^{-3}.

The suction head, ψ_f was determined as follows: (i) soil samples collected from various locations inside the pond were first analyzed for ascertaining the particle size distribution, (ii) based on the particle size distributions, textural classes were ascertained employing the USDA soil textural classification criteria, (iii) making use of the identified textural classes of soils to the standard table describing representative value of ψ_f for different classes of soil textures, the value of ψ_f was determined.

7.6 RESULTS AND DISCUSSION

7.6.1 Rainfall-Runoff Modeling

The rainfall events occurred during the year 2006 and 2007 on the catchment of the pond given in Table F.2(a, b) (Appendix-F) shown in Fig. 7.2(a, b). It is evident from Fig. 7.2(a, b) that the effective monsoon months were largely lingered for three months, from mid-June to mid-September. The duration of the rainfall event was recorded for few minutes to several hours. In an average, there were about 25 rainfall events in each year, which exceeded the threshold value of 2.5mm/day (the limiting value of rainfall to categorize as a rainy day). The total monsoon rainfall during the years 2006 and 2007, respectively, was, 362.4 and 505 mm, which indicated an average daily rainfall of 14.5 mm/day and 20.2 mm/day respectively, against the minimum of 2.5 mm/day and maximum of 51mm/day during the year 2006, and minimum of 2.5 mm/day and maximum of 115mm/day during the year 2007. The runoff yields corresponding to each rainfall event are the inflows on the respective day to the pond

To estimate runoff yields, Q(t) resulted from the recorded rainfalls events, P(t) on the catchment area of the pond , the parameters *a*, b, and c of the proposed NAPI based model (Eq.5.17) are to be known *a priori*. Having known *a*, b, and c and by ascertaining NAPI corresponding to a rainfall event, Q(t) for each of the rainfall event can be determined using Eq.(5.16). The parameters a, b, and c are watershed specific, while the experimental watershed is an un-gauged one. These parameters are, therefore, estimated from the gauged micro-watershed located inside the BK watershed, and thereafter the estimated parameters are extended to the experimental watershed. The experimental watershed of area 15.32 ha and the gauged watershed of area 29.2 ha being parts of the BK watershed, the hydrological deviations between these two micro-watersheds can be propounded to be very negligible.

Employing the proposed NAPI based model (Eq. 5.16) to the rainfall-runoff data of the gauged micro-watershed together with the respective values of the rainfall based NAPI, derived using Eq.(5.10), the parameters are estimated by least squares approximation using Marquardt algorithm. The NAPI corresponding to a rainfall event is derived considering $k = 0.9$. Out of the total 42 rainfall–runoff events, 23 events are considered for calibration and remaining events are used for validation. The estimated value of the parameters is found to be: $a = -0.1625$; $b = 0.0046(mm^{-1})$ and $c = -0.0169$. The statistical correlations between the observed runoffs and the runoffs computed using the estimated value of the parameters is worked out as: coefficient of determination, $R^2 = 0.9914$, index of agreement, $D = 0.8893$ and relative bias, $RB = -2.6883$, which conform a close match between the two series. The parameters a, b, and c so obtained is considered as the value of the parameters for this experimental watershed.

Using these values of the parameters, *a*, b and c and ascertaining the NAPI corresponding to each rainfall event, runoff yield resulted from each rainfall event during the year 2006 and 2007 on the catchment of the experimental pond are computed and shown in Fig 7.2(a, b). It can be seen from Fig.7.2 (a, b) that the runoff yields from the pond's catchment vary between 10% and 42% of the corresponding rainfall events with a mean of 20%.

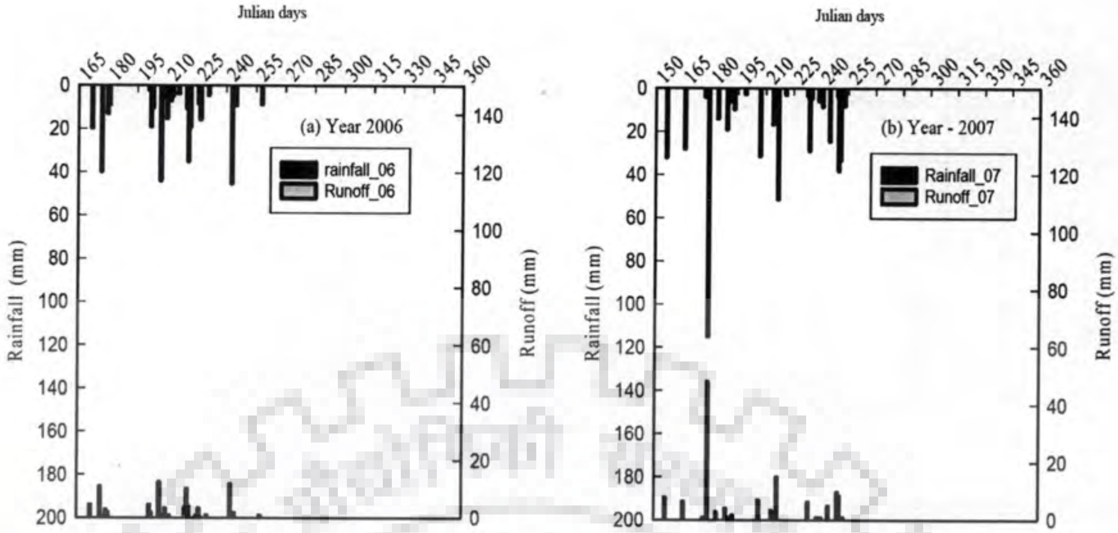

Fig.7.2. Rainfall events and the corresponding runoff yields generated using the proposed NAPI based model; (a) for the year 2006, and (b) for the year 2007.

7.6.2 Estimation of Evaporation Rate

To estimate the evaporation rate from the Bowen ratio energy balance (BREB) method (Eq. 6.2)[Chapter-6], the parameters R_n, G and β are required. Using the required observed data, the daily value of R_n, G and β is calculated employing equations [(C.1) through (C.8), (C.9) and (C.10) through (C.13)] given in the Appendix-C. R_n is calculated using Eqs.(C.1) through (C.9) one after anther, G is by Eq. (C.9) and β is by Eqs. (C.11) through (C.13). The values of R_n and G computed from the daily data series are found to be from 1.93 to 16.03MJ m^{-2}/day and 0.01 to 1.81MJ m^{-2}/day, respectively while β is estimated to be between 0.06 and 0.08. Utilizing the estimated daily values of R_n, G and β in Eq.(6.2), the daily evaporation rate is calculated. The variation of daily evaporation rates during the respective periods of the year 2006 and 2007 when the pond retained water is shown in Fig. 7.3(a, b). The surface evaporation rates are estimated to be varied from 1.2mm/day to 5.7 mm/day with a mean of 3.2 mm/day.

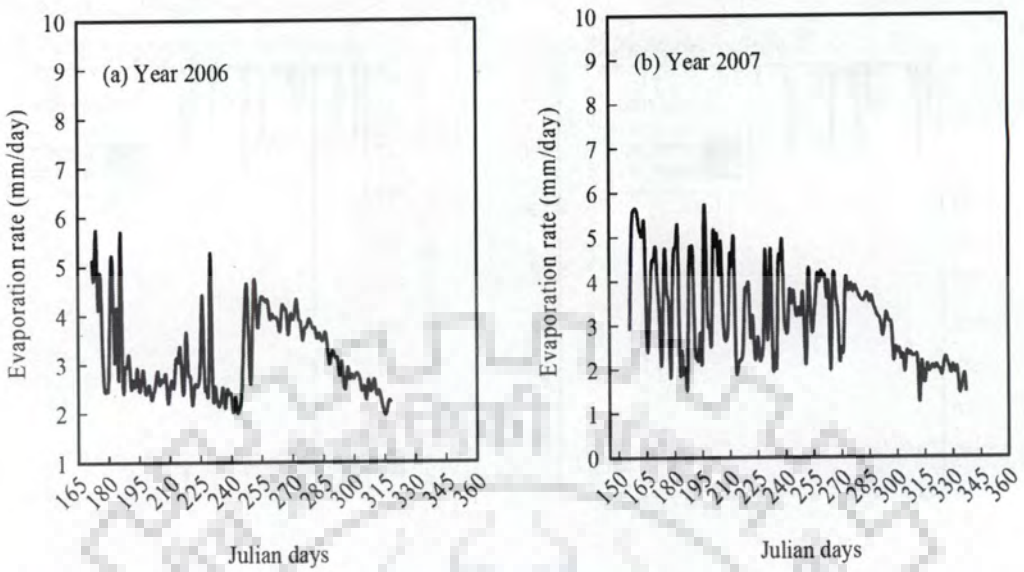

Fig.7.3. Variation of evaporation rate in the pond; (a) during the year 2006, and (b) during the year 2007.

7.6.3 Surplus Flow from the Pond

Surplus flow from the recharge pond is estimated using the formula of rectangular weir suggested by Murthy (1991) as; $q = 1.71 L_c H_f^{3/2}$, in which q is the rate of overflow over the crest of weir [m^3/s]; L_c is the length of crest[m]; and H_f is the depth of flow over the crest[m]. Volume of surplus flow is obtained by multiplying q with the time of flow of the surplus water. H_f was measured manually in the field for each the event, which exceeded the storage capacity of the pond. During the year 2006 and 2007, only 7 times in the year 2007 the pond had surplus flow, while there was no overflow during the year 2006.

7.6.4 Soil Properties

The saturated hydraulic conductivity, K_s is estimated utilizing the data of the infiltration tests in the Green-Ampt equation. For example, to estimate K_s from the Green-

Ampt model, one requires infiltration rate, cumulative infiltration and suction head. The infiltration rate and cumulative infiltration are known from the infiltration test, while suction head is known from soil textural class analysis. Making use of the particular dataset, K_s are estimated to be 0.94mmhr^{-1} for the year 2006 and 0.82mmh^{-1} for the year 2007. From the laboratory analysis of the soil samples, following characteristics and values of the soil properties are ascertained:

Soil properties	Estimated value
Soil textural class	Silty-clay
Bulk density, ρ_b (gm/cm^3)	1.48
Volumetric moisture content at near saturation, θ_s (cm^3/cm^3)	45.36 to 46.21
Suction head, ψ_f (m)	0.34
Initial soil moisture content, θ_i (cm^3/cm^3)	0.20

The depth to groundwater table below the pond is measured prior to the onset of the monsoon runoff in each year, and they are found at 5.2 m below in the year 2006 and 6.0 m below in the year 2007. These depths are considered as the initial depth to groundwater table in the respective year. The measured water table data indicated a time lag of 30 and 33 days between the initiation of recharge process and the rising the water table in the year 2006 and 2007, respectively. The horizontal hydraulic conductively, K and the storage coefficient, ϕ of the aquifer material are assumed to be equal to the bed material of the pond.

7.6.5 Simulation of Depth of Water in the Recharge Pond

We have time-variant water balance components of the pond P(t), Q(t), E(t) and Q_o(t) estimated; soil properties $K_s, \Psi_f, \eta, K, \theta_s, \theta_i$ and ϕ determined; pond geometry, and depth to groundwater table, D_w measured. The data of the respective year, 2006 and 2007, are extended separately to Eq.(7.3) that represents, the case till wetting front touches the groundwater table and Eq. (7.6) that explains the case of water table rise due to subsequent recharges after the pond is hydraulically connected to the aquifer. To simulate the variation of depth of water in the pond, H(t) consequent to the time-variant inputs acted during the years 2006 and 2007, following conditions and data are utilized.

Variables	Year : 2006	Year : 2007
Period of simulation	June 21 to November 14 (147 days)	June 6 to December 3 (182 days)
Initial conditions: (i) Depth of water in the pond (ii) Depth to ground water table (D_w).	(i) zero (ii) 5.2 m	(i) zero. (ii) 6.0 m
Time step size, Δt	1 day	1 day
Saturated hydraulic conductivity, K_s	0.94 $mmhr^{-1}$	0.82 $mmhr^{-1}$
Volumetric moisture content at near saturation, θ_s	45.36 ($cm^3\ cm^{-3}$)	46.21 ($cm^3\ cm^{-3}$)
Stresses: P(t), Q(t), E(t) and $Q_o(t)$	As computed for year 2006	As computed for 2007
Other Soil properties; Ψ, K, θ_i and ϕ	Ψ=0.34 m; K = K_s; θ_i = 0.20; $\phi = \eta$	Same, as in year 2006.
Pond geometry	Trapezoidal in shape. Bottom length = 75 m, width = 40 m; and depth = 2.75 m, Side slope = 1 V: 0.5 H	Same as in year 2006.

Procedure of Simulation

The procedure adopted for simulating the depth of water in the pond and the corresponding groundwater recharge rate are given below:

Case I: Estimation of time varying depth of water, H(t) and potential recharge, $R_p(t)$.

1. Depth of water in the recharge pond consequent to Q,(t) P(t), E(t), $Q_o(t)$, $R_p(t)$ is estimated using Eq.(7.3).

2. For the first time step Δt, i.e., n =1, considering H (0) = 0, L_f (0) = 0, the coefficients A_i, B_i and C_i of the first segment and the respective soil properties, the

depth of water in the recharge pond is estimated consequent to $Q(\Delta t)$, $P(\Delta t)$, $E(\Delta t)$ and $Q_0(\Delta t)$. After that, $L_f(\Delta t)$ is determined consequent to the time step Δt using Eq.(4.13). Thereafter, $L_f(\Delta t)/(H(\Delta t)+\psi_f)$ is ascertained to recognize the segmental equation. This segmental equation is considered for the next time step, i.e., $2\Delta t$.

3. $H(\Delta t)$ computed from step-2 form the initial head of water for the second time step, ($2\Delta t$.). Considering the inputs and outputs for the second time step, $H(2\Delta t)$ is determined by iteration as given in Appendix-D.

4. The subsequent $H(n\Delta t)$, n = 3,4,5… are calculated by repeating step 3 till L_f is equal to D_w.

5. The potential recharge rate, $R_p(n\Delta t)$, n =1,2,3….., for the corresponding $H(n\Delta t)$ are computed using Eq.(7.5).

6. The time for the wetting front to reach the water table is ascertained by the summation of time from the onset of recharge process till the wetting front touched the water table. The cumulative of inflows (Q_c), rainfalls(P_c), evaporations(E_c), out flows(Q_{oc}) and the potential recharge (R_{pc}) corresponding to this total time is estimated.

Case II: Estimation of actual recharge rate, R_a (t) and H(t)

1. The time at which the wetting front touches the water table is considered as the initial time for computation of $R_a(t)$. The depth of water in the pond corresponding to this initial time is considered as the initial depth of water.

2. Consequent to the stresses, $Q(n\Delta t)$, $P(n\Delta t)$, $E(n\Delta t)$ and $Q_0(n\Delta t)$, n =1,2,3…, of respective time steps, the head of water, $H(n\Delta t)$ in the pond for different time steps and the corresponding actual recharge rate, $R_a(n\Delta t)$ are computed in succession of

time step by iteration method as given in Appendix-D using Eqs.(7.6) and (7.7), respectively.

3. The cumulative of Q_c, P_c, E_c, Q_{oc} and the actual recharge, R_{ac} is ascertained considering the time from the onset of the actual recharge process and till end of the simulation period.

Extending the above procedures to the field data as given in section 7.6.5, $H(n\Delta t)$ and the corresponding $R_p(n\Delta t)$ and $R_a(n\Delta t)$ are computed for 147 and 182 days of the year 2006 and 2007, respectively. The computed $H(n\Delta t)$ are compared with the observed depth of water measured during the respective period of the year 2006 and 2007. The comparison is shown in Fig.7.4 (a, b). It can be seen from Fig. 7.4(a, b) that the simulated and the measured depth of water graphs match closely. To ascertain the goodness-of-fit between the simulated and the observed depth of water, statistical parameters R^2 and D and RB are estimated. The values of the statistical parameters (Table 7.1) also confirm a close match ($R^2 \geq 0.99$; and $D \geq 0.99$) between the simulated and the observed depth of water in the pond. It can also be seen from Table 7.1 that the proposed model slightly overestimated (RB > 0) $H(n\Delta t)$ for the period in year 2006 and slightly underestimated (RB< 0) for the period in year 2007 in comparison the observed values. Figure 7.5 showing 1:1 line between the observed and simulated $H(n\Delta t)$ in the pond also represents a close match. These clearly indicate the effectiveness and competence of the derived models [(Eqs. (7.3 and 7.6)]. The models can successfully be used to other areas to ascertain the groundwater recharge rate from a pond.

Table 7.1 Goodness-of-fit for different statistical measures computed between the observed and the simulated values of *H*

Years	R^2	D	RB
2006	0.9968	0.9984	0.0407
2007	0.9973	0.9985	-0.7376
Pool datasets	0.9975	0.9987	-0.4852

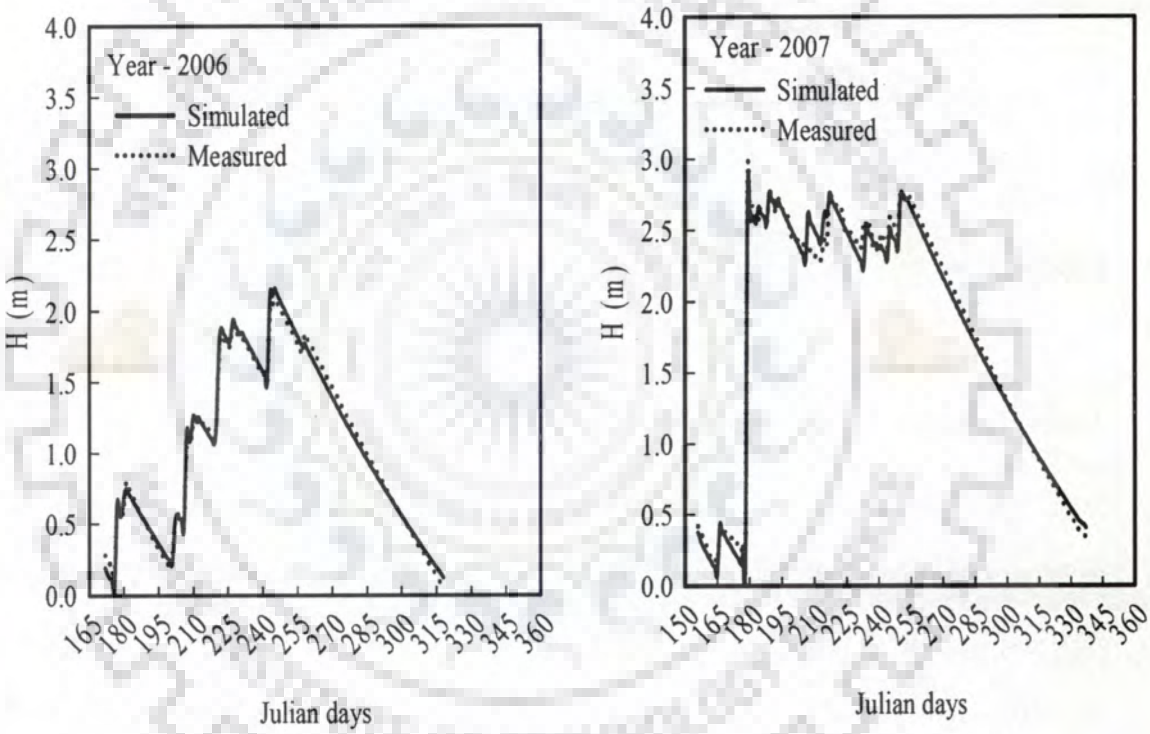

Fig.7.4. Comparison of the simulated values of *H* by the proposed models with the observed H of the experimental pond; (a) for the year 2006, and (b) for the year 2007.

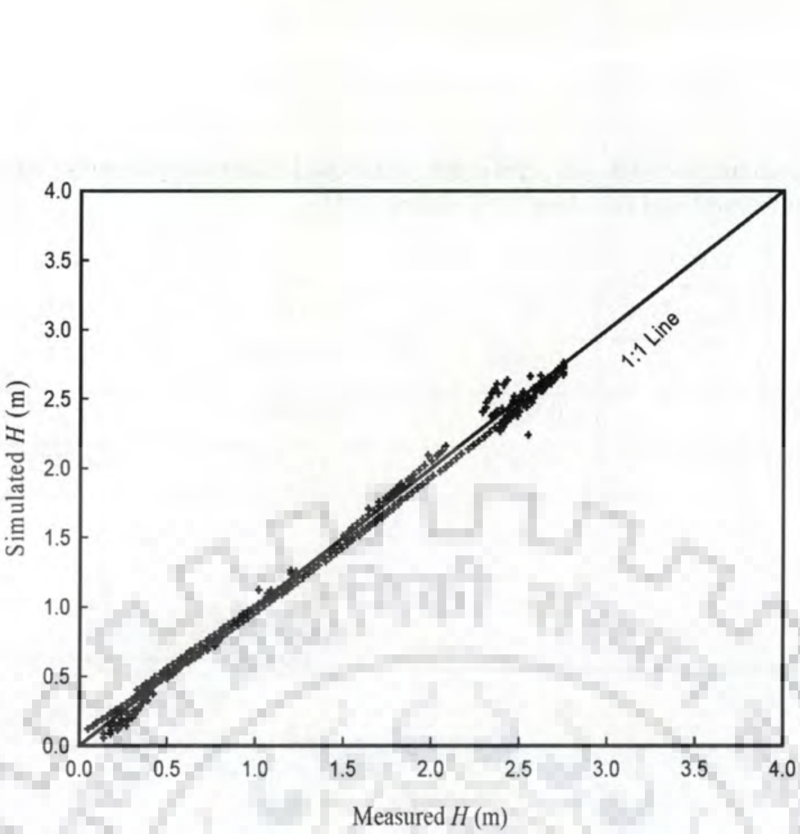

Fig.7.5. Relation between the observed and the simulated H in the experimental pond.

7.6.6 Estimation of Groundwater Recharge

Having computed the time varying depth of water, $H(t)$, the corresponding potential recharge rate, $R_p(t)$ and the actual recharge rate, $R_a(t)$ are computed using Eqs.(7.5) and (7.7) respectively . The computed profile of $R_p(t)$ and $R_a(t)$ for the respective period of the year 2006 and 2007 are given in Fig. 7.6(a, b). It can be seen from the figures that the recharge rate is high in the beginning of the recharge process and reduced gradually with time during the period 2006 and 2007. These are because, as the time progresses the potential difference of heads between the pond and the groundwater level reduced, which resulted in gradual decrease in the recharge rate. It can further be seen that the recharge rates fluctuated during the monsoon period. It is because of variation of inflows into the pond that in turn, changed the depth of water. These characteristics are in the expected line. The range and mean values of the groundwater recharge for the period 2006-2007 given in Table 7.2

indicate that the recharge rates varied between 0.019 and 0.051m/day with a mean of 0.025m/day.

The cumulative of the volumetric runoff into the pond Q_c, the rainfall over the pond P_c, the evaporation from the pond, E_c, the outflow from the pond Q_{oc} and the recharge through the pond's wetted surface, R_c are estimated from the volumetric rate of each component for each time interval. The graphs of variation of cumulative components of each variable are shown in Figs.7.7 (a, b) for the periods in the year 2006 and 2007. It can be seen from Figs. 7.7(a, b) that Qc and Q_{oc} sharply varied during the monsoon period (July–August) in both the years 2006 and 2007. The sharp rise in Q_c and Q_{oc}, respectively represent large volumetric inflows to and outflows from the pond. It can further be seen that there is a seasonal biasness in Q_c and Q_{oc} between 2006 and 2007. A similar trend in E_c and R_c component in the corresponding period of 2006 and 2007 is also noted (Fig.7.7). The cumulative groundwater recharge volume for the year 2006 and 2007 are estimated to be 11885 m^3 and 15542 m^3, respectively (Table 7.3) that gives a total of 27427m^3 of water with an average of 13714 m^3/year recharged artificially from the pond to the underneath aquifer during the period 2006-2007. The total loss of water from the recharge pond in the year 2006 and 2007 by the evaporation is worked out to be 1454 to 1861 m^3, respectively. The average storage in the recharge pond is estimated to be 94 m^3 at the end of the simulation period.

The dimensionless water balance partitioning factors, namely; the ratio of total volume of water recharged into the aquifer R_t to the total volume of inflows, which include: the volume of runoff into the pond and the volume of rainfall over the pond, (Q_t + P_t), i.e. $(R_t/(Q_t + P_t))$; the ratio of total volume of water loss by evaporation to the total volume of inflows, $(E_t/(Q_t + P_t))$; the ratio of total volume of outflows from the pond to the total volume of inflows $(Q_{ot}/(Q_t + P_t))$; and the ratio of total volume of water remained as storage in pond at the end of the simulation period to the total volume of inflows $(S_t/(Q_t + P_t))$ are estimated and given in Table 7.4. It can be seen from Table 7.4 that a large fraction of the accumulated runoffs into the pond that varied between 72% and 89% in the respective years has been recharged in to the aquifer, while the fraction of evaporation losses is found to be varied between 9% and 11% during the year 2006 and 2007, respectively. The fractions of outflows from the recharge pond and the storage in the pond are respectively varied between 0 (2006) and 12% (2007), and 1% of the total inflows.

Table 7.2. Statistical values of the recharge rate computed for the experimental pond for the year 2006 and 2007 by the proposed models.

Years	Simulation period (days)	Statistical values	
		Range(m/day)	Mean (m/day)
2006	147	0.020-0.051	0.025
2007	182	0.019-0.049	0.025
Pool dataset	329	0.019-0.051	0.025

Table 7.3. Estimated water balance components of the pond for the year 2006 and 2007

Years	Simulation period (days)	Water balance components					
		Q_t (m^3)	P_t (m^3)	E_t (m^3)	Q_{ot} (m^3)	R_t (m^3)	Storage (S_t) (m^3)
2006	147	12209	1205	1454	0	11885	+74
2007	182	19934	1679	1861	4096	15542	+113
Mean	165	16072	1442	1658	2048	13714	+94

Table 7. 4. Partition factors of the water balance components of the experimental pond for the year 2006 and 2007.

Years	Water balance partition factors(percent)			
	$\frac{R_t}{Q_t + P_t}$	$\frac{E_t}{Q_t + P_t}$	$\frac{Q_{ot}}{Q_t + P_t}$	$\frac{S_t}{Q_t + P_t}$
2006	88.60	10.84	0	0.56
2007	71.91	8.61	18.95	0.52
Mean	78.30	9.46	11.69	0.52

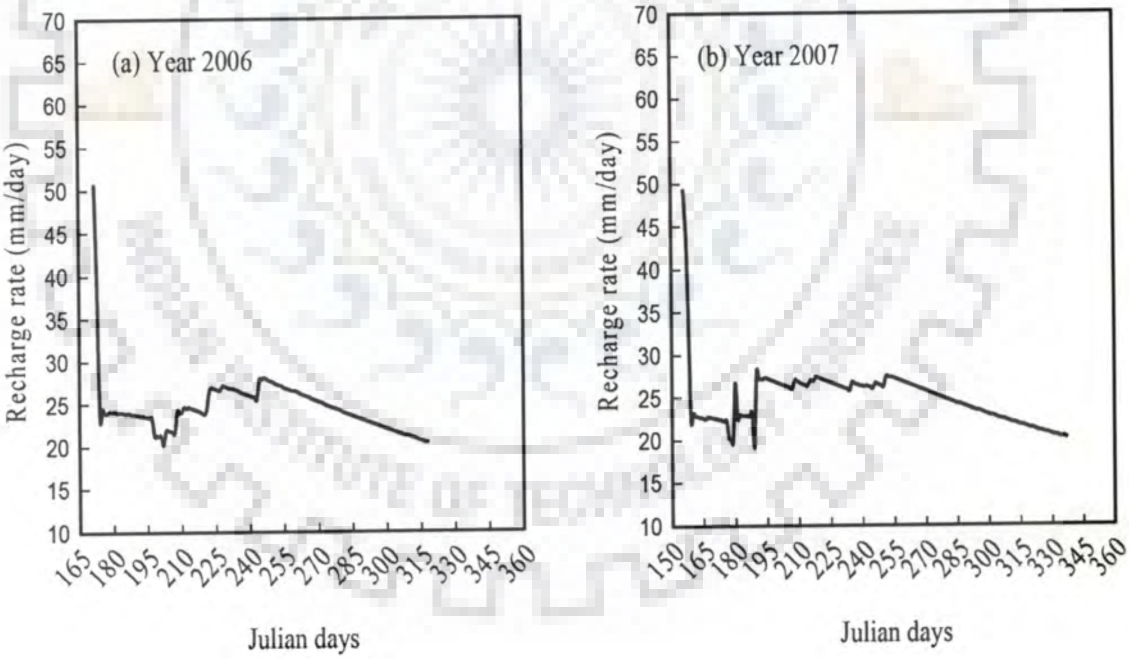

Fig.7.6. Variation of computed recharge rates of the experimental pond; (a) for the year 2006, and (b) for the year 2007.

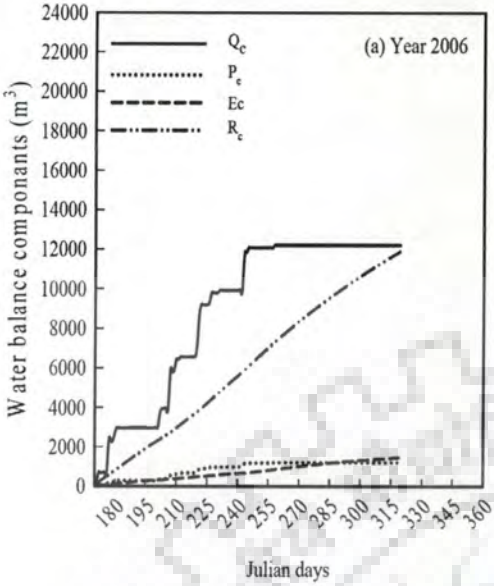

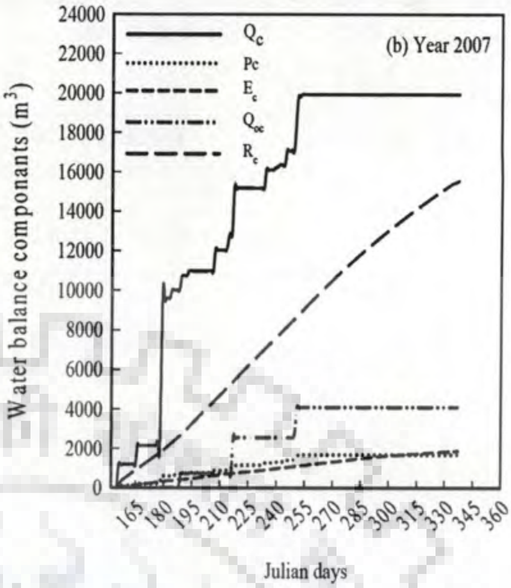

Fig.7.7. Variation of cumulative amount of water balance components of the experimental pond: (a) for the year 2006, and (b) for the year 2007.

7.7 CONCLUSIONS

1. Incorporating the rainfall-runoff, evaporation and recharge estimation models in the water balance equation of the pond, the integrated models for computing the time varying depth of water, the potential and the actual groundwater recharge rate have been derived.
2. The integrated models have been tested and validated by the data collected from an experimental pond located in the semi-arid area in Rajasthan. The instrumentations and data collections activities to fulfill the data requirement formed one of these challenging tasks of this research study.
3. The hydrological and hydro-meteorological data and subsurface soils samples collected from the field have been analyzed to ascertain the required input values.

4. The integrated models have been found effective to simulate the time varying depths of water in the pond and to estimate the potential and the actual groundwater recharge rate from the pond.
5. The comparison between the observed and the simulated depths of water by the integrated models showed a good correlation signifying $R^2 \approx 1$ and $D \approx 1$.
6. The derived integrated models can be extended to other field cases to determine the groundwater recharge for time varying depths of water in a pond.

CHAPTER-8

SUMMARY AND CONCLUSIONS

The components, namely (i) rainfall-runoff in a small catchment in a semi-arid region, (ii) evaporation from water surface in a small pond, and (ii) groundwater recharge from a shallow pond, of water balance equation for a recharge pond have been studied. The potential recharge rate from the pond has been derived based on the Green-Ampt infiltration model. The process level model for estimation of the actual recharge rate has been developed using the Hantush's analytical equation for predicting water table evolution due to constant recharge rate from a rectangular recharge basin. The runoff yields from rainfall events have been estimated from the water balance equation of a watershed using the concept of normalized antecedent precipitation index suggested by Heggen. By evaluating the performances of four commonly used evaporation methods, namely; Bowen ratio energy balance (BREB), Mass transfer (MT), Priestley-Taylor(PT) and Pan evaporation (PE), the most suitable and reliable model for estimation of the evaporation rate from the pond has been identified. The process level models developed are less data driven, easy to use and also capable of simulating the respective responses with a reasonable accuracy. These process level models have been incorporated in the water balance equation for a trapezoidal pond for estimation of the time varying depth of water in the pond and the corresponding potential recharge and the actual recharge rate from the pond.

The performances of the potential and the actual recharge rate estimation models have been analyzed using the published data of four textural soil groups. The performance of the rainfall-runoff model has been tested using the field data collected from the watersheds located in the semi-arid area in Rajasthan. The suitable evaporation estimation model applicable to semi-arid area has been selected by comparing the performances of the widely used models using four years observed data in a watershed in Rajasthan. The performances of the process level integrated model have been studied using the databases collected from an experimental trapezoidal pond located in the semi-arid area in Rajasthan. The experimental pond has specifically been instrumented for monitoring and collection of the required data for the present study. The field data collection and data analysis to ascertain required inputs for testing of the water balance model formed one of the major tasks in this dissertation work.

For evaluating the performance between two data series, the statistical parameters namely; coefficient of determination, index of agreement, percentage relative error, standard error of estimate, and relative bias have been chosen as the guiding factors.

Based on the study and analyses following conclusions are drawn:

1. Accurate estimation of the recharge component from an artificial recharge pond is indispensable to evaluate effectiveness of that pond for devising future groundwater development and management projects and for well field design, particularly for groundwater scarce areas like, Rajasthan.
2. For estimation of the position of advancing wetting front, L_f, approximating the logarithmic term, $ln\{1+L_f/(H+\psi_f)\}$ of the Green-Ampt model by the different second order polynomials, applicable in different ranges of $\lfloor L_f/(H+\psi_f)\rfloor$, five explicit expressions for L_f have been derived. The different ranges are: (i) $|x| \leq 1$; (ii) $1 < |x| \leq 5$; (iii) $5 < |x| \leq 15$; (iv) $15 < |x| \leq 50$; and (v) $|x| \geq 50$; where $x = L_f/(H + \psi_f)$. The coefficients of the polynomial in each segment have been

determined. Unlike estimation of L_f by the trial and error method as required in the GA model, the proposed polynomial expressions estimate L_f explicitly.

3. The solution for L_f has been used to estimate the time varying potential recharge. The responses of the potential recharge estimation model have been studied using published textural data of four soil groups. From the study it is found that recharge from a pond is significant if the subsoil is comprised of sand. For clay type sub soil recharge rate is insignificant. The generalized models for estimation of L_f and the potential recharge rate along with their values of the numerical factors have been determined. These generalized models can be used for estimation of L_f and the potential recharge rate for all ranges of soil groups.

4. The process level model for estimation of the actual recharge rate for time varying depth of water and water spread area has been developed using discrete kernel coefficients derived from Hantush's basic solution and applying the Duhamel's principle. The actual recharge has been estimated using data of four textural soil groups.

5. The Heggen's lumped NAPI based rainfall-runoff model has analytically been derived from the basic water balance equation. The Heggen's model has further been simplified to a rational form to make it comparable with the SCS-CN model. The simplified model has three watershed specific parameters, and requires rainfall and one rainfall dependent variable 'NAPI' as inputs to estimate runoff yields. The parameters of the model can easily be estimated from observed data of rainfall-runoff events using least squares optimization technique. The comparison of the Heggen's model and the proposed model with the SCS-CN model showed a superior match by the proposed model to the Heggen's model. The parametric characteristics of the proposed model described better resonance with the CN of the SCS model

than the Heggen's model. The proposed rainfall-runoff model can successfully be used for rainfall-runoff modeling in small watersheds.

6. The inter-comparison of the performances of four evaporation estimate models, namely; Bowen ratio energy balance (BREB), Mass transfer (MT), Priestley-Taylor (PT) and Pan evaporation (PE) has shown that the BREB, the PT and the PE model estimate evaporation rate from a pond very closely where as the MT model estimates higher/lower evaporation rate. In the present study, the BREB method has been used for the computation of evaporation rate, as the data required for use of the BREB model were available from the field investigation.

7. Integrating the process based models for estimation of the potential and actual recharge, runoff from a watershed and evaporation from a shallow pond, a water balance equation in a trapezoidal pond has been carried out for simulating the time varying depth of water in a pond from which the potential and actual groundwater recharge have been computed. Performance of the water balance model has been tested successfully using the experimental field data obtained from the experimental trapezoidal pond and its watershed located in the semi-arid region in Rajasthan. The observed and the simulated depths of water in the experimental pond have shown a close agreement. The potential and the actual recharge rates estimated based on the simulated time varying depth of water indicate the effectiveness of the artificial recharge through pond.

8. It has been found that during the year 2006 and 2007, out of the total accumulated runoffs in the pond, the components of water balance of the pond have been estimated to be, 78 percent as the recharge to the aquifer, 9 percent as the loss due to water surface evaporation, 12 percent as the surplus flow from the pond, and 1 percent as the storage in the pond.

8.1 MAIN CONTRIBUTIONS FROM THIS STUDY

The main contributions from this research study are as follows:

1. Process level models expressing explicit equations for prediction of advancement of wetting front, seepage rate and potential recharge rate have been presented.
2. A process based model for estimation of actual recharge rate from a pond in which depth of water and wetted perimeter change with time, has been developed.
3. A simple NAPI based rainfall-runoff model for predicting runoff yields from small watersheds has been proposed.
4. A suitable evaporation estimate model applicable to the arid and semi-arid areas in Rajasthan has been suggested.
5. An integrated process based model for estimation of potential and actual recharge rate from an artificial groundwater recharge pond has been presented.

REFERENCES

1. Abbott, M. B., Bathurst, J. C. Cunge, J. A., O'Connell, P. E., and Rasmussen, J. (1986a). An introduction to the European Hydrological System-systeme Hydrologique European, "SHE", 1. History and Philosophy of a physically-based, distributed modeling system. *J. Hydrol.*, **87**: 45-59.
2. Abdulrazzak M.J. and Morel-Seytoux, H.J.(1997). Groundwater recharge estimation from ephemeral streams: case study: wadi Tabalah, Soudi Arabia, *Hydrol. Process.*, **11**:1607-1619.
3. Abdulrazzak, M.J and Morel-Seytoux, H.J. (1983). Recharge from an ephemeral stream following wetting front arrival to water table. *Wat. Resour. Res.*, **19:**194-200.
4. Abtew, W. (2001). Evaporation estimation for Lake Okeechobee in south Florida. *J. Irri. Drain. Eng., ASCE*, **127**(3): 140-146.
5. Ali shakir, and Sharda, V.N. (2008) A comparison of curve number based methods for runoff estimation from small watersheds in a semi-arid region of India. *Hydrol. Res.*, **39**(3): 191-200.
6. Ali Shakir, Ghosh, N. C., and Singh, Ranvir (2009). Rainfall-runoff simulation using normalized antecedent precipitation index. *Hydrol. Sci. J.*, **55**(2): (*in press*).
7. Ali, S., Ghosh, N.C., and Singh, R. (2008), Evaluation of evaporation estimate model for water surface evaporation in semi-arid region, India. *Hydrol. Process.*, **22(8)**:1093-1106.
8. Ali, Shakir, Singh, K.D., Prasad, S.N., Kumar, A. and Mewar, Suresh (2002). Traditional water harvesting system in south -eastern Rajasthan. *J. wasteland,* **18**(2): 59-61.
9. Allen, R. G., Pereira, L. S., Raes, D., and Smith, M.(1998). Crop Evapotranspiration: guidelines for computing crop water requirement. *FAO Irrigation and Drainage Paper No.56, Food and Agricultural Organization of United Nations*, Rome.
10. Al-Muttair, F. F., and Al-Turbak, A. S. (1989). Estimation of recharge from a reservoir using two water budget models. *Water Resour. Bull.,* **25**(4): 727-732.
11. Amorocho, J., and Hart, W. E. (1964). A critique of current methods of hydrologic system investigation. *EOS trans. Am. GeophyS. Union*, **45**: 141-166.
12. Anderson, E. R. (1954). *Energy - budget study. US Geological Survey Professional Paper,* **269**: 71-119.

13. Angstrom, A. (1956). On the computation of global radiation from records of sunshine. *Ark. Geofys.*, **2**(22): 471-476.
14. Asano, T. (1992). Artificial recharge of groundwater with reclaimed municipal wastewater: current status and proposed criteria. *Wat. Sci. Tech.*, **25**: 87-92.
15. ASCE Task Committee on Application of Artificial Neural Networks in Hydrology. (2000). Artificial Neural Networks in Hydrology I: Preliminary concept. *J. Hydrol. Eng.*, **5**(2): 115-123.
16. Asmar, B. N., and Ergenzinger, P. (1999). Estimation of evaporation from Dead Sea. *Hydrol. Process.*, **13**: 2743-2750.
17. Assouline, S., and Mahrer, Y. (1993). Evaporation from lake Kineret 1. eddy correlation system measurements and energy budget estimates. *Water Resour. Res.*, **29**(4): 901-910.
18. Barry, D.A., Parlange, J.Y., Sander, G.C., and Sivapalan, M.(1995), Comment on explicit expression for Green-Ampt(delta function diffusivity) infiltration rate and cumulative storage. *Water Resour. Res.* , **31**(5): 1445-1446.
19. Barry, P. J., and Robertson, E. (1975).The energy budget of Perch lake in hydrological studies on small basin on the Canadian shield, edited by *P.J.Barry, Rep, AECL-5041/II, pp-376-415*, Chalk River Nucl. Lab, Chalk River, Ont., Canada.
20. Basha, H.A. (2000). Simple nonlinear rainfall-runoff model. *J. Hydrol. Eng.*, **5**(1):25-32.
21. Baumann, P. (1952). Groundwater movement controlled through spreading. *Trans. ASCE,* **177**(5): 1024-1060.
22. Benson, S. J.(1986). The sensitivity of evaporation rate to climate change-results of an energy-balance approach. *U.S. Geological Survey Water Resour. Invest.,* 86 - 4148, 40p.
23. Beven, K. J., Calver, A., and Morris, E. M. (1987). The institute of hydrology distributed model. Rep. 81, Institute of Hydrology, Wallingford, UK.
24. Bianchi, W.C., and Muckel, D.C. (1966). *Groundwater Recharge Hydrology*. U.S. Department of Agriculture, Agriculture Research Service Pub. No. 41-161.
25. Bishop, C. M. (1994). Neural networks and their applications. *Rev. Sci. Instrum.,* **65**: 1803-1832.
26. Bose, R. K., Vasudevan, N., Sinha, P. K. and Gupta, S. (1998). Water, In: India's Environment pollution and Protection Report No. 1997/ed/52. The Energy and Resources Institute, New Delhi.(Chapter 3).

RESEARCH PUBLICATIONS

Following publications have been made from this research work:

1. Ali, Shakir, Ghosh, N.C., and Singh, Ranvir (2008). Evaluation of evaporation estimate model for water surface evaporation in semi-arid region, India. *Hydrol. Process.*, **22**(8):1093-1106.

2. Ali Shakir, Ghosh, N. C., and Singh, Ranvir (2009). Rainfall-runoff simulation using normalized antecedent precipitation index. *Hydrol. Sci. J.*, **55**(2): (*in press*).

3. Ali, Shakir, Singh, Ranvir, Ghosh, N. C., and Somasundaram, J. (2009). Estimating saturated hydraulic conductivity of recharge structures in a small watershed. *Hydrol. J. IAH* (accepted).

27. Boszany, M. (1989). Generalization of SCS curve number method. *J. Irrig. Drain. Eng., ASCE,* 115(1): 139-144.

28. Boughton, W. C. (1984). A simple model for estimating the water yield of ungauged catchments. *J. Civ. Eng. Trans. Inst. Eng. Aust.,* **CE26**(2):83-88.

29. Boughton, W. C. (1968). A mathematical catchments model for estimating runoff. *J. Hydrol. (N.Z.),* **7**(2): 75-100.

30. Bouwer, H. (1978) *Groundwater Hydrology*. 1st ed. New York, wiley.

31. Bouwer, H. (1962). Analyzing groundwater mound by resistance network. *J. Irrig. Drai. Div., ASCE,* **88**(RJ3): 15-36.

32. Bouwer, H. (2002). Artificial recharge of groundwater: hydrogeology and engineering, *Hydrogeol. J.*, **10**: 121-142.

33. Bouwer, H. (1969). Infiltration of water into non-uniform soils. *J. Irrig. Drain. Eng., Div. ASCE,* **95**(IR4): 451-462.

34. Bowen, I.S. (1926). The ratio of heat losses by conduction and evaporation from any water surface. *Physical Review*, **27**: 770-787.

35. Brutsaert, W. (1982). Evaporation into atmosphere: *Theory, History, and Applications.* D. Reidel Publishing Company, Boston, Massachusetts.

36. Brutsaert, W., and Stricker, H. (1979). An advection-aridity approach to estimate actual regional evapotranspiration. *Water. Resour. Res.*, 15(2): 443-450.

37. Burman, R. D., and Pochop, L. O. (1994). Evaporation, Evapotranspiration and climatic data. Development in atmospheric science, vol 22, *Elsevier Science,* Amsterdam, The Netherlands.

38. Campolo, M., Andreussi, P., and Soldati, A. (1999). River flood forecasting with a neutral network model. *Water Resour. Res.,* **35**(4): 1191-1197.

39. CGWB (Central Ground Water Board), (1994), Manual on artificial recharge of Groundwater, Technical Series: Monograph No.3, *Ministry of Water Resources, Government of India* ,PP 215.

40. Chahar, B.R. (2006). Analytical solution to seepage from a soil channel with a curvilinear bottom. *Water Resour. Res.*, **42**: W01403, doi:10.1029/2005WR004140.

41. Chahar, B.R. (2007). Seepage analysis from polygonal canals. *J. Hyd. Div., ASCE,* **133**(4):451- 460.

42. Chaudhary. M. and Chahar, B.R. (2007). Recharge/seepage from an array of rectangular channels. *J. Hydrol.,* **343**: 71-79.

43. Chen, L., and Young, M.H. (2006). Green-Ampt infiltration model for sloppy surfaces. *Water Resour. Res.,* **42**: W07420. dot:10.1029/2005WR004468.

44. Chiew, F. H. S., Stewardson, M. J., and McMohan, T. A. (1993). Comparison of six rainfall-runoff modeling approaches. *J. Hydrol.,* **147**: 1-36.

45. Childs, E.C, and Bybordi, M. (1969). The vertical movement of water in stratified porous material 1. Infiltration. *Water Resour. Res,.* **5**(2):446-459.

46. Coulibali, P., Hache, M., Fortin,V., and Bobee B. (2005). Improving daily reservoir inflow forecasts with model combination. *J. of Hydrol. Eng., ASCE.,* **10**(2) : 91-99.

47. Dagan, G., and Bresler, E. (1983). Unsaturated flow in spatially variable fields I-Derivation of models of infiltration and redistribution. *Water Resour. Res.*, **19**(2): 413-420.

48. Dalton, J. (1802). Experimental essays on the constitution of mixed gases: on the force of steam or vapour from water or other liquids in different temperatures, both in a Torricelli vacuum and in air; on evaporation; and on expansion of gases by heat, Manchester Lit. Phil. Soc. Mem. Proc. **5**:536-602.

49. Dawson, C. W., and Wilby, R. E. (1998). An artificial neural network approach to rainfall-runoff modeling. *Hydrol. Sci. J.*, **43**: 47-66.

50. de Silva, C.S., and Rushton, K.R. (2007). Groundwater recharge estimation using improved soil moisture balance methodology for a tropical climate with distinct dry seasons. *Hydrol. Sci. J.,* **52**(5): 1051-1067.

51. de Vries, J. J., and Simmers, I.(2002). Groundwater recharge: an overview of processes and challenges. *Hydrogeol. J.*, **10**: 5-17.

52. deBruin, H.A.R. (1979). A simple model for shallow lake evaporation. *J. Appl. Meteorol.*, **17**: 1132-1134.

53. deBruin, H.A.R., and Keijman, J.O. (1978). The Priestley-Taylor evaporation model applied to large shallow lake in the Netherlands. J. evaporation. *J. Appl. Meteorol.,* **18**: 898:903.

54. Descroix, L., Nouvelot, J. F., and Vauclin, M. (2002) Evaluation of an antecedent index to model runoff yield in the western Sierra Madre (North-west Mexico). *J. Hydrol.,* **263:** 114-130.

55. Dingman, S.L. (1994). *Physical Hydrology*. Macmillan, New York.

56. Doorenbos, J., and Pruitt, W.O. (1977). Crop water requirement. Irrig. Drain. Paper No. 24, FAO (United Nations), Rome, pp.144.

57. Dowson, C. W., and Abrahat, R. J. (2007). Evaluation of two different methods for the antecedent precipitation index in neural network river stage forecasting. *Geophys. Res. Abstract,* **9:** 07522.

58. Eagleson, P.S.(1978). Climate, soil and vegetation. A simplified model of soil moisture movement in the liquid phase. *Water Resour. Res.,* **14**(5): 722-730.

59. Eaton, A. K., Rouse, W. R., Lafleur, P. M., Marsh, P., and Blanken, P. D. (2001). Surface energy balance of the western and central Canadian subarctic: variation in the energy balance among five major tarrain types. *J. climate,* **14**: 3692-3698.

60. Enciso-Medina, J., Martin, D. and Eisenhauer,D.(1998). Infiltration model from furrow irrigation. *J. Irrig. Drain. Eng.,* **124**(2): 73-80.

61. Fahimuddin, M, Mishra, G.C., and Kansal, M.L. (2009). Groundwater Recharge through a Multiaquifer Shaft near a Flooding Stream. *J. Hydrol. Eng.,* **14**(1): 84-90.

62. Fayer, M.J. (2000). UNSAT-H Version3.0; unsaturated soil water and heat flow model. Publ. PNNL-13249, Richland, Washington, Pacific Northwest National Laboratory.

63. Fedora, M. A., and Beschta, R. L. (1989). Storm runoff simulation using an antecedent precipitation index (API) model. *J. Hydrol.,* **112**: 121-133.

64. Fitzgerald, D. (1886). Evaporation. *Trans. Am. Soc. Civ. Eng.,* **98**(HY12): 2073-2085.

65. Flerchinger, G.N.Watt, F.J., Bloomsburg, G.L. ((1988). Explicit solution to Green-Ampt equation for non-uniform soils. *J. Irrig. Drain. Eng.* ASCE, **114**(3): 561-565.

66. Freeze, R. A., and Harlan, R.L. (1969). Blueprint for physically-based, digitally-simulated hydrologic response model. *J. Hydrol.,* **9**: 237-258.

67. Freyberg, D. L., Reeder, J. W., Franzini, J. B., and Remson, I. (1980) Application of Green-Ampt model to infiltration under time dependent surface water depths. *Water. Resour. Res.,* **16**(3): 517-528.

68. Gale, I.N., Newmann, I., Calow, R.C., and Moench, M. (2002). The effectiveness of artificial recharge of groundwater: a review. British Geological Survey Report CR/02/108N, pp 51. British Geological Survey Keyworth England.

69. Ganji, A., Khalili, D., Karamouz, M., Ponnambalam, K., and jawan, M. (2008). A fuzzy stochastic dynamic Nash game analysis of policies for managing water allocation in a reservoir system. *Water Resour. Manage.,* **22**:51-66.

70. Garen, D., and moore, D.S. (2005). Curve number hydrology in water quality modeling, use, abuse and future directions. *J. Am. Water Resour. Assoc.,* **41**(2): 377-388.

71. Garg, N.K., and Ali, A. (2000). Groundwater management for lower Indus basin. *Agric. Water Manage,* .**42**(3): 273-290.

72. Garg, S. K. (1987). *Hydrology and Water Resources Engineering.* 7th edition, Khanna Publishers, New Delhi.

73. Glover, R.E. (1960). Mathematical derivation as pertain to ground water recharge. Agriculture Research Service, USDA, Ft. Collins, Colo.

74. Govindraraju, R. S., Kavvas, M. L., Jones, S. E., and Rolston, D. E. (1996). Use of Green- Ampt model for analyzing one- dimension convective transport in unsaturated soils. *J. Hydrol,,* **178**: 337-350.

75. Goyal, R., and Chawala, A.S. (1997). Seepage from canals with infiltration from free surface zone. *J. Irrig. Drai. Eng., ASCE,* **123**(4): 257-263.

76. Goyal, V.C., Rai, S.P., and Kumar, V. (2002). Hydrological evaluation of groundwater contribution in Mansar lake (Jmmu &Kashmir). *Hydrol. J.,* **25**(4): 81-88.

77. Grayson, R. B., Moore, I. D., and MacMogan, T.A. (1992). Physically based hydrologic modeling-2. Is the concept realistic?. *Water Resour. Res.,* **28**(10): 2659-2666.

78. Green, W. H., and Ampt, G. (1911). Study in soil Physics. I. The flow of air and water through soils. *J. Agric. Sci.,* **4**: 1-24.

79. Greskowiak, J., Prommer, H., Massmann, G., Johnston, C. D., Nutzmann, G., and Pekdeger, A. (2005). The impact of variably saturated conditions on hydrogeological changes during artificial recharge of groundwater. *Applied Geochemistry*, **20**:1409-1426.

80. Gua, J.C.Y (2001). Design of circular infiltration basin under mounding effects. *J. water Resour. Plan. Manage.,* **127**(1): 58-65.

81. Guitjens, J. C. (1982). Model of alfalfa yield and evapotranspiration. *J. Irri. Drain. Div., ASCE.,* **108**(IR3): 212-222.

82. Haan, C.T., (1972). A water yield model for small watersheds. *Water Resour. Res.* **8**(1): 58-69.

83. Haan, C.T., Allred, T. B., Storm, D.E. Sabbagh, G. J. and Prabhu, S.(1995). A statistical procedure for evaluating hydrologic/water quality models. *Trans. ASAE,* **38**(3): 725-733.

84. Haltiner, J. P. and Salas, J.D. (1988). Short-term forecasting of snow melt runoff using ARMAX models. *Water Resour. Bull.*, **24**(5): 1083-1089.

85. Hantush, M.S. (1967). Growth and decay of groundwater mounds in response to uniform percolation. *Water Resour. Res.*, **3:** 227–234.

86. Harbeck, G. E. (1962). A practical field technique for measuring reservoir evaporation utilizing mass-transfer theory. US Geological Survey Professional Paper272-E,7. US Government Printing Office, Washington, D.C. PP.101-105.

87. Harbeck, G.E. et al. (1954). Water losses investigations Vol. I. Lake Hefner studies. U.S. Geological Survey Paper 269. US Government Printing Office, Washington, D.C.

88. Harbeck, G.E. et al. (1958). Water losses investigations, Lake Mead studies. U.S. Geological Survey Paper 298. US Government Printing Office, Washington, D.C.

89. Hawkins, R.H. (1978). Infiltration and curve numbers: Some pragmatic and theoretical relationships. *Proc., ASCE Irrig. Drain. Div. Symp. on watershed management, ASCE*, New York, Vol. II, 925-937.

90. Heggen, R. J. (2001). Normalized antecedent precipitation index. *J. Hydrol. Eng. ASCE*, **6**(5): 377-381.

91. Helweg, O. J. (1985). Role of artificial recharge in groundwater basin management. In: *Artificial recharge of groundwater,* ed T. Asano, Butterworth Publisher, Boston, USA.

92. Henderson-Sellers, B. (1986). Calculating the surface energy balance for lake and reservoir modeling: A review. *Review of Geophysics*, **24**: 625-649.

93. Hillel, D. (1990). *Application of Soil Physics.* Academic Press, Inc., New York.

94. Hjelmfelt, A.T. Jr. (1991). Investigation of curve number procedure. *J. Hydraulic Engineering,* **117:** 725-737.

95. Horton, R.I. (1933). The interception and application of runoff plot experiments with reference to soil erosionproblems. *Proc. Soil Sci. Soc.Am.,* **3**:340-349.

96. Horton, R.E. (1917). Rainfall interception. *Monthly Weather Rev.,* **47**(9): 603-623.

97. Hostetler, S. W., and Bartlein, P. J. (1990). Simulation of lake evaporation with application to modeling lake level variations of Harney-Malheur Lake, Oregon. *Water Resour. Res.,* **26**(10): 2603-2612.

98. Houston, J. (2002). Groundwater recharge through an alluvial fan in the Atacama Desert, northen Chile: Mechanisms, magnitudes and causes. *Hydrol. Process.,* **16**:3019-3035.

99. Hsu, K. L., Gupta, H. V., and Sorooshian, S. (1995). Artificial neural network modeling of the rainfall-runoff process. *Water Resour. Res.,* **31**(10): 2517-2530.

100. Hugo, A.L. (2002). Reservoir design and operation with variable lake hydrology. *J. Water Resources Planning Manage.,* **128**(6): 399-405.

101. Hunt, B.W. (1971). Vertical recharge of unconfined aquifers. *J. Hydrau. Div., ASCE, 96(HY7):*1017–1030.

102. Hussain, A.S.A, (1999). Grass ET estimates using Penma-type equations in central Sudan. J. *Irrig. Drain. Eng.,* **125**(6):324-329.

103. Imbeau, M.E. (1892) La Durance: Regime, crues et inundations. *Ann. Ponts Chaussees, Mem. Doc. Ser.,* **3**(1): 5-18(in French).

104. Istok, J. D. and Boersma, L. (1986). Effect of antecedent rainfall on runoff during low intensity rainfall. *J. Hydrol.*, **88**: 329-342.

105. Jain, A., and Indurthy, S. K.V.P. (2003). Comparative analysis of event-based rainfall-runoff modeling techniques - Deterministic, statistical, and artificial neural networks, *J. Hydrol. Eng.,* **8**(2): 93-98.

106. Jain, M. K., Mishra, S. K., and Singh, V. P.(2006). Evaluation of AMC-dependent SCS-CN-based models using watershed characteristics. *Water Resour. Manage.***20**: 531-552.

107. Jenson, M. E. (1973). Consumptive use of water and irrigation requirements. *Am. Soc. of Agri. Engrs.,* New York.

108. Kashyap, P.S., and Panda, R.K. (2001). Evaluation of evaporation methods and development of crop coefficients for potato crop in a sub-humid region. *Agric. Water mange.* , **50**: 9-25.

109. Kebede, S., Travi, Y., Alemayehu, T., and Marc, V. (2006). Water balance of lake Tana and its sensitivity to fluctuation in rainfall, Blue Nile basin, Ethiopia. *J. Hydrol.,.***316***:233-245.*

110. Kenabatho, P.K., parida, B.P. (2005). Evaporation losses as a major factor in determining allowable releases from water supply reservoirs: the case of botswana's major reservoirs. River basin Management III. *WIT trans. Ecol. Environ.* **83**:631-638.

111. Knapp, H.V., Yu, Y.S., and Pogge, E.C. (1984). Monthly evaporation for Milford lake in Kansas. *J. Irrig. Eng.,* **110**(2): 138-148.

112. Knisel, W.G. (1980) CREAMS: A field scale model for chemicals, runoff and erosion from agricultural management systems. Conservation Research Report No. 26, Washington, D.C.; USDA-SEA.

113. Knudsen, J. Thomsen, A. and Resfgaard, J.C. (1986). WATBAL: A semi-distributed physically based hydrological modeling system. *Nordic Hydrol.*, **17**(4-5): 347-362.

114. Kohler, M. A., Nordenson,T. J., and Fox, W. E.(1955). Evaporation from pans and lakes. *U S Weather Bureau Res. Paper 38*, 21p.

115. Kohler, M. A., and Parmele, L.H.(1967). Generalized estimates of free water surface evaporation. *Water Resour. Res.,* **3**: 997-1005.

116. Kohler, M.A., and Linsley, R. K.(1951).Predicting the runoff from storm rainfall. Weather Bureau, US Department of Commerce, Research Paper No. 34,Washington p 9.

117. Kraatz, D.B. (1971). Irrigation canal lining. *Food and Agricultural Organization of the United Nations Irrigation and Drainage Paper,* **2:** 1-199.

118. Kumar, M., Raghuwanshi, N.S., Singh, R., wallender, W.W., and Pruitt, W.O. (2002). Estimating evapotranspiration using artificial neural network. *J. Irrig. Drain. Eng.* 128(4): 246-251.

119. Kuzmin, O.P. (1957). Hydrophysical investigations of land water. *Int. Assoc. Sci. Hydrol. Publ.,* **3**: 468-478.

120. Latinopoulos, P.(1984). Periodic recharge to finite aquifers from rectangular areas. *Adv. Water Resour.,* **7:**137–140.

121. Lee, D. R. (1977). A device for measuring seepage flux in lakes and estuaries. *Limnol. Oceanogr.* **22**: 140-147.

122. Lee, D. R. and Cherry, J. A.(1978). A field exercise on groundwater flow using seepage meters and mini-piezometers. *J. Geol. Educ.,* **27:** 6-10.

123. Legates, D.R., and McCabe, G.J.(1999). Evaluating the use of "goodness-of-fit" measures in hydrologic and hydroclimatic model validation. *Water Resour. Res.,* **35** (1), 233-241.

124. Leonard, R.A., Knisel, W.G and Still, D.A. (1986). GLEAMS: Groundwater loading effect of agricultural management systems. American Society of Agricultural Engineers. Paper No. 86-2511. Chicago, II.

125. Lerner, D. N., Issar, A.S. and Simmers, I.(1990). Groundwater Recharge, A guide to understanding and estimating natural recharge. *In. Assoc. Hydrogeol.,* Kenilworth, Rep. 8, pp 345.

126. Lewis, D., Singer, M.J. and Tate, K.W. (2000). Applicability of SCS curve number method for a California oak woodland watershed. *J. Soil and Water Conservation,* **2:** 226-230.

127. Li, R.M., Steven, M.A., and Simons, D.B.(1976). Solutions to Green-Ampt infiltration equation. *J. Irrig. Drain. Eng., Div. ASCE,* **102**(IR2): 239-248.

128. Lloyd, J.W. (1986). A review of aridity and groundwater. *Hydrol. Process.,* **1**: 63-78

129. Lorrai, M. and Sechi, G. M.,(1995). Neural nets for modeling rainfall-runoff transformations. *Water Resour. Manage.*, **9**(4): 299-313.

130. Mailapalli, D.R., Wallender, W.W., Singh, R., and Raghuwanshi, N.S.(2009). Application of a nonstandard explicit integration to solve Green and Ampt infiltration equation. *J. Hydrol. Eng., 14*(2): 203-206.

131. Marquardt, D. W. (1963) An algorithm for least squares estimation of nonlinear parameters. *J. Soc. Indust. Appl. Mat.*, **11**(2): 431-441.

132. Mathur, V.N. (2006). Groundwater resources management in the state of Rajasthan. Groundwater Governance, ownership of groundwater and its pricing. (Eds Saleem Romani, K. D. Sharma, N. C. Ghosh and Y.B. Kaushik), Capital publishing Company, New Delhi, pp. 267-269.

133. Mein, R.G., and larson, C.L. (1973). Modeling infiltration during steady a rain. *Water Resour. Res.*, **9**(2): 384-394.

134. Meyer, A.F. (1915). Computing runoff from rainfall and other physical data. *Trans. Am. Soc. Civ. Eng.,79*): 1055-1155.

135. Mishra, G.C., and Fahimuddin, M. (2005). Stream Multiaquifer Well Interactions. *J. Irrig. and Drain. Eng.* **131**(5): 433-439.

136. Mishra, G.C., and Ghosh, N.C. (2002). Unsteady seepage from a large water body. Proc. Artificial Recharge of Groundwater held at Bhopal, India. pp 12c-1.

137. Mishra, G. C., and Jain, S. K.(1999). Estimation of hydraulic diffusivity in stream-aquifer system. *J. Irrig. Drain. Eng. ASCE*, **125**(2): 74-80.

138. Mishra, S.K. and Singh, V.P., (1999). Another look at SCS-CN method. *J. Hydrol. Engg,,* **4**(3): 257-264.

139. Mishra, S.K. Jain, M.K, Pandey, R. P., and Singh, V.P.(2005). Catchment area-based evaluation of the AMC-dependent SCS-CN-based rainfall- runoff models. *J. Hydrol. Process.,* **19:** 2701-2718.

140. Mishra, S.K., Tyagi, J.V., Singh, V.P., and Singh, R.(2006). Catchment area-based evaluation of the AMC-dependent SCS-CN-based rainfall- runoff models. *J. Hydrol. Process.,* **19:** 2701-2718.

141. Mishra, S.K., and Singh, V.P.(2004). Validity and extension of the SCS-CN method for computing infiltration and rainfall-excess rates. *J. Hydrol. Process.,* **18**(7): 1291-1313.

142. Mockus, V. (1949). Estimation of total (peak rate of) surface runoff for individual storm. Exhibit A of Appendix B, Interim Survey Rep. grand (Neosho) River watershed, USDA, Washington, D.C.

143. Moglen, G.E. (2000). Effect of orientation of spatially distributed curve numbers in runoff calculations. *J. Am. Water Resour. Assoc.,* **36**(6):1391-1400.

144. Molden, D.J., Sunada, D.K., and Warner, J.W.(1984). Microcomputer model of artificial recharge using Glover's solution. *Ground Water,* **22**(1): 73-79.

145. Monteith, J.L. ((1965). Evaporation and Environment. *Symposia of the Society of Experimental Biology*, **19**: 205-239.

146. Morel-Seytoux, H.J., Miracapillo, C., and Abdulrazzak, M.J. (1990). A reductionist physical approach to unsaturated aquifer recharge from a circular spreading basin. *Water resour. Res.,* **26**(4): 771-777.

147. Morel-Seytoux, H.T., and Khanji, J. (1974). Derivation of an equation of infiltration. *Water Resour. Res.,* **4**(10): 795-800.

148. Morel-Seytoux, H.J. (1964). Domain variation in channel seepage flow. *J. Hydraul. Div. ASCE*, **90**(HY2)*: 55-79.*

149. Morel-Seytoux, H.J.(1985). Conjunctive use of surface and groundwaters. In: *Artificial Recharge of Groundwater*. Eds. T. Asano, Butterworth, Roston, Mass. pp.35-68.

150. Morel-Seytoux, H.J. (1984). From excess infiltration to aquifer recharge: a derivation based on the theory of flow of water in unsaturated soils. *Water Resour.Res*., **20***: 1230-1240.*

151. Morton, F.I. (1983). Operational estimates of lake evaporation. *J. Hydrol.,* **66**: 77-100.

152. Morton, F.I. (1990). Studies in evaporation and their lessons for environmental sciences. *Canadian Water Resour. J.,* **15**(3): 261-285.

153. Morton, F.I. (1994). Evaporation research- A critical review and its lessons for environmental sciences. *Critical Rev. Environ. Sci. Tech.,* **24**(3): 237-280.

154. Morton, F.I. (1979). Climatological estimates of lake evaporation. *Water Resour. Res.*, **15**(1):64-76.

155. Mulvany, T.J. (1850) On the use of self registering rain and flood gauges. *Proc. Inst. Civ. Eng.,* **4**(2): 1-8.

156. Nair, A.R. Jain, S.K. Rao, S.M. and Eapen, A.C. (1980). Radio tracer technique to study the efficacy of Bangarawadi percolation tank . Proc. Workshop on Nuclear Techniques in Hydrology held at NGRI, Hyderabad, India. pp.219-230.

157. Nath, S.S., and Bolte, J.P. (1998). A water budget for pond aquaculture. Aquacultural Engineering. Elsevier Science B.V. 18: 175-188.

158. O'Hare, M.P., Fairchild, D.M. Hajali, P.A., and Canter, L.W.(1982). Artificial recharge of Groundwater. Status and potential in the continuous United States, Norman, Okalahoma.

159. Oaksford, E.T. (1985), Artificial recharge: methods, hydraulics, In: Artificial Recharge of Groundwater. T. Asano, (ed), *Butterworth Publishers*, Boston, pp. 69-127.

160. Pandey, R.K., Panda, S.N., and Panigrahi, B. (2006). Sizing of farm reservoirs for crop-fish integration in rainfed farming systems in eastern India. *Biosystems Engineering,* **93**(4): 475-489.

161. Panigrahi, B., and Panda, S.N. (2001). Simulation of ponding and soil moisture status through water balance model for rain-fed upland rice. *Agric. Eng. J.,***10**(1-2): 39-56.

162. Panu, U.S., and Nguyen, T. (1994). Estimation of mean areal evaporation in Northwestern Ontario. *Can.Water Resour. J.,* **19**(1): 69-82.

163. Parker, B. D., Eisenhauer, D.E. Schulte, D.D., Nienaber, J.A. (1999). Seepage characteristics and hydraulic properties of a feedlot runoff storage pond. *Trans. ASAE,* **42**(2): 369-380.

164. Penman, H. L.(1948). Natural evaporation from open water, bare soil and grass. *Proceeding of Republic society of London,* **193**: 120-145.

165. Pennequin, D.F. and Anderson, M.P. (1983). The ground water budget of Lake Wingra, Dane County, Wisconsin, National Technical Information Service, Springfield, VA, 22161, PB83-220525, 43pp.

166. Philip, J. R. (1957). Theory of infiltration: Sorptivity and algebraic equations. *Soil Sci.,* **84**: 257-265.

167. Philip, J. R. (1992). Falling head ponded infiltration with evaporation. *J. Hydrol.,* **17**:1-21.

168. Ponce, V.M., and Hawkins, R.H. (1996). Runoff curve number: Has it reached maturity?. *J. Hydrol. Eng. ASAE,* **1**(1): 11-19.

169. Prasad, S. N., Singh R.K. Kumar, A., Parandiyal, A.K., Ali, Shakir, Somasundaram, J., Sethy, B.K., and Sharda V.N. *eds.* (2008) *Natural Resources Management for Sustainable Development in Western India.* Allied publishers Private limited, New Delhi.

170. Priestley, C. H. B., and Taylor, R. J. (1972). On the assessment of surface heat flux and evaporation using large scale parameters. *Monthly Weather Review,* **100**: 81-92.

171. Pruess, K., Oldenburg, C. and Moridis, G. (1999). TOUGH2 user's guide version 2.0. Rep. LBNL-43134. Lawrence BerkeleyTatl. Lab., Berkeley, CA.

172. Pyne, R.D. (1995). Groundwater recharge and well: a guide to aquifer storage recovery. Lewis Publishers, Boca Rotan, Florida.

173. Quinn, F.H. (1978). Hydrological response model of the North American Great Lake. *J. Hydrol.,* **37**(3-4): 295-307.

174. Rai, S.N, and Singh, R.N. (1995). Two-dimensional modeling of water table fluctuation in response to localized transit recharge. *J. Hydrol.,* **167**: 167-174.

175. Rai, S.N, and Singh, R.N. (1992). Water table fluctuations in an aquifer system due to time varying surface infiltration and canal recharge. *J. Hydrol.,* **136**: 381-387.

176. Rai, S.N, and manglik, A. (1999). Modelling of water table variation in response to time varying recharge from multiple basins using the linearized Boussinesq equation. *J. Hydrol.,* **220**: 144-148.

177. Raju, K.C.B. (1985). Recharge through percolation tanks and subsurface dyke, India. Proc. Semi. Artificial Recharge of Groundwater held at Ahmadabad, India. pp 12c-1.

178. Rallison, R.E.(1980). Origin and evaluation of the SCS runoff equation. *Proc. Irrig. Drain. Symposia on Watershed Management,* Vol.2 ASCE, New York, 912-924.

179. Rallison, R.E., Cronshey, R.C. (1979). Discussion on runoff curve number with site varying moisture by R.H. Hawkins, *J. Irrig. Drai.. Div., ASCE,* **105**(IR4(:439-441.

180. Ramos, H. (2007). A non-standard explicit integration scheme for initial value problems. *Appl. Mat. Comput.,* **189**(1): 710-718.

181. Rao, M.D., Raghuwanshi, N.S., and Singh, R. (2009). Development of a physically based 1D-infiltration model for seal formed irrigated soils. *Agric. Water. Manage.,* **84**(1-2): 164-174.

182. Rathore, M. S. (2005). Groundwater exploration and augmentation efforts in Rajasthan. Institute of Development Studies, Jaipur, India, pp 33.

183. Rawls, W. J. Brakensiek, D.L., and Saxon, K.E. (1982). Estimation of soil water properties. *Trans. ASAE.*, **25**: 1316-1320.

184. Reeder, J. W., Freyberg, D.L., Franzini, J. B., and Remson, I.(1980). Infiltration under rapidly varying surface water depths. *Water Resour. Res.,* **8**(5): 97-104.

185. Reis, R. J. D., and Dias N.L. (1998). Multi-season lake evaporation: energy budget estimates and CRLE model assessment with limited meteorological observations. *J. Hydrol.*, **208**: 135-147.

186. Richards, L.A. (1931). Capillary conduction of liquids through porous mediums. *Physics,* **1**: 318-333.

187. Rohwer, C. (1931). Evaporation from free water surfaces. Technical Bulletin 271, US Department Agriculture, Washington, D.C.

188. Romanenko, V.A.(1961). Computation of the autumn soil moisture using a universal relationship for a large area. Proc. Ukrainian Hydrometeorological Research institute, No.3. Kiev.

189. Rose, S. (1998). A statistical method for evaluating the effects of antecedent rainfall upon runoff: application to the coastal plain of Geogia. *J. Hydrol.,* **211:** 168-177.

190. Rosenberry, D.O., Sturrock, A.M., and Winter, T.C. (1993). Evaluation of energy budget method of determining evaporation at William Lake, Minnesota, using alternative instrumentation and study approaches. *Water Resour. Res.,* **29**(8): 2473-2483.

191. Rushton, K. (1997). Recharge from permanent water bodies. In. Simmers, I. (ed.) recharge of phreatic aquifers in semi-arid areas. A.A. Balkema, Rotterdam, pp215-255.

192. Sacks, L. A., Lee,T. M., and Radell, M. J. (1994). Comparison of energy-budget evaporation Losses from two morphologically different Florida seepage lakes. *J. Hydrol.,* **156**: 311-334.

193. Sajikumar, N and Thandaveswara, B.S. (1999). A non-linear rainfall-runoff model using an artificial neural networks. *J. Hydrol.,* **216**: 32-55.

194. Salvucci, G. D., and Entekhabi, D. (1994). Explicit expressions for Green-Ampt (delta function diffusivity) infiltration rate and cumulative storage. *Water Resour. Res.,* **30**(9): 2661-2663.

195. Sarkar, R., Kumar, S., Kumar, Y., and Sharma, H.C. (2007). Groundwater modeling for prediction of water table in Ramganga-Bahgul interbasin of Uttar Pradesh. *Hydrol. J.,* **30**(1-2): 123-133.

196. Scanlon, B.R., Healy, R.W., and Cook, P.G. (2002). Choosing appropriate techniques for quantifying groundwater recharge. *Hydrogeol. J.,* **10**:18-39.

197. Schneider, L.E., and McCuen, R.H.(2005). Statistical guidelines for curve number method for a California oak woodland watershed. *J. Soil and Water Conservation*, **2**: 226-230.

198. Schwartz, F.W., Zhang, H. (2003). Fundamentals of groundwater. John Wiley and Sons, Inc. U.K.

199. SCS, (1956, 1985, 1993). Hydrology-National Engineering Handbook, Supplement A, Section 4, Chapter 10, Soil Conservation Service. United State Department of Agriculture (USDA), Washington, DC.

200. Selvarajan, M., Bhattacharya, A. K., and de Vries, F. W. T. (1995). Combined use of watershed, aquifer and crop simulation model to evaluate groundwater recharge through percolation ponds. *Agriculture Systems*, **47**: 1-24.

201. Serrano, S.E. (2001). Explicit solution to Green and Ampt infiltration equation. *J. Hydrol. Eng.*, **6**(4): 336-340.

202. Serrano, S.E. (2003). Improved decomposition solution to Green and Ampt infiltration equation. *J. Hydrol. Eng.*, *8*(3): 158-160.

203. Sharda, V.N., Kurothe, R.C. Sena, D.R., Pandey.V.C., and Tiwari, S.P. (2006). Estimation of groundwater recharge from water storage structure in a semi-arid climate of India. *J. Hydrol.*, **329**(1-2): 224-243.

204. Sharma, P.B.S., and Rao, N.H.(1980). Growth of groundwater mound in response to recharge. *Ground Water*, **8**(6):587-595.

205. Sharma, S.C.(1985). Artificial recharge in Gujarat state by injection, spreading through percolation tanks, chek dams, Bandharas, and other methods. Proc. Semi. on Artificial Recharge of Groundwater held at Ahmadabad, India.pp 16c-1.

206. Sherman, L.K. (1932) Stream flow from rainfall by the unit graph method. *Eng. News-Rec.*, **108**: 501-505.

207. Shinogi, Y., Makin, I.W., and Witharana, P. (1998). Simulation of water the balance in a dry zone tank cascade. Paper presented at the National Conference of the Status and Future direction of Water Research in Sri Lanka, November 4-6, 1998, at BMICH, Colombo, Sri Lanka.

208. Shuttleworth, W. J.(1993).Evaporation. *Handbook of Hydrology*, D.R.Maidment, ed., MaGraw-Hill, New York.

209. Simon, E., and Mero, F. (1985). A simplified procedure for the evaluation of the lake kinneret evaporation. *J. Hydrol.*, **78:** 291-304.

210. Simunek, J., Sejna, M., and van Genuchten, M.Th. (1998). The HYDRUS-1D software package for simulating water flow and solute transport in one –dimensional variably saturated media, Version 2.0. IGWMC-TPS-70. Int. Groundwater modeling Centre, Colorado School of Mines, Golden, Colorado, pp202.

211. Singh R.K, Prasad, S. N. Ali, S., Kumar, A., and Parandiyal, A.K.(2004). *Participatory Watershed Management for Sustainable Development in Badakhera Watershed.* Allied publishers Private limited, Kota.

212. Singh, V. P. (1989).Hydrologic system, Vol. II, Watershed Modeling. *Prentice-Hall, Inc*.

213. Singh, V. P., and Xu, C. Y.(1997). Evaluation and generalization of 13 mass transfer equations for determining free water evaporation. *Hydrol. Process.*, **11**: 311-323.

214. Sittner, W.T., Schauss, C.E., and Monro, J. C. (1969). Continuous hydrograph synthesis with an API type hydrologic model. *Water Resour. Res.*, **5**(5): 1007-1022.

215. Sivapragasam, C., Vasudevan, G., Maran, J., Bose, C., Kaza, S., and Ganesh, N. (2009). Modeling evaporation seepage losses for reservoir water balance in semi-arid regions. *Water Resour. Manage.*, **23**: 853-867.

216. Small, E. E . (2005). Climate controls on diffuse groundwater recharge in semiarid environments of the southwestern United States. *Water Resour, Res.*, **41**: W04012, doi: 10.1029/2004WR003193.

217. Smith, R. E. (1972). The infiltration envelopes: Results from a theoretical infiltration model. *J. Hydrol.*, **138**: 215-296.

218. Smith, R.A., and Parlange, Y.J.(1978). A parameter efficient hydrologic infiltration model. *Water Resour. Res.*, **14**(3):535-538.

219. Sorman, A.U., and Abdulrazzak, M.J (1993). Infiltration recharge through wadi beds in arid regions. *Hydrol. Sci. J.*, **38**(3):173-186.

220. Sorooshian, S., Daun, Q., and Gupt, V. K. (1993). Calibration of rainfall-runoff models: Application of global optimization to the Sacramento soil moisture accounting model. *Water Resour. Res.*, **29**(4): 1185-1194.

221. Springer, E.P., McGurk, B.J., Hawkins, R.H., and Goltharp, G.B. (1980). Curve numbers from watershed data. *Proc. Irrig. Drain. Symp. On Watershed management*, ASCE, New York, N.Y. pp. 938-950.

222. Srivastava, R.C., Das, M. and Panda, D.K.(2007). Pre-estimation of seepage loss for site selection and design of rain water management structures. *Indian J. Soil Conservation*, 35(3): 255-256.

223. Srivastava, S. K., Singh, O. P., and Pandey, G. P. (1993). Estimation of global solar radiation in Uttar Pradesh (India) and comparison of some existing correlations. *Solar Energy*, **51**(1):27-29.Stannard, D., and Rosebarry, R. (1991). A comparision of short-term measurement of lake evaporation using eddy-correlation and energy budget methods. *J. Hydrol.*, **122**: 15-22.

224. Stauffer, R. E. (1991). Testing lake energy budget under varying atmospheric conditions. *J. Hydrol.*, **128**: 115-135.

225. Stewart, R.B., and Rouse, W.R. (1976). A simple method for determining the evaporation from shallow lakes and ponds. *Water Resour. Res.*, 12: 623-628.

226. Stuff, R. G. and Dale, R. F. (1978). A soil moisture budget model accounting for shallow water table influences. *Soil Sci. Soc. Am. J.,* **42(4)**: 637-643.

227. Sturrock, A. M., and Winter, T. C., and Rosenberry, O. D. (1992). Energy- budget evaporation from Williams Lake: a closed lake in north central Minnesota. *Water Resour. Res.,* **28**(6): 1605-1617.

228. Subramanya, K. (2006). *Engineering Hydrology.* 2nd Edition, McGraw Hill, New Delhi.

229. Sukhija, B.S., Reddy, D.V. Nandakumar, M.V. and Rama (1997). A method for evaluation of artificial recharge through percolation tanks using environmental chloride. *Ground Water*, **35**(1): 161-165.

230. Sukhija, B.S. and Reddy, D.V. (1987). Study of artificial recharge through Potharam percolation tanks using environmental chloride method. *Geophysical Research Bulletin*, **25**(1): 27-31.

231. Swammee, P.K., Mishra, G.C., and Chahar, B.R. (2000). Design of minimum seepage loss canal sections. *J. Irrig. Drai. Eng., ASCE,* **126**(1): 28-32.

232. Swartzendruber, D. (1974). Infiltration of constant flux rainfall into soil as analyzed by the approach of Green and Ampt. *Soil Sci.,* **117**:272-281.

233. SYSTAT (2006) SigmaPlot User Guide, Release 10.0 Edtion, Systate Sotware inc., Sanjose, California, USA.

234. Szumiec., M. (1979). Hydrometeorology in pond fish culture. In: Pillay, T.V.R. (Ed.), Advances in Aquaculture. FAO, Fishing News Books, London, pp. 117-120.

235. Tan, S.B.K., Shuy, E.B., Chau, L.H.C., and Yee, W.K.(2007). Studies on groundwater recharge characteristics at a reclaimed land site with an equatorial climate using time series and spectrum analyses. *Hydrol. Process.,* **21**: 939-948.

236. Thom, A.S., and Oliver, H.R. (1977). On Penman's equation for estimating regional evaporation . *Quarterly Journal of Royal Meteorological Society*, **103**: 345-357.

237. Thornthwaite, C. W., and Holzman, B. (1939). The determination of land and water surfaces. *Monthly Weather Review*, **67**: 4-11.

238. Todd, D.K. (1980). Groundwater Hydrology. Second edition, John and Wily Sons, New York, pp.535.

239. Tokar, A. S., and Johnson, P. A. (1999). Rainfall-runoff modeling using neural networks. *J. Hydrol. Eng.*, **4**(3): 232-239.

240. Topper, R., Barkmann, P.E., Bird, D.R. and Sare, M.A.(2004). Artificial recharge of ground water in Colorado: a statewide assessment. Colorado Geological Survey Department of Natural Resources, Colorado.

241. Tracy, J.C., and Marino, M.A.(1987). Seepage into variably saturated porous medium. *J. Irrig. Drain.Eng. ASCE,* **113**(2):198-211.

242. Tsykin, E. N. (1985). Multiple nonlinear statistical models for runoff simulation and prediction. *J. Hydrol.*, **77**: 209-226.

243. Van Mullem, J.A. 9(1989). Runoff and peak discharge using Green-Ampt infiltration model. *J. hydrol. Eng.,* **117**(3): 354-370.

244. Vardavas, I. M., and Fountoulakis, A. (1996). Estimation of lake evaporation from standard meteorological measurements: application to four Australian lakes in different climatic region. *Ecological Modeling*, **84**: 139-150.

245. Viessman, W. Jr., and Lewis, G.L. (1996) *Introduction to Hydrology*. 4th edition, HarperCollins, New York.

246. Wang, X. K., Lu, W. Z. Cao, S. Y., and Fang, D. (2007). Using time-delay neural network combined with genetic algorithm to predict runoff level of Linshan watershed, Sichuan, China. *J. Hydrol. Eng.,* **19**(2): 231-236.

247. Warrick, A. W., Zerihun, D., Sanchez, C. A., and Furman, A. (2005). Infiltration under variable ponding depths of water. *J. Irrig. Drain. Eng.,* **131**(4): 358-363.

248. Weeks, E.P.(2002). A historical overview of hydrological studies of artificial recharge in the U.S. Geological Survey, U.S. Geological Survey Open File Report02-89.

249. Weeks, W.D., and Hebbert, R. H. B. (1980). A comparison of rainfall-runoff models. *Nordic Hydrol.,* **11**: 7-24.

250. White, D. (1988). Grid based application of runoff curve numbers. *J. Water Resour. Plann. Manage., ASCE,* **114**(6): 601-612.

251. Wilcon, B., Rawls, W., Brakensiek, L., and Wright, R. (1990). Predicting runoff from rangeland catchments: a comparison of two models. *Water Resour. Res.* , **26**: 2401-2410.

252. Winter, T. C. (1981). Uncertainties in estimating the water balance of lakes. *Water Resour. Bull.*, **17**(1): 82-115.

253. Winter, T. C., Rosenberry, O. D., and Sturrock, A. M. (1995). Evaluation of 11 equations for determining evaporation from a small lake in the north central United State. *Water Resour. Res.,* **31**(4): 983-993.

254. WMO (1985). Casebook on operational assessment of areal evaporation. Operational Hydrology Report *NO. 22. Secretariat of the World Meteorological Organization,* Genewa, Switzerland, 194p.

255. Woessner, W.W. and Sullivan, K.E. (1987). Results of seepage meter and mini-piezometers study. Lake Mead, Nevada. *Ground Water,* **22**: 561-568.

256. Xia, J., O'Connor, K.M., Kachroo, R. K., and Liang, G. C. (1997) A non-linear perturbation model considering catchment wetness and its application river flow forecasting. *J. Hydrol., Delft, The Netherlands,* **200**(1-4): 164-178.

257. Xu, Y., and Breekman, H.E. (2003). Groundwater recharges estimation in southern Africa. UNESCO IHP Series No. 64. UNESCO Paris.

258. Yadev, B., and Keshari, A.K. (2006). A coupled mathematical water and salt balance model of flat bay. *Asian Journal of Water, Environment and Pollution,* **4**(2): 55-59.

259. Young, A. A. (1947). Evaporation from water surface in California: summary of pan records and coefficients. Bulletin 54, Public Works Department, Sacramento, CA, 1881-1946.

260. Young, R.A., Onstad, D.D. Bosch and Anderson, W.P. (1985). Agricultural non-point surface pollution model (AGNPS) I and II model documentation. Pollution Control Agency, St. Paul and U.S. Department of Agriculture, Agricultural Research Service, Washington, D.C.

261. Yuan, Y., Mitchell, J.K., Hirschi, M.C., and Cook, R.A.C.(2001). Modified SCS curve number method for predicting subsurface drainage. *Trans. ASAE.,* **44**(6): 1673-1682.

APPENDIX–A

EQUATIONS FOR ESTIMATION OF STATISTICAL PARAMETERS

A.1 COEFFICIENT OF DETERMINATION (R^2)

Coefficient of determination (R^2) that gives a measure of correlation between a pair of data values, is given by:

$$R^2 = \frac{\sum_{i=1}^{N}(X_i - \overline{X})(Y_i - \overline{Y})}{\left[\sum_{i=1}^{N}(X_i - \overline{X})\right]^{0.5}\left[\sum_{i=1}^{N}(Y_i - \overline{Y})\right]^{0.5}} \tag{A.1}$$

where X_i is the observed values; $\overline{X}$ is the mean of the observed values; Y_i is the estimated values; $\overline{Y}$ is the mean of estimated values; i is an integer varying from 1 to N, and N is the number of data points.

The values of R^2 vary from 0 to 1. R^2 greater than 0.9 signifies a very good agreement, R^2 between 0.8 and 0.9 specifies a fairly good agreement and less than 0.8 indicates an unsatisfactory agreement (Coulibaly et al., 2005).

A.2 INDEX OF AGREEMENTS (D)

Index of agreement, *D* that gives a measure of agreement between a data pair (Legate and McCabe, 1999) , is defined as:

$$D = 1.0 - \frac{\sum_{i=1}^{N}(X_i - Y_i)^2}{\sum_{i=1}^{N}\left(|Y_i - \overline{X}| + |X_i - \overline{X}|\right)^2} \tag{A.2}$$

The value of *D* varies between 0 and 1, where 0 indicates no agreement and 1 means perfect agreement of a data pair.

A.3 RELATIVE BIAS (RB)

Relative bias (RB) is an index of the systematic error, which indicates the amount that a model underestimates or overestimates and is defined as:

$$RB = \frac{1}{N}\sum_{i=1}^{N}(Y_i - X_i) \tag{A.3}$$

RB = 0 indicates the perfect match, RB >0 indicates towards over prediction and RB <0 indicates towards under prediction.

A.4 STANDARD ERROR OF ESTIMATE (SE)

Standard error of estimate that gives a measure of accuracy of predictions by fitting a regression line is expressed as:

$$SE = \left[\frac{\sum_{i=1}^{N}(X_i - Y)}{N - DF}\right]^2 \tag{A.4}$$

in which DF is the degree of freedom.

A.5 RELATIVE PERCENTAGE ERROR (RPE)

RPE that represents the relative differences between a pair of data values, is given by:

$$RPE = \frac{(Y_i - X_i)}{X_i} \times 100 \tag{A.5}$$

APPENDIX-B

DATA OF TEXTURAL SOIL GROUPS USED IN THE STUDY

Table B.1. Hydrological properties of four textural soil groups (after Rawls and Brakensiek, 1982).

Soil textural classes	Mean volumetric moisture content at near saturation or mean total porosity (θ_s) (cm^3 cm^{-3})	Mean residual saturation (θ_i) (cm^3 cm^{-3})	Suction pressure head (ψ_f)(cm)	Geometric mean pore size distribution index (λ)	Mean saturated hydraulic conductivity (K_s) (cm h^{-1})
Sand	0.437	0.020	7.26	0.591	21.00
Loam	0.463	0.027	11.15	0.220	1.32
Clay loam	0.464	0.075	25.89	0.194	0.23
Sandy clay	0.430	0.109	29.17	0.168	0.12

APPENDIX–C

EQUATIONS FOR ESTIMATION OF PARAMETERS OF DIFFERENT EVAPORATION MODELS
[Ref. Chapter-6]

C.1ESTIMATION OF THE BOWEN RATIO ENERGY BALANCE'S PARAMETERS

C.1.1 Net Radiation (R_n)

The equation for R_n is given (Hostetler and Bartlien, 1990; Dingman, 1994) as :

$$R_n = (1-\alpha_w)\, R_s - \left[\varepsilon_w \, \varepsilon_a \sigma \left(T_a + 273.15 \right)^4 - \varepsilon_w \, \sigma \left(T_a + 273.15 \right)^4 \right] \tag{C.1}$$

where R_s is the net radiation [MJm $^{-2}$]; α_w is the albedo or reflection coefficient of water surface [dimensionless]; R_s is the incoming solar or short wave radiation [MJm^{-2}]; ε_w is the emissivity of the water surface [dimensionless]; ε_a is the emissivity of the atmosphere [dimensionless]; σ is the Stefan-Boltzmann constant = 4.903 x10^{-9} MJM^{-2} K^{-4}; and T_a is the air temperature above the pond surface [^{0}K].

α_w in Eq. (C.1) is defined (Henderson seller, 1986; Hostetler and Bartlien, 1990) by:

$$\alpha_w = \left(\frac{a_c \, t_d}{2 \, \pi \, w_s} \right) F_i \tag{C.2}$$

where a_c is a parameter; t_d is the number of second in a day; w_s is the half- day length; and F_i is the integral factor.

a_c in Eq. (C.2) is:

$$a_c = 0.02 + 0.01 \left(0.5 - C_c \right) \left\{ 1.0 - \sin \left(\frac{\pi \, (J - 81)}{183} \right) \right\} \tag{C.3}$$

In which C_c is the fraction of the sky obscured by cloud; and J is the Julian day.

C_c of Eq. (C.3) is defined (Vardavas and Fountoulakis, 1996) as:

$$C_c = 1 - \frac{24\; w_s\; n_a}{\pi} \tag{C.4}$$

where n_a is the actual duration of sunshine (hour).

F_i in Eq.(C.2) is given by:

$$F_i = 2\left(b^2 - c^2\right)^{-\frac{1}{2}} tan^{-1}\left(B^{\frac{1}{2}}\right) \qquad b^2 - c^2 > 0 \tag{C.5a}$$

$$F_i = \left(-b + c^2\right)^{-\frac{1}{2}} ln\left\{\frac{\left[1 + \left(-B\right)^{\frac{1}{2}}\right]}{1 - \left(-B\right)^{\frac{1}{2}}}\right\} \qquad b^2 - c^2 < 0 \tag{C.5b}$$

in which,

$$b = a + sin\,\theta \;\; sin\,\delta \tag{C.5c}$$

$$c = cos\,\theta \;\; cos\,\delta \tag{C.5d}$$

$$B = \left(\frac{b-c}{b+c}\right) tan^2\left(\frac{\pi\; w_s}{2\,t_d}\right) \tag{C.5e}$$

where θ is the latitude[degree]; and δ is the solar declination [degree].

R_s in Eq. (C.1) is defined (Angstrom, 1956; Allen *et al.*,1998) by:

$$R_s = \left(a_s + b_s\,\frac{n_a}{N_m}\right) R_a \tag{C.6}$$

where R_a is the extraterrestrial radiation [MJm^{-2}/day]; N_m is the maximum duration of sunshine or daylight hours [hour]; a_s and b_s are the regression constants expressing the fraction of extraterrestrial radiation (R_a) reaching the earth surface[dimensionless]; The R_a of a day in a year for a specific location is computed using Allen et al., (1998) equation. The value of $a_s = 0.2006$ and $b_s = 0.5313$ is used as suggested by Srivastava et al., (1993).

ε_a in Eq.(C.1) can be computed (Henderson – Seller, 1986) by:

$$\varepsilon_a = 0.84 - \left(0.1 - 9.973\times10^{-6}\,e_a\right)\left(1-C\right) + 3.491\times10^{-5}\,e_a \qquad \text{for, } 1\text{-}C > 0.4 \tag{C.7}$$

$$\varepsilon_a = 0.87 - \left(0.175 - 29.92 \times 10^{-6}\, e_a\right)\left(1 - C\right) + 2.693 \times 10^{-5}\, e_a \quad \text{for, } 1\text{-}C < 0.4 \tag{C.8}$$

in which e_a is the actual vapour pressure at air temperature (kpa).

ε_w in Eq.(C.1) is considered to be 0.97 (Anderson, 1954; Hostetler and Bartlein, 1990).

C.1.2 Heat Stored or Lost by Water (*G)*

The equation for G is:

$$G = 4.186\, d\, \frac{T_w(t) - T_w(t-1)}{\Delta t} \tag{C.9}$$

where ρ_w is the density of water = 1000 kg/m^3; C_{pw} is the heat capacity of water $= 4.186 \times 10^{-3}$ MJ/kg/^{0}C; d is the depth of water for temperature measurement (m); $T_w(t)$ is the water temperature at time, t (^{0}C) and $T_w(t\text{-}1)$ is the water temperature at time, $t\text{-}1$ (^{0}C).

C.1.3 Bowen Ratio (*β)*

The equation for β is given (Bowen, 1926) as:

$$\beta = c_k\, \frac{P_a}{100} \left(\frac{T_w - T_a}{e_s - e_a}\right) \tag{C.10}$$

where c_k is the empirical constant [dimensionless]; P_a is the atmospheric pressure [kpa]; T_a is the air temperature above the pond surface [^{0}C]; and e_s is the saturated vapour pressure at water temperature [kpa]; The constant c_k is considered as *0.665* at standard atmosphere of 20 ^{0}C, and pressure 101.3 kpa.

P_a in Eq.(C.10) *(*Allen et al., 1998) is:

$$P_a = 101.3 \left(\frac{293 - 0.0065\, Z}{293}\right)^{5.26} \tag{C.11}$$

where Z is the elevation[m].

The e_s in Eq.(C.10) is defined (Asmar and Ergenzinger, 1999) as:

$$e_s = 0.6108 \exp\left[\frac{17.269\,T_w}{T_w + 237.3}\right] \tag{C.12}$$

e_a in Eq.(C.10) is estimated (Burman and Pochop,1994; Allen et al., 1998) as:

$$e_a = \frac{e^0\left(T_{min}\right)\frac{RH_{max}}{100} + e^0\left(T_{max}\right)\frac{RH_{min}}{100}}{2} \tag{C.13}$$

in which $e^0(T_{max})$ is the saturated vapour pressure at maximum air temperature[kpa]; $e^0(T_{min})$ is the saturated vapour pressure at minimum air temperature[kpa]; RH_{max} is the maximum relative humidity [%]; and RH_{min} is the minimum relative humidity [%].

C.2 ESTIMATION OF THE MASS TRANSFER'S PARAMETERS

The equation for the mass transfer coefficient (μ) is given (Shuttleworth, 1993; Abtew, 2001) as:

$$\mu = 2.909\,A^{-0.05} \tag{C.14}$$

in which μ in mm s m^{-1} kpa^{-1}; and A is the water surface area of the pond [km^2].

The μ can be also determined from the slope of straight line passing through the origin that shows the relationship between the mass transfer product $(U_2\,(e_s - e_a))$ as an independent variable and an independent measurement of evaporation rate as a dependent variable (Sturrock et al., 1992; Sacks et al., 1994).

The equation for wind speed (U_2) is described (Allen et al., (1998) as:

$$U_2 = U_z\left[\frac{4.87}{ln\left(67.8\,Z - 5.42\right)}\right] \tag{C.15}$$

where U_2 is the wind speed at 2 m above the water surface[ms^{-1}]; U_z is the wind speed at 'Z' m above the ground surface[ms^{-1}]; and Z is the height at which wind speed is measured above the ground surface[m].

C.3 ESTIMATION OF THE PRIESTLEY-TAYLOR'S PARAMETERS

The equation for Priestley-Taylor's coefficient α is expresses (Eaton et al., 2001) as:

$$\alpha = \frac{\Delta + \gamma_c}{\Delta(1+\beta)} \tag{C.16}$$

Δ in Eq.(C.16) is defined as:

$$\Delta = \frac{4098\left[0.6108\ \exp\left(\frac{17.27\,T_w}{T_w + 237.3}\right)\right]}{(T_w + 237.30)^2} \tag{C.17}$$

γ_c in Eq.(C.16) is estimated (Allen et al., 1998; Asmar and Ergenzinger, 1999) as:

$$\gamma_c = \frac{C_{pa}\ P_a}{0.622 \times 1000\ \lambda_h} \tag{C.18}$$

where C_{pa} is the specific heat capacity $= 1.013\text{MJ/kg/}^0\text{C}$; and 0.622 is the ratio of water to dry air molecular weights (Brutsaert, 1982).

APPENDIX–D

ITERATION PROCEDURE FOR DETERMINING IMPLICIT VARIABLES

The iteration procedure given in the flow chart below is used for determining the state variables of Eqs. (7.3), (7.5) and (7.6)[Chapter-7], which appear both in L.H.S. and R.H.S. of the equation, let us take Eq.(7.3).

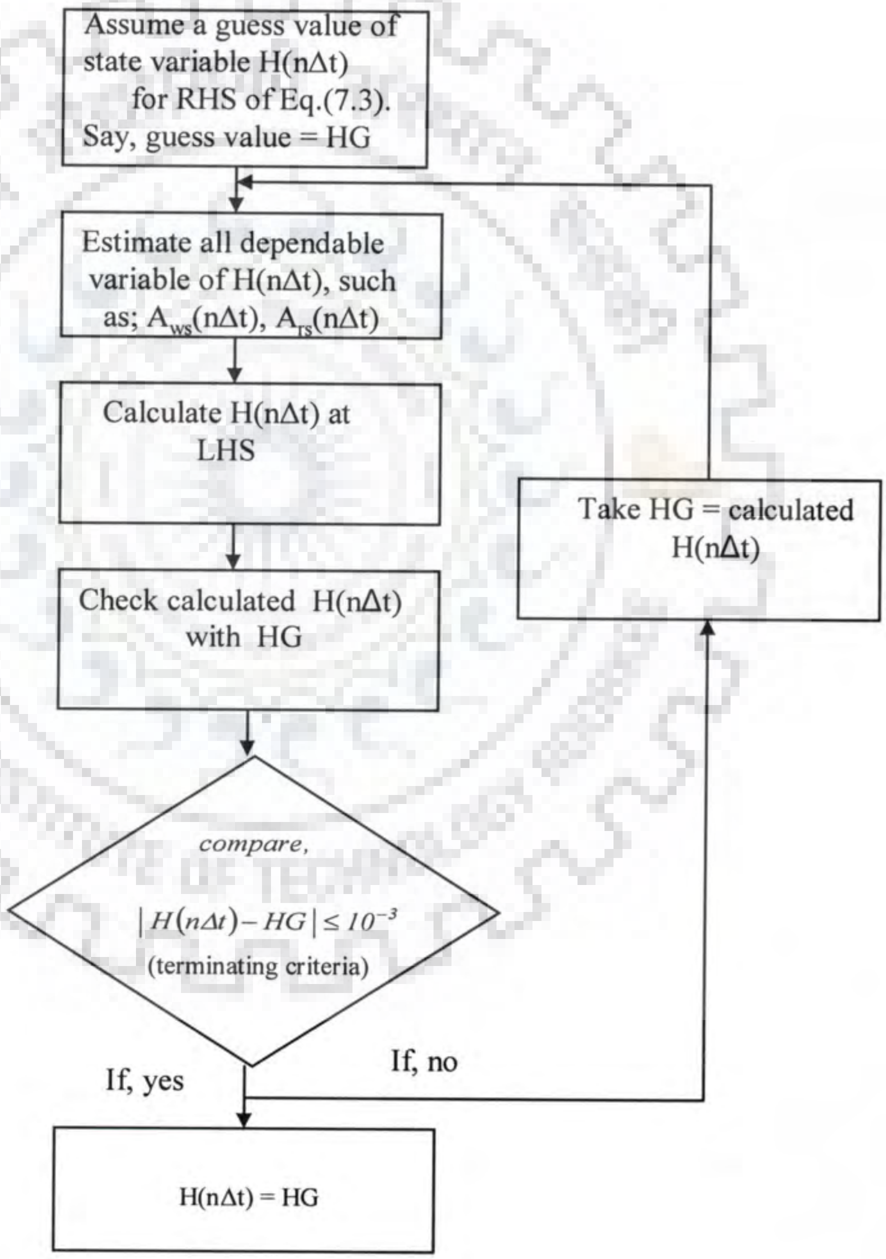

APPENDIX–E

RELATIONSHIPS OF GEOMETRICAL VARIABLES FOR A TRAPEZOIDAL POND

A sketch of plan and cross-section of a trapezoidal pond along with its geometrical variables is shown below.

L = bottom length of the pond [m];

W = bottom width of the pond[m];

n_s = side slope of the pond;

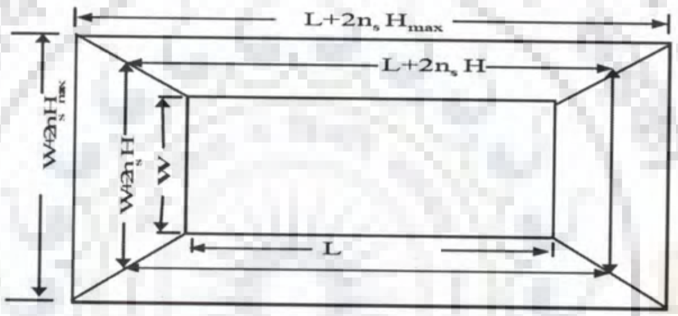

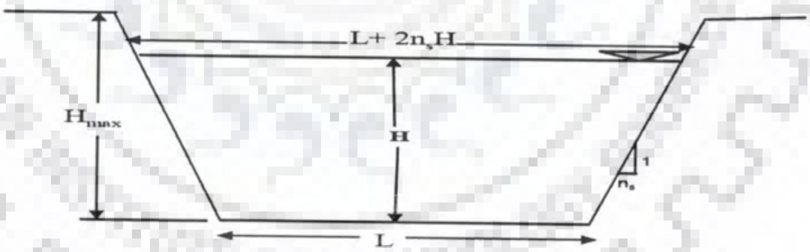

Surface Area of the Pond at the Top (A_s):

$$A_s = L\,W + 2\,n_s\,H_{max}(L+W) + (2\,n_s\,H_{max})^2 \tag{E.1}$$

Water Surface Area of the Pond (A_{ws}):

$$A_{ws} = L\,W + 2\,n_s\,H(L+W) + (2\,n_s\,H)^2 \tag{E.2}$$

Wetted Surface Area of the Pond (A_{rs}):

$$A_{rs} = L\,W + 2\,H\sqrt{1+n_s^2}\,(L + W + 2\,n_s H) \tag{E.3}$$

APPENDIX-F

HYDROLOGICAL AND HYDRO-METEOROLOGICAL DATA OF THE BADAKHERA WATERSHED IN RAJASTHAN

Table F.1. Observed rainfall-runoff data of three small watersheds in the semi-arid region of Rajasthan, India.

AG watershed			RAV watershed			BK watershed		
P(mm)	NAPI	Q(mm)	P(mm)	NAPI	Q(mm)	P(mm)	NAPI	Q(mm)
54.6	1.55	7.2	39	2.01	5.4	29.5	2.40	9.6
25.2	1.42	4.7	25.2	2.59	4.9	12.8	2.00	3.8
25.8	1.59	5.3	15	2.21	1.9	33.4	1.70	11.4
78.6	2.48	24.4	30.8	1.78	5.9	16	1.50	4.9
171.2	2.06	103.5	9.4	1.72	2.0	6.6	2.70	2.5
92.4	1.69	86.0	27.5	2.8	0.6	23	2.10	5.7
32.2	1.54	22.8	14	2.79	0.4	46	4.70	13.9
45.4	4.33	19.9	33.4	1.98	6.3	9.2	5.40	1.1
48.4	3.01	35.0	22	2.05	5.6	14.2	5.20	2.4
73.2	2.94	40.8	95.7	2.16	30.9	23.6	3.20	12.3
93.6	2.08	57.8	36.2	1.95	11.9	48	2.20	5.9
10	1.83	6.0	23.2	1.59	4.5	184	1.90	94.2
13	1.81	5.7	24.5	4.81	5.1	13.8	1.70	2.9
46	1.89	15.4	40.2	3.09	9.6	20.2	1.40	2.8
82.5	1.96	10.8	17	1.61	0.5	87.4	1.70	59.1
49	2.41	3.1	42	1.57	9.4	8.4	2.70	1.5
50	1.93	1.5	13.6	1.45	3.0	26	2.40	6.4
38.5	1.7	4.1	15.1	1.36	2.7	14	2.60	2.7
40.5	1.74	22.5	52.6	1.37	10.8	25	1.40	11.3
67	1.72	9.1	30.8	1.79	6.1	5.6	7.60	0.1
33	1.54	4.0	26.7	2.55	5.1	2.8	6.60	0.8
21.75	1.44	1.4	26.4	3.23	5.0	11.4	4.00	0.1
14.5	1.36	11.9	26	4.23	4.0	18.6	1.60	0.1
25.5	2.51	6.1	59.6	2.29	11.6			
44.5	2.48	7.2	15.8	1.99	3.3			
17.5	2	1.9	8.4	1.74	1.2			
32	2.19	10.9	14.4	3.74	2.4			
25.5	2.41	8.8	34.6	1.64	7.9			
20	1.41	2.7	62.4	1.42	19.8			
129	11.53	31.3	12.2	1.41	3.0			
21.5	2.33	4.8	21	4.68	3.3			
21.75	2.56	9.4	57.5	1.62	12.8			
26.5	1.73	8.5	48.8	1.53	10.9			
195	2.25	8.9	15	2.35	3.5			
63.8	1.99	2.3	24.8	2.02	6.4			
24.4	1.9	1.3	38.3	1.70	3.0			
48.1	2	18.3	37.4	2.44	6.9			
66.7	2.34	7.4	44.4	1.95	11.2			
50.7	2.01	2.8	73.5	1.85	24.5			
35.4	1.61	2.1	12.2	1.66	1.6			

22.2	2.92	1.9	24.2	1.84	1.6			
28.6	1.87	3.0	38.6	4.25	11.4			
38.2	1.71	3.3						
28	1.69	3.9						
77.1	1.73	45.0						
96.1	1.67	71.6						
28.6	1.57	3.4						
20.3	1.57	16.6						
42.6	3.91	35.7						
37	3.31	18.3						
31.7	2.96	7.6						
62	1.23	6.9						
66	1.59	26.4						
28.1	3.99	1.2						
27.9	3.13	1.3						
15.7	2.04	1.0						
69.4	2.21	2.5						
40.2	1.91	2.0						
75.9	1.63	50.1						
58.6	1.57	28.3						
28.8	1.39	10.8						
62	1.66	4.6						
61.8	3.07	21.3						
115.5	1.75	56.4						
31.1	2.49	1.1						
91.5	1.66	36.7						
55	1.96	9.4						
29	4.44	4.4						
30.7	2.79	9.8						
31.8	2.21	12.6						
56.8	1.62	18.5						
101	1.89	29.9						
15.6	1.64	4.3						

Table F.2(a). Observed hydro-meteorological data of the experimental pond during the year 2006.

J (day)	P (mm)	NAPI	H ((m)	N_{max} (hr)	T_{max} (^0C)	T_{min} (^0C)	RH_{max} (%)	RH_{min} (%)	D_f (m)	T_f (min)
172	19.6	2.2	0.28	9.6	40.5	27	41	23	0	0
173	0	2.0	0.27	9.1	41	28.5	36	22	0	0
174	0	1.8	0.22	10.8	43	29	45	24	0	0
175	0	1.6	0.18	8.1	42.2	31	48	27	0	0
176	0	1.4	0.14	9.5	42	30	58	72	0	0
177	39.8	1.3	0.59	6.7	38.6	28.5	68	50	0	0
178	0	2.2	0.59	5.1	37.5	28.5	77	48	0	0
179	0	2.0	0.55	5.4	36.6	29	75	95	0	0
180	13	1.8	0.63	5.3	35	25	83	49	0	0
181	9	1.6	0.79	8.9	37	23.5	90	55	0	0
182	0	1.5	0.77	9.6	35	28	78	70	0	0
183	0	1.3	0.73	6.1	36.6	28	76	48	0	0
184	0	3.4	0.69	8.2	39	27	79	66	0	0
185	0	3.0	0.66	5.5	36	29.5	69	41	0	0
186	0	2.7	0.62	10.8	39.5	29	68	46	0	0
187	0	0.0	0.58	5.5	36.5	26	92	64	0	0
188	0	0.0	0.55	5.7	32.5	28	79	52	0	0
189	0	0.0	0.51	5.9	34.8	28	70	46	0	0
190	0	0.0	0.48	6.3	35	28	73	51	0	0
191	0	0.0	0.45	5.1	34.4	28	70	50	0	0
192	0	0.0	0.41	5.6	34.4	28.5	69	86	0	0
193	0	0.0	0.38	5.1	34	25.5	79	58	0	0
194	0	0.0	0.35	5.8	33	28	72	45	0	0
195	0	0.0	0.33	5.1	35	28	74	45	0	0
196	0	0.0	0.3	5.3	34.8	28	70	39	0	0
197	0	0.0	0.27	5.9	36	29.5	78	47	0	0
198	0	0.0	0.24	5.1	37.2	29	63	37	0	0
199	0	0.0	0.22	5.2	38.5	28	69	37	0	0
200	0	0.0	0.19	5.4	38.6	28.5	74	57	0	0
201	2.2	0.0	0.27	5.1	33.5	26	89	98	0	0
202	19	6.7	0.49	5	29.5	24	95	86	0	0
203	10.4	2.1	0.57	5.2	30	24	93	65	0	0
204	0	1.8	0.55	6	33	26	92	73	0	0
205	0	1.6	0.53	5.3	31.2	25.5	86	74	0	0
206	0	1.5	0.5	5.5	30.5	26	86	68	0	0
207	44	1.3	1.02	5.7	32.5	25.5	86	86	0	0
208	4.4	1.5	1.07	5.9	29	25.5	86	86	0	0
209	5.8	1.8	1.09	5.3	28.5	24	98	100	0	0
210	15.2	1.9	1.2	5.1	26	24.5	100	77	0	0
211	2.6	1.7	1.2	5.6	30	25	95	72	0	0
212	7	1.5	1.23	5.7	38.8	25.5	97	77	0	0
213	4.8	1.4	1.24	6.6	29	24	93	73	0	0
214	0	2.7	1.22	6.3	28.2	24.5	84	67	0	0
215	0	2.7	1.19	7.1	31	25	86	64	0	0
216	3.8	2.9	1.19	6	32.5	25	98	83	0	0
217	0	4.7	1.16	5.4	31.6	26	90	70	0	0
218	0	4.9	1.13	8.1	32	26	92	76	0	0
219	0	8.0	1.1	6.2	29.5	25.5	89	78	0	0

220	10.6	16.2	1.22	6.1	30	25	97	79	0	0
221	35	5.1	1.64	5.1	30	24	96	95	0	0
222	19.2	2.5	1.82	5.1	27.2	24.5	95	79	0	0
223	0	2.2	1.81	5.4	29.5	24.5	96	86	0	0
224	0	2.0	1.78	5.2	29.5	24	92	72	0	0
225	0	1.8	1.74	7	31.2	26	92	93	0	0
226	8.4	1.6	1.78	9.5	33.5	26	93	79	0	0
227	15.8	1.7	1.89	5.7	32	24	100	79	0	0
228	0	2.8	1.87	5.3	31.2	25	97	72	0	0
229	0	4.5	1.84	5.5	31.8	26	87	62	0	0
230	0	4.1	1.81	11.4	34	24	95	72	0	0
231	4.4	3.7	1.81	5.7	31.8	24	98	87	0	0
232	0	3.2	1.79	5.2	26.5	24	87	74	0	0
233	0	4.3	1.76	4.8	30.5	25	87	67	0	0
234	0	47.4	1.73	4.5	31.2	25	82	78	0	0
235	0	42.7	1.7	4.9	30.5	25	87	76	0	0
236	0	38.4	1.67	5.3	31	23	81	70	0	0
237	0	34.6	1.64	4.4	30.5	24	85	68	0	0
238	0	0.0	1.61	5.3	30	24	84	68	0	0
239	0	0.0	1.58	5.3	30	25	87	78	0	0
240	0	0.0	1.55	5.2	29.5	23.5	88	70	0	0
241	0	0.0	1.53	4.3	30.5	25	84	59	0	0
242	0	0.0	1.5	5.1	31.8	23	87	58	0	0
243	45.2	0.0	1.98	5.7	32	23	100	100	0	0
244	5.4	2.1	2.04	5.1	25	23	100	92	0	0
245	9.2	1.9	2.08	5.1	26.8	23.5	84	60	0	0
246	0	1.7	2.06	7.8	32.2	23.5	90	71	0	0
247	0	1.5	2.03	10.1	31.6	24	88	64	0	0
248	0	1.4	2	10.4	32.6	25	92	65	0	0
249	0	1.2	1.96	7.2	32.8	26	93	86	0	0
250	0	4.5	1.93	6.8	29.5	24	87	63	0	0
251	0	6.5	1.9	10.5	31	23.5	88	60	0	0
252	0	0.0	1.87	10.5	31.5	23.5	92	35	0	0
253	0	0.0	1.83	9.2	33.4	28	87	61	0	0
254	0	0.0	1.8	10.1	33.50	25	86	60	0	0
255	0	0.0	1.77	10.6	33.00	24	85	58	0	0
256	0	0.0	1.74	10.6	33.50	24.5	87	57	0	0
257	0	0.0	1.7	10.5	33.5	24	85	53	0	0
258	8.6	0.0	1.83	10.7	34.5	24.5	95	51	0	0
259	0	4.6	1.81	9.9	35.0	24.5	83	52	0	0
260	0	4.2	1.78	10.2	35	24.5	84	52	0	0
261	0	3.7	1.75	10.1	35.2	25	80	49	0	0
262	0	3.4	1.72	10.2	35.5	24	86	51	0	0
263	0	3.0	1.68	10.1	36	25.5	84	52	0	0
264	0	2.7	1.65	9.8	35.2	25.5	80	53	0	0
265	0	0.0	1.62	10.1	35	22	96	51	0	0
266	0	0.0	1.59	10	34.2	24	79	48	0	0
267	0	0.0	1.55	10	33.6	25	84	49	0	0
268	0	0.0	1.52	9	34.5	23	82	51	0	0
269	0	0.0	1.49	10	34.5	23	79	52	0	0
270	0	0.0	1.46	10	34.5	26	80	49	0	0
271	0	0.0	1.43	10.3	34.5	24.5	81	48	0	0
272	0	0.0	1.4	11.1	35	24.5	84	44	0	0

273	0	0.0	1.36	10.1	35.5	21	90	35	0	0
274	0	0.0	1.33	9.9	34.4	23	52	34	0	0
275	0	0.0	1.30	9.4	35	27	42	36	0	0
276	0	0.0	1.27	10	35.5	26	51	27	0	0
277	0	0.0	1.24	10	36.5	21	61	25	0	0
278	0	0.0	1.21	10.5	37.5	21	52	18	0	0
279	0	0.0	1.18	10.4	37.8	19	68	18	0	0
280	0	0.0	1.15	10.5	36.5	24	76	35	0	0
281	0	0.0	1.11	10.5	35	23	76	39	0	0
282	0	0.0	1.08	10	34	22.5	73	33	0	0
283	0	0.0	1.05	10.4	36	22.5	61	23	0	0
284	0	0.0	1.02	10.2	36	21	65	33	0	0
285	0	0.0	0.99	10.2	36	21	61	19	0	0
286	0	0.0	0.96	10.6	35	19	69	29	0	0
287	0	0.0	0.93	10.2	34.8	22.5	72	29	0	0
288	0	0.0	0.9	9.1	35.5	18	84	24	0	0
289	0	0.0	0.87	9.7	34.6	18	75	21	0	0
290	0	0.0	0.84	10.1	36.6	19	66	28	0	0
291	0	0.0	0.81	9.9	36.6	19	76	29	0	0
292	0	0.0	0.78	10.1	36.5	22	71	28	0	0
293	0	0.0	0.75	9.2	35.6	19	77	50	0	0
294	0	0.0	0.72	9.8	30.8	18	94	34	0	0
295	0	0.0	0.69	8.8	33.8	18.5	90	36	0	0
296	0	0.0	0.66	8.7	33.4	18	87	34	0	0
297	0	0.0	0.64	9.8	32.5	17.5	87	32	0	0
298	0	0.0	0.61	9.3	32	18.4	96	32	0	0
299	0	0.0	0.58	9.5	32.5	16	72	32	0	0
300	0	0.0	0.55	9.3	31.8	15.5	75	32	0	0
301	0	0.0	0.52	9.7	31.5	16	74	28	0	0
302	0	0.0	0.49	9.7	31.5	14	89	25	0	0
303	0	0.0	0.47	9.5	31.8	15	90	27	0	0
304	0	0.0	0.44	9	32.5	15.5	74	24	0	0
305	0	0.0	0.41	9.4	32.8	14.5	89	25	0	0
306	0	0.0	0.38	8.7	32	16	69	26	0	0
307	0	0.0	0.35	9.1	31	15	90	33	0	0
308	0	0.0	0.32	8.6	31	14.5	93	30	0	0
309	0	0.0	0.3	9.1	35.5	15	88	32	0	0
310	0	0.0	0.27	9.5	32	14	89	41	0	0
311	0	0.0	0.24	8.8	32.5	14	90	44	0	0
312	0	0.0	0.21	9	31.5	14	79	39	0	0
313	0	0.0	0.18	8.8	32.2	15	89	31	0	0
314	0	0.0	0.16	8.2	31	14	89	35	0	0
315	0	0.0	0.13	7.8	29.8	15	98	32	0	0
316	0	0.0	0.1	8	29.6	15	85	35	0	0
317	0	0.0	0.08	8.8	30.5	14.5	85	34	0	0
318	0	0.0	0.05	8.8	30.5	14.5	76	28	0	0

Table F.2(b). Observed hydro-meteorological data of the experimental pond during the year 2007.

J (day)	P (mm)	NAPI	H ((m)	N_{max} (hr)	T_{max} (^0C)	T_{min} (^0C)	RH_{max} (%)	RH_{min} (%)	D_f (m)	T_f (min)
156	32	0.5	0.42	6.8	35.5	27.5	50	26	0	0
157	0	0.7	0.39	10.80	40.2	30.5	49	25	0	0
158	0	0.9	0.35	11.8	41.6	32.2	47	28	0	0
159	0	1.0	0.31	11.8	41.5	32	47	21	0	0
160	0	1.1	0.28	11.8	43	33	40	20	0	0
161	0	1.0	0.24	11.2	43.5	32	50	20	0	0
162	0	0.0	0.20	10.9	43.5	31.5	48	23	0	0
163	0	0.0	0.18	10.9	42.5	32	48	22	0	0
164	0	0.0	0.18	11.1	42.5	32	48	24	0	0
165	0	0.0	0.14	7.4	42	33.6	47	33	0	0
166	28	0.0	0.40	6.6	42	33.5	70	43	0	0
167	0	0.0	0.38	7.9	38	25.5	68	43	0	0
168	0	0.0	0.38	9.5	37.8	26	69	32	0	0
169	0	0.0	0.37	9.8	41	28	68	35	0	0
170	0	0.0	0.35	10.1	39.5	27	61	37	0	0
171	0	0.0	0.34	8.7	39.5	27	68	45	0	0
172	0	0.0	0.33	7.5	38.5	28	66	49	0	0
173	0	0.0	0.32	5.4	37.5	26.5	76	34	0	0
174	0	0.0	0.30	8.2	40.5	30.5	59	38	0	0
175	0	0.0	0.27	10.1	38.5	30	56	38	0	0
176	0	0.0	0.24	8.4	38	28.5	64	47	0	0
177	4	2.6	0.23	7.7	36.5	28	65	44	0	0
178	0	1.9	0.21	5.1	37.5	29	67	42	0	0
179	115	1.4	2.75	9.3	37.5	24	100	89	0.04	8
180	0	1.0	2.70	10.2	38	26	82	57	0	0
181	0	0.7	2.68	10.3	34.5	27	78	58	0	0
182	0	0.4	2.64	10.6	35	27	78	55	0	0
183	0	0.2	2.59	5.5	33.5	24.5	96	92	0	0
184	14	0.4	2.56	5.9	30	25	89	76	0	0
185	0	2.2	2.65	5.1	30	23	100	86	0	0
186	0	2.1	2.61	5.5	28	24	98	95	0	0
187	0	1.9	2.58	4.5	28	24.5	90	83	0	0
188	0	2.0	2.52	10.2	33	29.5	87	97	0	0
189	19	2.0	2.75	10.1	32.8	29.6	85	82	0.18	25
190	6.4	2.2	2.75	9.5	30.2	26.5	82	78	0.1	12
191	0	1.8	2.73	5.2	30	25	95	77	0	0
192	0	1.7	2.62	4.5	31	25	93	82	0	0
193	9.6	1.8	2.72	4.6	29.5	26.5	85	100	0	0
194	0	1.6	2.70	5.6	29.5	24.5	85	73	0	0
195	0	2.0	2.66	4.2	34	26	83	63	0	0
196	0	1.5	2.63	11	34	26	83	63	0	0
197	0	1.4	2.61	11	34.5	27	86	71	0	0
198	0	1.2	2.59	6.8	34	25	80	93	0	0
199	2.6	4.4	2.47	6	34	25	79	54	0	0
200	0	4.0	2.46	5.3	34.5	27	78	52	0	0
201	0	3.6	2.45	10.4	34.5	26	78	52	0	0
202	0	3.2	2.43	9.9	34.5	26	78	49	0	0

203	0	2.9	2.43	10.5	34.2	27	69	47	0	0
204	0	2.6	2.41	8.5	33.5	26.5	70	44	0	0
205	0	0.0	2.40	10.3	35.5	26	82	52	0	0
206	0	0.0	2.39	7.7	36.4	27.2	70	96	0	0
207	31.4	0.4	2.37	5.6	34.2	25	80	69	0	0
208	0	0.4	2.36	5.5	33	26.5	79	61	0	0
209	0	0.3	2.34	6.5	34	27	79	59	0	0
210	0	0.3	2.33	9.9	35	27	85	59	0	0
211	0	0.3	2.31	9.1	35	27	82	29	0	0
212	0	0.3	2.31	10.8	35	27.5	87	65	0	0
213	0	0.0	2.29	5	34	28	85	68	0	0
214	16.6	0.7	2.38	4.1	34	25	86	87	0	0
215	13	0.9	2.43	4.5	30	25	95	78	0	0
216	0	0.8	2.41	4.5	32	25	87	70	0	0
217	51.4	0.9	2.75	5.6	34.4	24.5	93	72	0.28	40
218	0	0.8	2.74	8.2	31	25	89	70	0	0
219	0	0.7	2.71	8.3	34	25.5	89	64	0	0
220	0	0.6	2.68	8.8	35	26.5	92	74	0	0
221	2.8	0.6	2.66	5.8	31	25	92	63	0	0
222	0	0.6	2.64	6.6	33	25	89	73	0	0
223	0	4.9	2.63	4.8	30.5	25	81	69	0	0
224	0	4.4	2.51	4.5	31.2	25.5	81	65	0	0
225	0	4.0	2.50	5.5	31.2	26	81	66	0	0
226	0	3.6	2.50	4.6	31	25.5	81	86	0	0
227	0	0.0	2.48	4.5	29	25.5	85	65	0	0
228	0	0.0	2.46	5.8	31.5	25.5	80	55	0	0
229	0	0.0	2.43	9.8	33.2	25	84	58	0	0
230	0	0.0	2.42	5.7	32.5	24.5	84	58	0	0
231	0	0.0	2.41	7.5	32.4	24.5	79	57	0	0
232	0	0.0	2.39	10.3	32.5	25.5	83	89	0	0
233	3.8	1.5	2.55	4.5	27.5	24	97	87	0	0
234	28.8	0.9	2.54	5.5	29.5	23	90	98	0	0
235	4.8	1.2	2.51	4.3	31.5	24.5	89	60	0	0
236	0	1.0	2.53	9.5	32.5	24.5	86	62	0	0
237	0	0.9	2.40	9.8	33.5	25.5	88	63	0	0
238	0	0.8	2.36	10.9	34	26	83	68	0	0
239	5.8	0.9	2.37	7.7	34.5	25	92	83	0	0
240	0	1.4	2.34	6.5	31	24	89	78	0	0
241	8.4	1.2	2.47	6.5	31.6	25	90	66	0	0
242	0	0.9	2.45	8.6	33	25	90	67	0	0
243	0	0.8	2.42	7.9	33.5	26	85	63	0	0
244	0	0.8	2.39	8.8	34.5	25.5	90	73	0	0
245	24.4	0.7	2.58	7.8	34.5	23.6	93	66	0	0
246	0	0.6	2.57	7.4	33	25.5	85	61	0	0
247	0	0.6	2.54	8	34.2	26	87	67	0	0
248	0	0.4	2.50	7.7	34.2	26	89	67	0	0
249	3.6	0.8	2.49	9.5	33.5	25.5	86	93	0	0
250	38.2	0.9	2.75	6.8	32	25	93	80	0.16	19
251	33.2	1.1	2.75	5.8	30.2	24.5	92	93	0.25	30
252	0	1.0	2.75	10	32.6	25	87	65	0	0
253	8.2	1.2	2.75	9.3	33.5	25.5	84	83	0.04	6
254	0	1.3	2.75	7	33.00	25	83	55	0	0
255	0	1.2	2.71	7.7	34.00	25	86	56	0	0

256	0	2.1	2.68	9	33.50	24	90	57	0	0
257	0	9.6	2.65	10.3	33.5	24.5	84	56	0	0
258	0	10.4	2.62	9.8	33.5	23	79	53	0	0
259	0	0.0	2.58	10.5	33.6	22.5	90	51	0	0
260	0	0.0	2.55	10.4	33.5	24.5	90	56	0	0
261	0	0.0	2.52	10.5	34.5	25	87	53	0	0
262	0	0.0	2.49	9.4	35	25.5	86	49	0	0
263	0	0.0	2.45	10.3	36	26	85	52	0	0
264	0	0.0	2.42	5.6	34	25	87	61	0	0
265	0	0.0	2.39	8.9	35	24	84	63	0	0
266	0	0.0	2.36	10.2	34.4	24	87	52	0	0
267	0	0.0	2.33	8.8	33.5	22.5	68	44	0	0
268	0	0.0	2.30	8.7	33.5	23.5	79	88	0	0
269	0	0.0	2.27	5.6	26	22	93	65	0	0
270	0	0.0	2.24	6.5	31	25	85	49	0	0
271	0	0.0	2.21	6.4	33	22.5	85	39	0	0
272	0	0.0	2.17	9.9	35	20.5	78	33	0	0
273	0	0.0	2.14	10	35	18.5	81	42	0	0
274	0	0.0	2.11	9.6	34	17.5	82	33	0	0
275	0	0.0	2.08	10	34.5	17	82	20	0	0
276	0	0.0	2.05	9.7	35.5	17	78	20	0	0
277	0	0.0	2.01	10.2	36.5	18	79	25	0	0
278	0	0.0	1.98	10.1	35.5	18	68	32	0	0
279	0	0.0	1.95	9.9	34.6	18.5	77	26	0	0
280	0	0.0	1.92	9.8	35	18	83	32	0	0
281	0	0.0	1.89	9.7	34.2	18.5	52	24	0	0
282	0	0.0	1.86	9.9	34.5	18.5	66	34	0	0
283	0	0.0	1.82	10.2	34	17	82	22	0	0
284	0	0.0	1.79	10.4	33	18.5	85	25	0	0
285	0	0.0	1.76	9.8	33.5	14	81	17	0	0
286	0	0.0	1.73	10.2	33.5	13.5	65	16	0	0
287	0	0.0	1.70	9.9	34	14	78	19	0	0
288	0	0.0	1.67	9.7	34	14	83	18	0	0
289	0	0.0	1.64	9.5	34	14	81	18	0	0
290	0	0.0	1.61	9.4	34	13	90	13	0	0
291	0	0.0	1.58	9.3	34.8	13.5	83	26	0	0
292	0	0.0	1.55	8.6	33	14.5	92	18	0	0
293	0	0.0	1.52	9.3	35.5	13	79	13	0	0
294	0	0.0	1.48	10.2	34.6	13.5	75	18	0	0
295	0	0.0	1.45	10	34.5	15.5	74	10	0	0
296	0	0.0	1.42	10	34.5	16	72	21	0	0
297	0	0.0	1.39	9.7	34.6	15.5	86	23	0	0
298	0	0.0	1.36	7.6	33.5	13	91	18	0	0
299	0	0.0	1.33	8.5	33	13	86	19	0	0
300	0	0.0	1.31	8.4	33.6	14.5	87	22	0	0
301	0	0.0	1.28	8.8	34	15.5	89	14	0	0
302	0	0.0	1.25	8.2	34	15	85	24	0	0
303	0	0.0	1.22	8.5	33.2	14	83	20	0	0
304	0	0.0	1.19	7.3	32	10	84	36	0	0
305	0	0.0	1.16	8.5	31.8	7.5	89	24	0	0
306	0	0.0	1.13	8.6	32	11	88	23	0	0
307	0	0.0	1.10	8	31.2	10.8	90	22	0	0
308	0	0.0	1.07	8	32.2	12.6	80	16	0	0

309	0	0.0	1.05	8.2	32.4	13.4	89	22	0	0
310	0	0.0	1.02	8.4	33.4	13.6	91	23	0	0
311	0	0.0	0.99	8	33.8	13.2	95	33	0	0
312	0	0.0	0.96	5.5	34	12.4	80	31	0	0
313	0	0.0	0.93	8.2	32.8	14.2	89	31	0	0
314	0	0.0	0.91	7.5	32	15	92	36	0	0
315	0	0.0	0.88	7.1	31	14.5	87	36	0	0
316	0	0.0	0.85	8.3	32	14	91	24	0	0
317	0	0.0	0.82	8	33	13.5	87	28	0	0
318	0	0.0	0.80	8.1	32.5	12	86	26	0	0
319	0	0.0	0.77	8.3	31	11.5	91	25	0	0
320	0	0.0	0.74	8.1	31.2	11.2	88	15	0	0
321	0	0.0	0.72	8.5	32	11	76	19	0	0
322	0	0.0	0.69	8.1	29.5	8.8	87	26	0	0
323	0	0.0	0.66	8	28.5	8.5	92	20	0	0
324	0	0.0	0.64	7.7	28.5	8.5	87	16	0	0
325	0	0.0	0.61	8.6	29.5	9	64	19	0	0
326	0	0.0	0.58	9.3	30.6	9	82	21	0	0
327	0	0.0	0.56	9.1	30	10	88	24	0	0
328	0	0.0	0.53	8.7	29.6	9.5	82	24	0	0
329	0	0.0	0.50	8.4	30.2	9.4	90	22	0	0
330	0	0.0	0.48	9	30	8.5	85	24	0	0
331	0	0.0	0.46	8.6	30.4	9.6	83	23	0	0
332	0	0.0	0.43	9	30	8.5	87	24	0	0
333	0	0.0	0.41	8.1	28.5	11.5	86	32	0	0
334	0	0.0	0.38	7.4	29.5	12	84	33	0	0
336	0	0.0	0.36	8.7	27.5	10	88	27	0	0
337	0	0.0	0.33	7.9	27.2	14.5	85	59	0	0
338	0	0.0	0.31	6.5	23.5	10.4	95	58	0	0
339	0	0.0	0.28	7.5	23.2	8.5	95	45	0	0
340	0	0.0	0.26	7.8	23.8	7.5	92	37	0	0
341	0	0.0	0.24	7	25.5	7.5	97	43	0	0
342	0	0.0	0.22	6.5	22.4	7	91	48	0	0
343	0	0.0	0.19	7.8	24.4	7	94	34	0	0
344	0	0.0	0.17	8.3	24	6.5	89	34	0	0
345	0	0.0	0.15	8	25	7.5	94	42	0	0
346	0	0.0	0.13	7.4	25.8	10.5	86	37	0	0
347	0	0.0	0.10	8	24.8	14.5	85	46	0	0
348	0	0.0	0.08	7.4	20.5	10.5	87	56	0	0
349	0	0.0	0.06	7	20.6	7.5	92	59	0	0
350	0	0.0	0.04	7.6	20.3	3.5	94	35	0	0
351	0	0.0	0.03	8.9	20.5	3.4	90	38	0	0
352	0	0.0	0.02	8.7	20.5	3.2	93	35	0	0
353	0	0.0	0.01	9	21.5	2	89	30	0	0